REFERENCE ONLY

UNIVERSITY OF LONDON THESIS

Degree PhD Year 2005 Name of Author ASANWALA L.

COPYRIGHT

This is a thesis accepted for a Higher Degree of the University of London. It is an unpublished typescript and the copyright is held by the author. All persons consulting the thesis must read and abide by the Copyright Declaration below.

COPYRIGHT DECLARATION

I recognise that the copyright of the above-described thesis rests with the author and that no quotation from it or information derived from it may be published without the prior written consent of the author.

LOANS

Theses may not be lent to individuals, but the Senate House Library may lend a copy to approved libraries within the United Kingdom, for consultation solely on the premises of those libraries. Application should be made to: Inter-Library Loans, Senate House Library, Senate House, Malet Street, London WC1E 7HU.

REPRODUCTION

University of London theses may not be reproduced without explicit written permission from the Senate House Library. Enquiries should be addressed to the Theses Section of the Library. Regulations concerning reproduction vary according to the date of acceptance of the thesis and are listed below as guidelines.

A. Before 1962. Permission granted only upon the prior written consent of the author. (The Senate House Library will provide addresses where possible).

B. 1962 - 1974. In many cases the author has agreed to permit copying upon completion of a Copyright Declaration.

C. 1975 - 1988. Most theses may be copied upon completion of a Copyright Declaration.

D. 1989 onwards. Most theses may be copied.

This thesis comes within category D.

☑ This copy has been deposited in the Library of UCL.

☐ This copy has been deposited in the Senate House Library, Senate House, Malet Street, London WC1E 7HU.

Photosystem I monomers and trimers in cyanobacteria

A thesis submitted for the degree of Doctor of Philosophy

by

Caroline L Aspinwall

Department of Biology

University College London

UMI Number: U592590

All rights reserved

INFORMATION TO ALL USERS
The quality of this reproduction is dependent upon the quality of the copy submitted.

In the unlikely event that the author did not send a complete manuscript
and there are missing pages, these will be noted. Also, if material had to be removed,
a note will indicate the deletion.

UMI U592590
Published by ProQuest LLC 2013. Copyright in the Dissertation held by the Author.
Microform Edition © ProQuest LLC.
All rights reserved. This work is protected against
unauthorized copying under Title 17, United States Code.

ProQuest LLC
789 East Eisenhower Parkway
P.O. Box 1346
Ann Arbor, MI 48106-1346

ABSTRACT

Photosystem I (PSI) is one of the chlorophyll-protein complexes located in the thylakoid membranes of photosynthetic organisms. It catalyses the oxidation of reduced plastocyanin or cytochrome c_6 and reduction of ferredoxin or flavodoxin during photosynthesis. The complex is composed of two core subunits, PsaA and PsaB, which bind electron-carrying cofactors, and numerous low molecular weight subunits. The precise composition of small subunits varies between prokaryotic and eukaryotic PSI and the function of many of these subunits remains unclear. This thesis describes studies of cyanobacterial mutants lacking small subunits in order to clarify the function of the PsaL and PsaE subunits.

The subunit PsaE has been implicated in the interaction of PSI with ferredoxin and in cyclic electron transport. In cyanobacteria a trimeric form of PSI predominates, with PsaL acting as the point of contact between three monomer units. Cyanobacterial mutants lacking this subunit therefore produce only monomeric PSI. No evidence of trimerisation has been found for PSI in eukaryotic organisms.

This study has established growth conditions in which PsaL-lacking mutants are disadvantaged compared to wild type. An investigation into the interaction of monomeric PSI with light-harvesting structures such as the phycobilisomes and the iron stress-induced CP43' antenna ring revealed that trimerisation of PSI is not required for interaction with either structure. However, the rates of state transitions and phycobilisome diffusion were measured and compared to those of wild type cells, revealing an increase in rate in both cells when PSI is monomeric. This suggests a change in the stability of the phycobilisome-PSI interaction. EPR analysis of electron transfer processes in cyanobacterial mutants lacking the PsaE subunit and of PSI in either monomeric (PsaL-lacking) or trimeric (wild type) forms has been conducted.

Possible functional roles for PSI trimerisation are discussed.

This thesis is dedicated to my family, particularly to my brother Paul.

ACKNOWLEDGEMENTS

First I wish to thank my supervisors, Dr Conrad Mullineaux and Prof Mike Evans, for giving me the opportunity to undertake this PhD and then for supporting me every step of the way.

I acknowledge the BBSRC for providing funding for this project. I must also thank Antonio Casal and Susan Jones for excellent technical assistance and Laura Wood for DNA sequencing. Peter Rich, Jasvinder Jassal and Nick Fisher assisted with the use of the homemade spectrophotometer. I thank Jim Barber, James Duncan and Tom Bibby at Imperial College London for collaborating to produce the electron microscopy images of PSI particles. I thank Mary Sarcina and Elinor Thompson from the UCL Photosynthesis Research Group for sharing advice, protocols and ideas.

Many people at UCL Photosynthesis Research Group have given me help in some form or another and I am grateful to them all. In particular I would like to mention the following people: Kulsam Ali, Antonio Casal, Mary Sarcina, Jasvinder Jassal, Alec Forsyth and Sally Marsh – they have been both colleagues and friends.

A great many other people have made the last few years enjoyable and to mention them all would form another chapter. To avoid this I mention only a few: Joanna Macve, Elizabeth White and Matthew Ramagge for providing electronic good wishes on a near daily basis, and my friends at the Mei Chuan tai chi academy for keeping me calm and sane even when my 'things to do' list seemed unending. Alec Forsyth provided tips and encouragement even as he travelled the world. To everyone else that has helped me scientifically or otherwise, I say a sincere thank you.

Last, but certainly not least, I thank my wonderful family for their love and support and for encouraging me with every crazy project I have ever taken on.

CONTENTS

FIGURES

TABLES

ABBREVIATIONS

A	Angstrom
A_0	Primary electron acceptor chlorophyll (of PSI)
A_1	Phylloquinone
ATP	Adenosine triphosphate
AU	Arbitrary units
Chl	Chlorophyll
CW	Constant wave
DCMU	3-(3,4-dichlorophenyl)-1,1-dimethylurea
DNA	Deoxyribonucleic acid
dNTP	Deoxyribonucleotide 5'-triphosphate
EDTA	Ethylene diamine tetra-acetic acid
EPR	Electron paramagnetic resonance
ESP	Electron spin polarised
F_A	Iron-sulphur centre F_A (of PSI)
F_B	Iron-sulphur centre F_B (of PSI)
F_X	Iron-sulphur centre F_X (of PSI)
FRAP	Fluorescence Recovery After Photobleaching
g	Acceleration due to gravity
GHz	gigaHertz
GT	Glucose-tolerant
HEPES	N-(2-hydroxythethyl)piperazine-N'-(2-ethanesulphonic acid)
hr	Hours
IPTG	Isopropyl ß-D-thiogalactopyranoside
kanR	Kanamycin resistance cassette
kb	Kilobases
LAHC	Light-activated heterotrophic conditions
LB	Luria-Bertani
LHCI	Light-harvesting complex I
LHCII	Light-harvesting complex II
µg	Microgram
µl	Microlitre
µm	Micrometre
µmole	Micromole
µs	Microsecond
mg	Milligram
min	Minute
ml	Millilitre
mM	Millimolar
mT	Milli Tesla
NADP(H)	Nicotinamide adenine dinucleotide phosphate
ns	Nanosecond
P680	Primary electron donor of PSII
P700	Primary electron donor of PSI
PAGE	Polyacryamide gel electrophoresis

PBS	Phycobilisome
PCC	Pasteur Culture Collection
PCR	Polymerase chain reaction
pH	A logarithmic unit of measurement for acidity or alkalinity
PSI	Photosystem I
PSII	Photosystem II
psi	Pounds per square inch
rpm	Revolutions per minute
s	Second
SD	Standard deviation
SDS	Sodium dodecyl sulphate
SE	Standard error
TES	Tris-ethylene diamine tetra-acetic acid-NaCl
Tris	Tris(hydroxymethyl)aminomethane
v/v	Volume per volume
w/v	Weight per volume
wt	Wild type
X-gal	5-bromo-4-chloro-indolyl-β-D-galactoside

CHAPTER ONE
INTRODUCTION

CHAPTER ONE

INTRODUCTION

1.1 Oxygenic photosynthesis

Oxygenic photosynthesis is the process by which light energy is harnessed and converted into chemical energy by photosynthetic organisms. The process yields oxygen and removes carbon dioxide from the air. Plants, algae and photosynthetic bacteria are essential for maintaining a breathable atmosphere and form the basis of the food chain. They are capable of converting the low-energy compounds carbon dioxide and water into energy-rich carbohydrates using energy from solar radiation. A thorough understanding of the process of photosynthesis will be required if we are to exploit solar energy in the future (Barber & Andersson, 1994).

1.1.1 Pigments

The energy from light is captured when it is absorbed by photosynthetic pigments, mainly the green chlorophylls. The pigments form complexes with proteins, which are described in later sections. A photosynthetic unit contains many chemically inactive pigments with light-harvesting functions and a few photochemically reactive pigments that constitute the reaction centre (Hillier & Babcock 2001).

Chlorophyll *a* is present in all oxygen-evolving photosynthetic organisms. It is blue-green in colour and is present in various forms in the cell. Plants and green algae also contain a smaller proportion of the yellow-green chlorophyll *b*. Satoh *et al* (2001) genetically engineered the cyanobacterium *Synechocystis* sp. strain PCC 6803 (abbreviated hereafter to *Synechocystis* 6803) to produce chlorophyll *b* and found that it accumulated to a level of 10% of the total chlorophyll, incorporating preferentially into photosystem I (PSI) and channelling light successfully to chlorophyll *a* molecules. This suggests flexibility in the pigment-binding capacity of photosystems.

Carotenoids (orange or yellow in colour) are present, channelling the light that they absorb to the chlorophyll *a* molecules and offering protection from excessive photo-

oxidation (Hall & Rao 1999). Carotenoids can also react with the singlet oxygen species ($O^{\cdot}$) that may be produced in chloroplast reactions.

Cyanobacteria also contain phycobilins, bound to proteins as phycobilisomes, and these act as light-harvesting complexes (LHC) for the cell. In eukaryotes (and prochlorophytes), there are specific LHCI and LHCII associated with each of the photosystems. These complexes contain numerous chlorophyll molecules for light absorption. LHCs channel energy into the photosynthetic reaction centres, where electrons are excited and transferred along an electron transfer chain.

1.1.2 Reaction centres

There are two classes of photosynthetic reaction centre. Type I reaction centres use iron-sulphur centres as terminal electron acceptors and include those found in green sulphur bacteria, the gram-positive heliobacteria and PSI. Type II reaction centres use quinone molecules as terminal electron acceptors and include those of sulphur and non-sulphur purple bacteria, some green filamentous bacteria and photosystem II (PSII).

Bacteria that carry out anoxygenic photosynthesis (i.e. they use light energy but they do not evolve oxygen as a result of this process) have either a type I or a type II reaction centre. For example, purple photosynthetic bacteria possess type II reaction centres with some homology with PSII. Heliobacteria and green sulphur bacteria contain type I reaction centres consisting of a homodimeric core (unlike the PSI core, which is heterodimeric).

Organisms capable of oxygenic photosynthesis have both type I and type II reactions centres (PSI and PSII), which are coupled in series to allow water oxidation and $NADP^+$ reduction to drive chemical reactions in the cell. It is this oxygen-evolving photosynthesis that is described here.

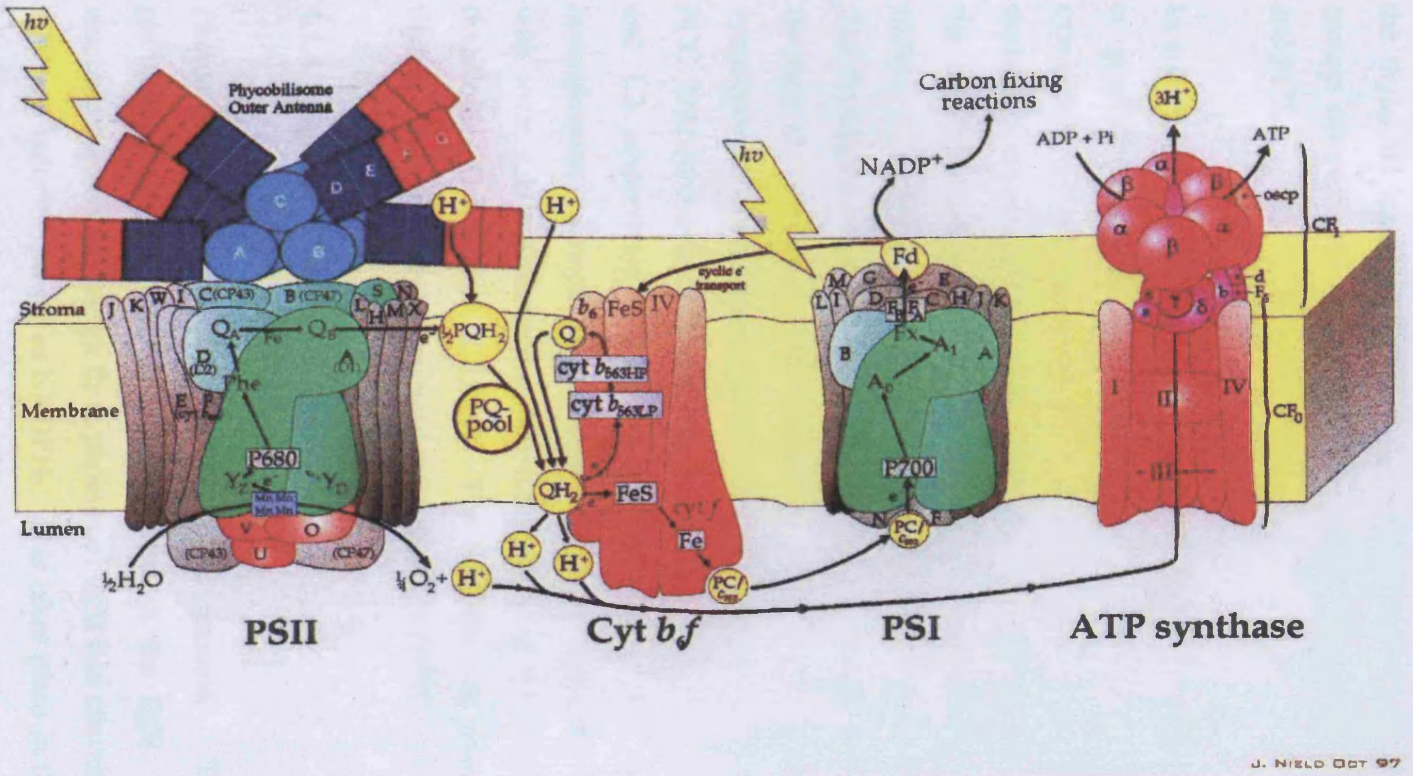

Figure 1.1 Schematic diagram of photosynthesis in cyanobacterial thylakoid membranes. The photosystems, PSI and PSII, absorb light energy and use it to drive electrons through a chain of bound cofactors. PSI is shown as a monomer for simplicity. The photosystems are linked by the cytochrome b_6f complex and mobile electron carriers such as the plastoquinone pool. The resulting electrochemical gradient across the membrane drives ATP synthesis by ATP synthase and reduction of $NADP^+$ to NADPH. The light-harvesting phycobilisomes are shown attached to PSII (the phycobilisomes are actually relatively much larger than shown on this diagram). Drawn by J. Nield, Imperial College London.

1.1.3 Thylakoid membranes

The photosynthetic complexes and their light-absorbing chlorophylls are located in the thylakoid membranes, as shown in Figure 1.1. A third thylakoid-embedded protein complex, the cytochrome b_6f complex, connects the two photosystems, PSI and PSII.

In eukaryotes, the thylakoids are contained within membrane-bound chloroplasts. It is generally accepted that chloroplasts evolved from the endosymbiosis of a cyanobacterial cell approximately 1.5 billion years ago (Yoon *et al* 2004). The thylakoids are arranged as stacks called grana, which are linked by looser membranes, the stromal lamellae. These membranes are embedded in the stroma, a colourless matrix. Cyanobacteria themselves, as with all prokaryotes, do not contain organelles. The thylakoids of cyanobacteria are present as parallel sheets of membranes running through the cytosol. The membrane arrangement within cells of the model cyanobacterial species used for this thesis, *Synechocystis* 6803 and *Synechococcus* sp. PCC 7942 (abbreviated hereafter to *Synechococcus* 7942), are shown in Figures 1.2 and 1.3 respectively. Cyanobacterial thylakoids are thought to be relatively homogeneous in composition, although there is evidence for some 'radial asymmetry' with some subtle difference in the composition of the inner and outer cylinders of thylakoids (Sherman *et al* 1994). The structure and dynamics of cyanobacterial thylakoid membranes are reviewed in Mullineaux (1999).

1.1.4 Light and dark reactions

Photosynthesis is essentially a two stage process. The first step involves photochemical reactions, which only occur in the light. These light-dependent reactions convert the energy from photons of light into chemical energy in the form of ATP and reducing power as $NADPH_2$. This takes place in the thylakoid membranes of chloroplasts and cyanobacteria. The energy from photons of light is used to move electrons across the membrane, via chains of cofactors bound to PSI and PSII reaction centres, eventually creating the strongly reducing agent NADPH. This process

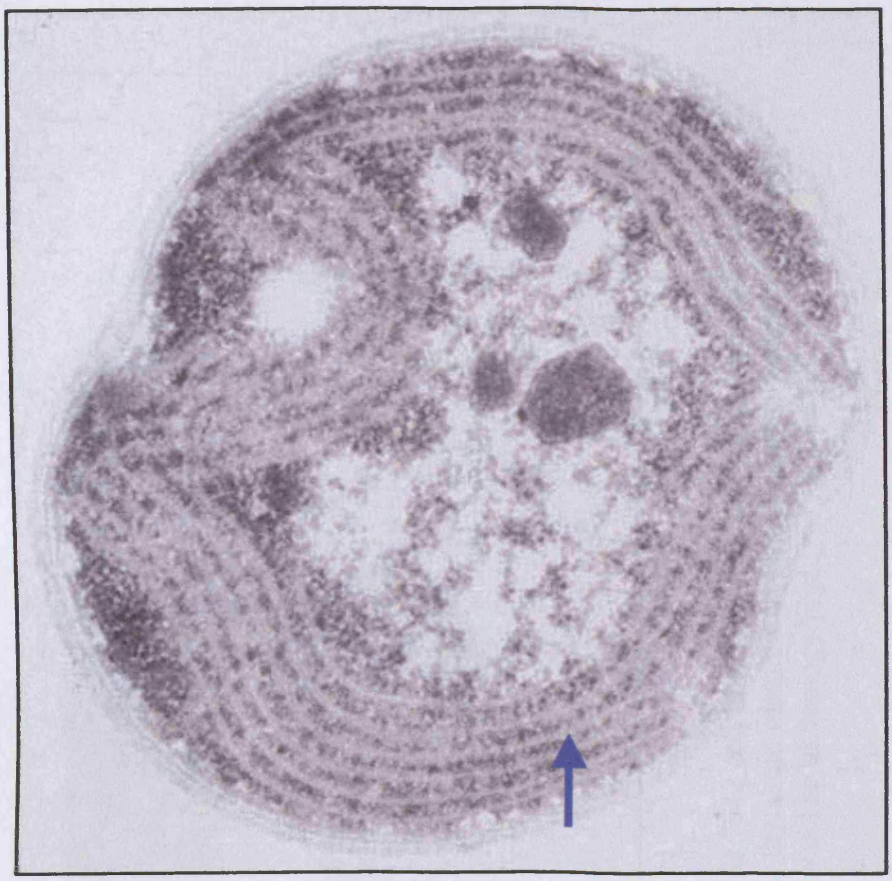

Figure 1.2 Electron micrograph image of a *Synechocystis* 6803 cell. The thylakoid membranes visible as continuous light grey lines as indicated (blue arrow). Image is reproduced from www.ucl.ac.uk/biology/prg/

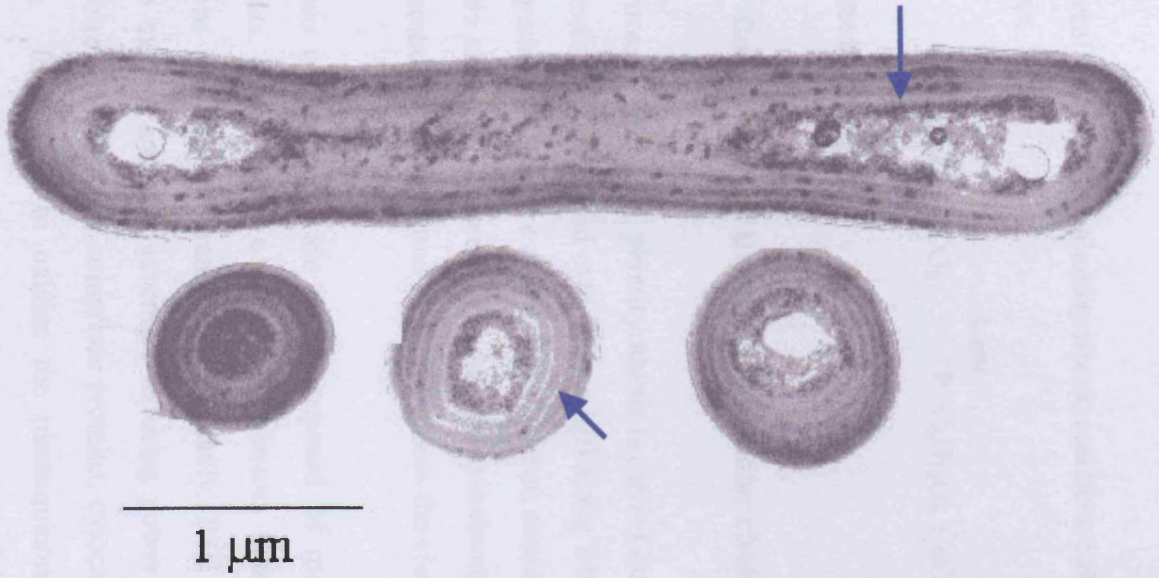

Figure 1.3 Electron micrograph image of a *Synechococcus* 7942 cell in longitudinal and transverse sections. The cell has been elongated using a cell division inhibitor. The thylakoid membranes (which appear as light grey lines) are indicated (blue arrows). Image is reproduced from www.ucl.ac.uk/biology/prg/

generates a proton gradient, which is in turn coupled to the synthesis of ATP by ATP synthase.

The second stage of photosynthesis is comprised of slower enzymatic steps known as the 'dark' reactions, meaning that they are light-independent processes. Enzymes in the chloroplast stroma or the cyanobacterial cytosol reduce carbon dioxide to produce carbohydrates using the ATP and $NADPH_2$ made during the light-dependent reaction.

The overall result of the photosynthetic reactions can be summarised by the following equation:

$$6H_2O + 6CO_2 \xrightarrow{\text{Light}} C_6H_{12}O_6 + 6O_2$$

1.2 Electron transfer

1.2.1 Components of the electron transfer chain

The process of oxygenic photosynthesis is carried out by the membrane-bound protein complexes (PSI, PSII and cytochrome b_6f) along with light-harvesting complexes and ATP synthase. There are also mobile electron carriers: the plastoquinone pool, which transfers electrons between PSII and the cytochrome b_6f complex, and plastocyanin (or alternatively cytochrome *c*), which passes the electrons on to PSI.

The two photosystems are both composed of multiple polypeptide subunits and pigments. Each binds a series of cofactors that are involved in photochemical reactions and electron transfer. Essentially, PSII drives the splitting of water to evolve oxygen and PSI generates reducing power in the form of $NADPH_2$. The cytochrome b_6f complex comprises proteins, cytochromes and a Rieske iron-sulphur centre. Its role is to oxidise the plastoquinone pool, reduce plastocyanin or cytochrome *c* and participate in the generation of the proton gradient. The complex links the electron transfer chains of PSI and PSII with the soluble electron carriers.

Pigments within the photosystem reaction centres absorb photons of light. The energy from photons absorbed by light-harvesting complexes is transferred rapidly to the

reaction centre pigments. The energy change induces a separation in charge between a primary donor (a chlorophyll molecule) and the first electron acceptor of a chain. The reaction centre pigments are excited and are altered from a slightly oxidising state to a highly reducing state. This allows the reduction of the primary electron acceptor of the electron transfer chain, a process that would not otherwise be energetically possible. The charge separation is stabilised as electrons are subsequently transferred along a chain of cofactors, each in turn being reduced and oxidised.

The chain of cofactors of PSI is described in more detail in Section 1.3. ATP is generated by photophosphorylation by either linear or cyclic electron transfer as described below. Energy conversion by PSI is likely to result from a combination of linear and cyclic processes with the proportion that each contributes being dependent on physiological conditions (it is estimated that the cyclic contribution is 3% of the linear under normal conditions) (Bendall & Manasse, 1995).

1.2.2 Linear electron transfer

Linear electron transfer can be described as an 'open' system and involves the generation of several products (ATP, oxygen, $NADPH_2$). There are two light reactions involved, each carried out by a different photosynthetic complex. In PSII, electrons from water are passed along the transfer chain and oxygen is evolved. Electrons are passed via the plastoquinone pool to the cytochrome b_6f complex and then from the mobile carrier plastocyanin to PSI. Electrons are carried by the chain of PSI cofactors to the stromal side of the complex. Here, ferredoxin is reduced and subsequently donates electrons to reduce $NADP^+$ to $NADPH_2^+$.

The transfer of electrons along a chain of cofactors is linked to the transfer of protons. An electrochemical potential across the membrane is created and this drives ATP synthesis by ATP synthase.

1.2.3 Cyclic electron transfer

Cyclic electron transfer is also a light-dependent reaction but is a 'closed' system from which the only net product is ATP. Only PSI and the cytochrome b_6f complex are involved. Once ferredoxin has been reduced, the electrons flow back via the plastoquinone pool, creating a cyclic pathway. The cytochrome b_6f complex probably functions in the same way in both the linear and cyclic systems. Ferredoxin is known to be the soluble cofactor but cyanobacteria may synthesise flavodoxin as an alternative when iron is unavailable and this has a different size and structure to ferredoxin. Flavodoxin substitutes for ferredoxin in linear electron transfer and may do in the cyclic process. The flow of electrons from ferredoxin to the plastoquinone pool generates a proton gradient that can be used to drive ATP synthesis without production of NADPH. As PSII does not participate in the cycle, no oxygen is evolved.

In plants and cyanobacteria there is a cyclic pathway directly from reduced ferredoxin to the plastoquinone pool via a ferredoxin:plastoquinone reductase enzyme (FQR), which is as yet unidentified (Munekage *et al* 2003; 2004). There may also be a cyclic pathway involving NADH dehydrogenase, which is shared with respiratory pathways (Fork & Herbert 1993).

The 'extra' ATP made by the cyclic system may be used during carbon dioxide fixation or other ATP-requiring reactions. A role for cyclic electron transfer in stress responses has been suggested; for example, an increase in output from the system is seen in photoinhibited *Chlamydomonas* cells and in salt-stressed *Dunaliella* (Bendall & Menasse 1995).

1.2.4 The Mehler reaction

Under some conditions, reduced ferredoxin reacts with oxygen rather than NADP and creates H_2O_2. Reduction of oxygen may generate a superoxide radical (O_2^-). Superoxide dismutase in chloroplasts converts two molecules of O_2^- into one H_2O_2 and

one O_2 (Hall & Rao 1999). The H_2O_2 can be converted to water by ascorbate peroxidase. This pseudocyclic electron transfer can produce extra ATP (without NADP reduction) and provides a mechanism for removing oxygen.

1.3 Photosystem I

PSI complexes catalyse the light-driven oxidation of the soluble electron carrier plastocyanin on the stromal side of the thylakoid membrane and the reduction of ferredoxin on the lumenal side. It is a large, multi-subunit pigment-protein complex. The reaction centre consists of a dimer of special chlorophyll *a* molecules called P700 to reflect the wavelength of maximal bleaching of 700 nm on oxidation (Brettel 1997).

1.3.1 A multi-subunit complex

The polypeptide subunits are present as one copy per P700 reaction centre (Chitnis 1996). They are named PsaA to PsaN plus PsaX (see Table 1.1). Cyanobacterial PSI lacks PsaH, PsaG and PsaN. As PsaG and PsaK are homologous, it has been suggested that cyanobacterial PsaK should be known as PsaGK (Scheller *et al* 1997). PsaM has not been identified in eukaryotic PSI. Despite differences in subunit composition, eukaryotic and cyanobacterial PSI are similar in structure and function, particularly with respect to the core subunits (Webber & Bingham 1998). PsaA and PsaB form the heterodimeric photosystem core, bind the majority of the cofactors and are essential for photosynthetic function. These two subunits are structurally similar although neither PsaA nor PsaB subunits can form a functional homodimer (Chitnis 1996). The individual subunits of PSI are discussed in detail in Section 1.4.

1.3.2 Light-harvesting for PSI

In plants and green algae, PSI associates with multiple LHC1, which are embedded in the membrane and specific to PSI. These antennae harvest light and channel it to the reaction centre to increase light-absorbing efficiency. Cyanobacteria do not have

Table 1.1 Subunits of PSI

Subunit	Location	Known cofactors	Function*
PsaA and PsaB	Transmembrane	P700, A_0, A_1, F_X, 100 chlorophyll *a*, 22 β-carotenes	Charge separation and stabilisation, electron transfer, light harvesting
PsaC	Stromal	F_A, F_B	Electron transfer
PsaD	Stromal		Ferredoxin docking, stabilisation of complex, orientation of PsaC
PsaE	Stromal		Ferredoxin docking, cyclic electron transfer
PsaF	Transmembrane		Plastocyanin docking
PsaG[a]	Transmembrane	Chlorophyll *a*?	Interaction with LHC1 in eukaryotes
PsaH[a]	Stromal	Chlorophyll *a*?	State transitions by binding LHCII in eukaryotes
PsaI	Transmembrane		Stabilisation of PsaL
PsaJ	Transmembrane	3 chlorophyll *a*	Stabilisation of PsaF
PsaK	Transmembrane	2 chlorophyll *a*	Binding LHCI in eukaryotes, function unknown in cyanobacteria
PsaL	Transmembrane	3 chlorophyll *a*	Trimerisation in cyanobacteria, stabilisation of PsaH in plants
PsaM[b]	Transmembrane	1 chlorophyll *a*	Stabilisation of trimers in cyanobacteria
PsaN[a]	Lumenal		Docking of plastocyanin in eukaryotes
PsaO[a]	Transmembrane		Unknown
PsaX[b]	Transmembrane	1 chlorophyll *a*	Unknown

a found only in eukaryotes
b found only in prokaryotes
* the precise function of many of the accessory subunits remains unclear, this table lists our current knowledge or suggested functions

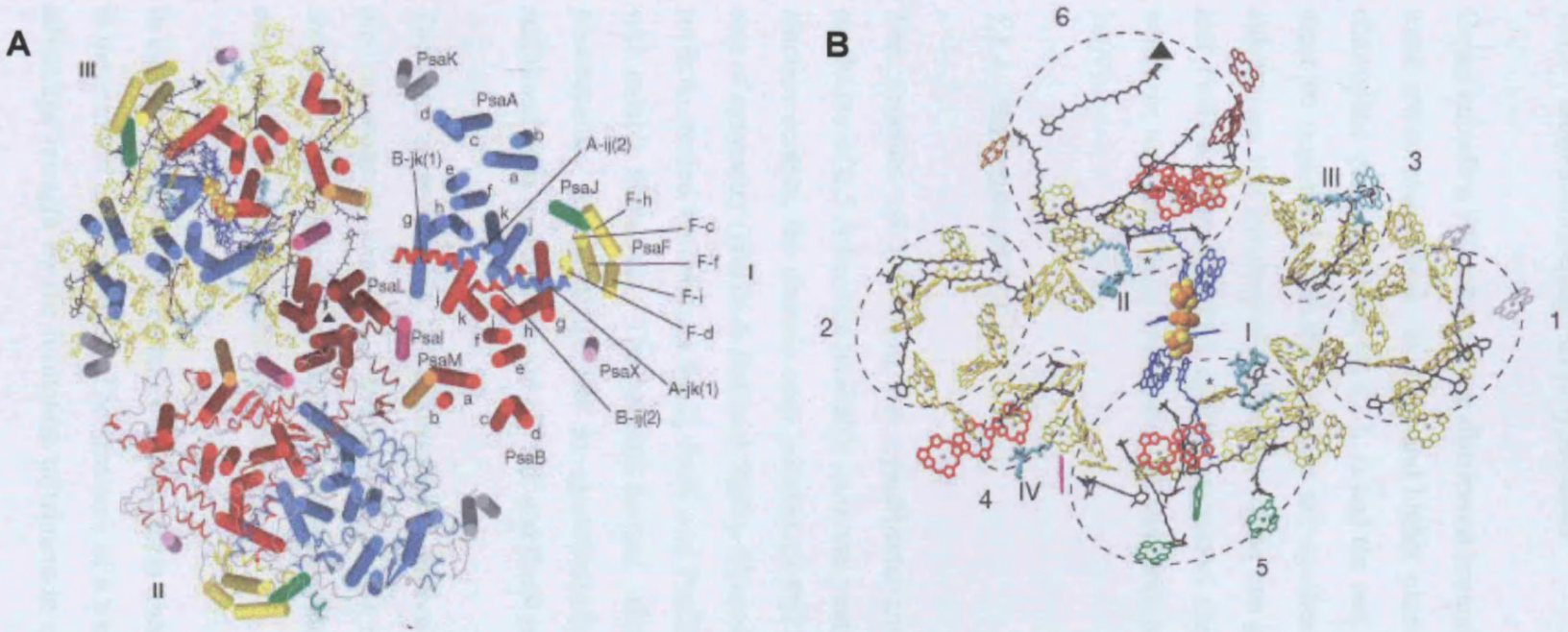

Figure 1.4 **A** Structural model of a PSI trimer from *Synechococcus* elongatus at 2.5 Å resolution. Stromal subunits are not shown. The core subunits PsaA and PsaB are shown as transmembrane a-helices (blue and red respectively) in the labelled monomer I on the right hand side of the image. **B** Spatial organisation of the cofactors and the antenna system in one monomer of PSI in a view from the stromal side onto the membrane plane. Chlorophylls coordinated by PsaA/PsaB are yellow, those bound to peripheral subunits in the colour of the coordinating subunits in as indicated in **A**, chlorophylls of the electron transfer chain in blue. The 22 carotenoids are arranged in clusters 1 to 6. Four lipids (turquoise) labelled with roman numerals. From Jordan *et al* (2001).

specific LHC for PSI but the mobile phycobilisomes associate with the photosystem under certain conditions.

1.3.3 Genes encoding PSI polypeptides

Genes encoding PSI subunits are distributed around the genome of cyanobacteria and some are co-transcribed. In algae and higher plants, some genes are encoded by the chloroplast genome (PsaA, B, C, I, J) and the rest by the nucleus. Gene expression must be organised such that subunits are synthesised in the correct ratio. In the eukaryotes, this involves co-ordination of the two genomes. The core subunits PsaA and PsaB are essential and appear to control the accumulation of other subunits, which in turn may have effects on the assembly of one another (Schwabe & Kruip 2000).

1.3.4 Structure of PSI

The structure of PSI from the cyanobacterium *Synechococcus elongatus* at a resolution of 2.5 Å became available in recent years (Jordan *et al* 2001). As in other reaction centres, the dimeric core proteins of PSI give rise to a pseudo-C2 (2-fold) axis of symmetry (Hillier & Babcock 2001). There is a prominent ridge on the stromal surface, created by subunits PsaC, PsaE and PsaD, where the photosystem interacts with soluble ferredoxin. The lumenal surface, where the photosystem interacts with plastocyanin, is essentially flat in cyanobacteria. In eukaryotes, PsaF has an additional helix and this portion of PsaF and PsaN are exposed on the lumenal face.

There are approximately 100 chlorophyll *a* molecules, 22 β-carotene molecules, two phylloquinones (vitamin K_1) and three [4Fe-4S] iron-sulphur centres bound to the complex. The chlorophyll *a* molecules act as an internal antenna for PSI, while the β-carotene molecules offer photoprotection.

In cyanobacteria the PSI complex tends to form trimers (Jordan *et al* 2001), whereas it is monomeric in eukaryotes. The structure of a trimer is shown in Figure 1.4. Any advantage brought by the formation of trimers in cyanobacteria is not known and is

the subject of much of the work presented in this thesis. It is possible that the eukaryotic PSI cannot form trimers (Ben-Shem *et al* 2003) due to steric hindrance, as the LHCI is permanently bound to the side of the complex (at PsaG/PsaK) and LHCII can bind transiently to the other side (at PsaH) during state transitions (Boekema *et al* 2001b, Scheller *et al* 2001).

1.3.5 The electron transfer chain of PSI

Plastocyanin is a copper protein found in the thylakoid lumen, which can be substituted by cytochrome *c* in some organisms when copper levels are limiting. Light energy drives oxidation of the primary electron donor, P700, which is then re-reduced by plastocyanin. Electrons are then transferred to the first acceptor in a chain of cofactors: A_0, a monomeric chlorophyll *a* molecule. The second electron acceptor in the chain, A_1, is a phylloquinone, one of the two phylloquinones present in the photosystem. The electrons are passed to Fx and then to F_A or F_B, all of which are [4Fe-4S] iron-sulphur centres. Finally, soluble ferredoxin is reduced. The low redox potential of the electron transfer chain allows $NADP^+$ to be reduced on the stromal side (Nugent 1996). Reduced ferredoxin is used by ferredoxin:$NADP^+$ oxidoreductase (FNR) to generate NADPH. The electron transfer chain cofactors are bound to the core polypeptides PsaA and PsaB, with the exception of $F_{A/B}$, which are bound to PsaC. The binding positions of the co-factors to are shown in Figure 1.4.

The reductants generated by PSI are used to drive numerous biochemical processes including the Calvin cycle, nitrite reduction, glutamate synthesis and many more (Chitnis 1996). PSI also participates in cyclic electron transfer in the thylakoid membrane, as mentioned earlier.

1.3.6 Two electron transfer pathways through the PSI core

There are two alternative, almost symmetrical, electron transfer pathways between P700 and Fx in PSI, one through the PsaA side of the core and one through the PsaB side. In the purple bacterial reaction centre, only one side of the photosystem has an active electron transfer pathway, although changes to some amino acids can 'activate'

the other branch (Hillier & Babcock 2001). PSI is analogous to the green bacterial reaction centre. It is not certain whether one or both of the two possible branches is active in PSI.

Initially, it was suggested that the PsaB side was the only active branch, as the electron spin density in $P700^{\bullet+}$ appears to be on the PsaB chlorophyll (Webber *et al* 1996). Some experimental evidence can be interpreted to support a model of uni-directional electron transfer through PSI (Biggins & Mathis 1988, Yang *et al* 1998, Xu *et al* 2003b). However, a number of observations suggesting bi-directionality have been made using a combination of site-directed mutagenesis strategies, optical spectroscopy and EPR measurements (Joliot & Joliot 1999, Guergova-Kuras *et al* 2001, Muhiuddin *et al* 2001, Rigby *et al* 2002). There were several reports of biphasic electron transfer to the iron-sulphur centre F_X, with two characteristic half-times of approximately 20 ns and 200 ns (Setif & Brettel 1993, Brettel 1997, Schlodder *et al* 1998). However, it was suggested that the electron transfer chain through PSI had been disrupted by the PSI preparation procedures employed in these studies and that this had affected the rates.

When oxidation of A_1^- and reduction of F_X was monitored spectrophotometrically in PSI from whole cells of *Chlorella sorokiniana*, a biphasic oxidation of A_1 was observed (Joliot & Joliot 1999). This result was found in whole cells and hence countered concerns about PSI sample preparation. The biphasic kinetics were also found in whole cells of *C. reinhardtii* (Guergova-Kuras *et al* 2001). Of the two phases, one showed a half-time of about 18 ns and the other of 160 ns. One of the explanations proposed was that the reaction centre uses the two branches but that they operate at different rates. During a study of site-directed *C. reinhardtii* mutants with altered tryptophan residues on the PsaA subunit, indirect evidence for electron transfer along the PsaA branch was found (Purton *et al* 2001).

Recent work demonstrated bi-directional electron transfer in PSI from *C. reinhardtii* (Fairclough *et al* 2003). Pulsed EPR measurements at 100 K were used to monitor the rate of decay of the signal arising from the $P700^{\bullet+}/A_1^{\bullet-}$ radical pair, which is believed to be influenced by both the PsaA and PsaB sides of PSI (Muhiuddin *et al* 2001).

Fairclough *et al* (2003) found evidence that electron transfer can occur via A_1 on either side of PSI and that the PsaB side, but not the PsaA side, was necessary for photoautotrophic growth. However, studies conducted by Xu *et al* (2003a and 2003b) using *Synechocystis* 6803 showed that electron transfer was predominantly via the PsaA branch in cyanobacteria. Further work is required to resolve this controversial issue.

1.4 Subunits of PSI

Table 1.1 summarises our current understanding of the function of each PSI subunit. The PsaA and PsaB subunits constitute the core of the photosystem, binding the reaction centre, other pigments and most of the electron transfer cofactors. These subunits are essential for photosynthetic function. The remaining subunits play various other roles. The function of some of the lower molecular weight polypeptides is undetermined but molecular genetic studies of mutants in several model organisms are increasing our knowledge of these subunits.

The majority of the accessory subunits (i.e. those other than PsaA, PsaB and PsaC) are dispensable for photosynthesis in cyanobacteria and often in eukaryotes. However, it is likely that at least some of these subunits have important roles to play, as they have been well conserved. In some cases, accessory subunits may have different roles in prokaryotes and eukaryotes (Scheller *et al* 1996). An overview of the subunits follows, with particular emphasis on PsaE and PsaL as these subunits were studied in more detail for this thesis.

1.4.1 Cofactor-binding subunits – PsaA, PsaB and PsaC

As stated previously, the PsaA and PsaB subunits form the membrane-spanning heterodimeric catalytic core of the reaction centre and bind the majority of the electron transfer cofactors. The proteins are highly conserved and contain several hydrophobic domains and numerous charged residues, the points at which they interact with the smaller subunits and the mobile electron carriers. The iron-sulphur centre Fx is liganded to the core at conserved cysteine residues.

PsaC is an acidic, hydrophilic protein of approximately 9 kDa. Conserved cysteine residues ligand to the iron-sulphur centres F_A and F_B. A lysine residue (K_{35}) has been identified as an essential point of interaction between PsaC and ferredoxin (Fischer *et al* 1998).

1.4.2 Reducing side subunits

The subunits PsaC, PsaD and PsaE form the stromal ridge, where the photosystem interacts with ferredoxin. Chemical cross-linking experiments and protease accessibility assays have shown that these subunits are exposed on the surface of the photosystem but that a large part of PsaC is buried beneath PsaD and PsaE (Xu *et al* 1994b).

PsaD is a conserved peripheral protein, with an N-terminal extension in the plant protein. It is implicated in the stable assembly of the other stromal ridge subunits and is thought to provide the docking site for ferredoxin and flavodoxin interaction. A mutant of *Synechocystis* 6803 lacking PsaD grew ten times more slowly than wild type cells and showed 40% of wild type levels of P700 activity (Chitnis *et al* 1989b). This is due to its inability to donate electrons to ferredoxin. PsaD is absent in etiolated leaves and is the first to reappear in greening chloroplasts, implicating it in the assembly process.

PsaE is also a well-conserved peripheral polypeptide. Studies to discover the function of this subunit have been ongoing for over a decade and a summary of this work is discussed in Section 1.4.6. It is thought to play a role in ferredoxin reduction and in cyclic electron transfer.

Although the PSI complexes from cyanobacteria and plants have an analogous stromal ridge, the model for ferredoxin binding differs between prokaryotes and eukaryotes (Ruffle *et al* 2000). In cyanobacteria, the ferredoxin is thought to bind on one side of the ridge, contacting PsaC, PsaE and mainly PsaD. In plants it is modelled to bind on the top of the ridge, contacting primarily PsaC and PsaE.

The alternative electron acceptor flavodoxin, a low molecular mass flavoprotein that is synthesised to substitute for ferredoxin under iron-limitation, has slightly different docking requirements than ferredoxin (Xu *et al* 1994c). The docking site still appears to consist of the stromal subunits and perhaps a few other low molecular weight subunits (Muhlenhoff *et al* 1996).

1.4.3 Oxidising side subunits

Plastocyanin interacts with PSI on the lumenal side of the thylakoid membrane. The PsaF subunit is thought to act as a site for this interaction. The eukaryotic form of the polypeptide has a larger lumenal portion, which is absent in cyanobacteria. When modified PsaF with the eukaryotic N-terminus was introduced into the cyanobacterium *Synechococcus elongatus*, the rate of reaction with plastocyanin was increased (Hippler *et al* 1999). This portion of the polypeptide is involved with plastocyanin binding and the fast kinetics seen in eukaryotes. *C. reinhardtii* cells lacking PsaF have reduced electron transfer from plastocyanin (Farah *et al* 1995). Plants lacking PsaF barely survive and are severely photoinhibited (Haldrup *et al* 2000). It would appear that PsaF is more important in eukaryotes. In cyanobacteria this subunit is dispensable, possibly because the N-terminal region is absent and the electrostatic attraction of the other subunits is sufficient to provide a binding site for plastocyanin, allowing its interaction with the PSI complex.

In addition, eukaryotic PSI includes the PsaN polypeptide. This 9 kDa polypeptide is located exclusively on the lumenal face of the complex. Its function is unknown as yet, although it has been found that *Arabidopsis* lacking PsaN has reduced $P700^+$ reduction by plastocyanin, suggesting that it may participate in the interaction with plastocyanin. Plants appear to compensate for this by increasing the amount of PSI present (Haldrup *et al* 1999). The PsaN polypeptide was recently found to be present in the PSI of *C. reinhardtii* (Ali 2004). PsaN has not been found in cyanobacteria.

1.4.4 Other accessory subunits

Subunits PsaG and PsaH are present only in eukaryotes. PsaG is involved in binding LHC1. PsaG shows some homology to PsaK. In transgenic *Arabidopsis* plants that lack PsaH, no state transitions could occur, possibly because the LHCI could not be correctly bound (Lunde *et al* 2000). PsaH is needed for stable PSI accumulation and efficient electron transfer (Naver *et al* 1999) and binds LHCII during state transitions. Plants compensate for a loss of PsaH by synthesising extra PSI.

The role of many of the remaining subunits is unknown. Some appear to be involved with the correct orientation of other subunits, for example PsaI is required for the correct assembly of PsaL (Xu *et al* 1995). PsaJ is a hydrophobic subunit of unknown function, although it is thought that PsaJ has some role in correctly orienting PsaF for efficient electron transfer from plastocyanin (Fischer *et al* 1999, Xu *et al* 1994d).

PsaM is very small (3 kDa) and is only found in cyanobacteria, although an open reading frame corresponding to the *psaM* gene is found in some eukaryotes such as liverwort but not others (Chitnis *et al* 1995). A *Synechocystis* 6803 PsaM-minus mutant showed a marked decrease (75% reduction from wild type) in trimeric PSI yield (Naithani *et al* 2000). This suggests that it may function to stabilise the trimerisation domain formed by PsaL subunits in cyanobacteria.

PsaK is an integral protein that is very tightly associated with the core but has unclear function. In *Arabidopsis* plants, PsaK has a role in organising the LHC1 and a lack of PsaK is compensated by increased synthesis of PSI (Jensen *et al* 2000). In cyanobacteria, PsaK is non-essential. Disruption of both the *psaK* genes in *Synechocystis* 6803 leads to only a very small reduction in the rate of electron transfer (Naithani *et al* 2000).

The PSI X-ray crystallography structure revealed the presence of a twelfth subunit, a single transmembrane helix with homology to a polypeptide found in thermophilic cyanobacteria (Jordan *et al*, 2001). This has been designated PsaX. There is currently no information on the function of this subunit.

1.4.5 PsaL

PsaL is an integral membrane protein approximately 16 kDa in size. It is present in both eukaryotic and prokaryotic photosynthesising organisms. It is less well conserved than other subunits except in some hydrophobic regions.

A lack of PsaL in the cyanobacterium *Synechocystis* sp. PCC 6803 does not affect the photosynthetic growth of the organism or assembly of PSI (Chitnis *et al* 1993). Wild type P700 kinetics are observed in PsaL-minus mutants, with PsaL having little or no effect on electron transfer. During preparation of PSI from such cells, only monomeric forms can be isolated. During early studies on this subunit, a role for PsaL in trimerisation of the complexes was therefore suggested. PsaL is resistant to proteolytic activity in trimeric but not monomeric photosystems and the subunit forms a structural component of the trimer-forming domain (Chitnis & Chitnis 1993). The purpose of trimerisation in cyanobacterial thylakoids is not understood. It is possible that trimerisation modulates light-harvesting efficiency. Trimerised PSI has not been found in plant thylakoid preparations.

There is a structural interaction between PsaL and PsaD, the absence of either polypeptide decreasing the level of association of the other into the complex, although the reduction in PsaD incorporation in the absence of PsaL is less marked (Xu *et al* 1994a). As a result of this, there is a reduced yield of trimers when PsaD is absent. PsaI has also been found to stabilise PsaL in the complex (Schluchter *et al* 1996).

A *Synechococcus* 7002 mutant lacking PsaL was found to perform state 2 to state 1 transitions three times faster than wild type (Schluchter *et al* 1996). Further work on this interesting result was performed (Aspinwall *et al* 2004b) for this thesis and is described in Chapter 5.

1.4.6 PsaE

This 8 kDa subunit is well conserved between species. Initial work on a *Synechocystis* 6803 mutant lacking PsaE led to reports that the absence of this subunit had only minor phenotypic effects (Chitnis *et al* 1989a). Subsequent studies have postulated various roles for PsaE, mostly suggesting some involvement with ferredoxin reduction or cyclic electron transport. However, the precise role of the subunit does not appear to have been determined. A brief overview of the work carried out so far follows.

FNR, the enzyme responsible for oxidising ferredoxin and reducing $NADP^+$ is thought to be bound by a PSI polypeptide. The stromal location of PsaE and a set of cross-linking experiments led to the suggestion that this was the FNR-binding site (Andersen *et al* 1992). This was later disproved when PSI was found to bind FNR after PsaE had been removed, although some sort of interaction between the proteins is not ruled out (Weber & Strotmann 1993).

In 1993, Rousseau *et al* used flash absorption spectroscopy to study photoreduction of ferredoxin in a *Synechocystis* 6803 PsaE-minus mutant and found that the rate of ferredoxin reduction was decreased from that of wild type by a factor of at least 25. A functional role for PsaE in the PSI-ferredoxin interaction was proposed, possibly a structural role in organising the photoreduction site. Studies by Sonoike *et al* (1993) found that although PsaD alone was sufficient to mediate the electron transfer to ferredoxin, PsaE may increase the efficiency of transfer. PsaE may alter the conformation of PsaD or PsaC to create an optimal binding site. PsaE could stabilise the acceptor side, orienting $F_{A/B}$ correctly and facilitating efficient transfer between redox centres (Weber & Strotmann 1993). However, there appears to be little change to the other subunits organisation when PsaE is lacking, suggesting a more direct interaction with ferredoxin (Xu *et al* 1994c). Flash absorption studies on *Synechocystis* 6803 mutants lacking PsaE or PsaD found that PsaD affects the association rate of ferredoxin and PSI (i.e. the binding) and PsaE affects the dissociation rate (i.e. controls the complex lifetime) (Barth *et al* 1998). PsaE is

needed for efficient binding to the alternative electron acceptor flavodoxin (Meimberg *et al* 1998).

A *Synechococcus* 7002 mutant lacking PsaE did not grow photoheterotrophically and only slowly under conditions favouring cyclic electron transfer (low light, low carbon dioxide level), leading to the suggestion that PsaE is involved in cyclic electron transfer around PSI (Yu *et al* 1993; Zhao *et al* 1993).

There are two copies of the gene encoding PsaE in *Arabidopsis*, *psaE1 and psaE2*. When plants with disrupted *psaE1* were studied, PsaE, PsaD and PsaC were all found to be absent and there was limited electron flow due to this disruption of the reducing side of PSI (Varotto *et al* 2000). The plants grew at 50% the normal rate and showed a marked increase in light sensitivity and photoinhibition. The presence of *psaE2* did not appear to compensate for the loss of *psaE1*. The effects of losing PsaE in plant PSI appear to be more drastic than when the subunit is absent in cyanobacterial mutants; additional roles for PsaE may have evolved in plants.

1.5 Cyanobacteria as model organisms

The cyanobacterial genera *Synechococcus* and *Synechocystis* (Figure 1.5) have been used by many researchers because of several clear advantages over working with plants. They offer a system for natural transformation, allowing DNA to be taken up into the cells where it undergoes homologous recombination with the chromosome (an advantage over the random nature of integration in plant and *C. reinhardtii* nuclear genomes). This is useful for generating gene disruptions or deletions. Some strains can be grown on glucose so that photosynthetic mutants can be grown even if a lethal mutation has been created in the photosynthetic system. The availability of the *Synechocystis* 6803 genome sequence (Kaneko *et al* 1996) simplifies the design and implementation of mutagenesis strategies. High-resolution structures of the photosystems are available (Fromme *et al* 2003, Iwata & Barber 2004).

Photosynthesis in cyanobacteria is essentially analogous to that of higher plants. Although there are some key differences from higher plants (the co-ordination of two

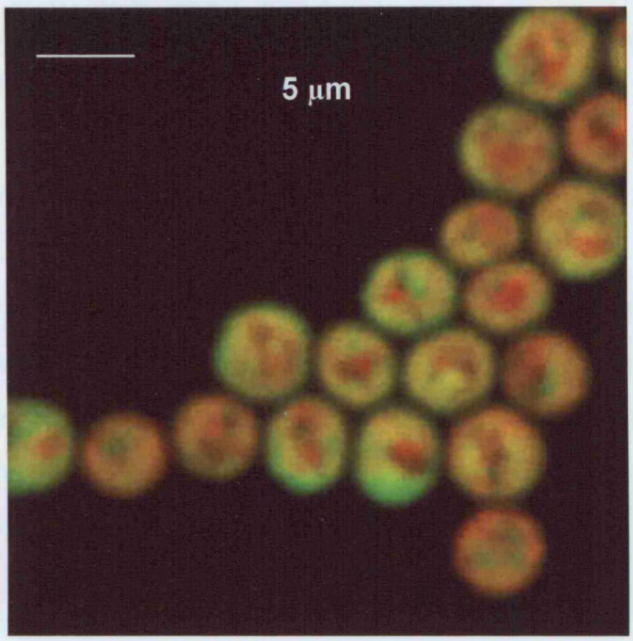

Figure 1.5 Confocal fluorescence micrograph of *Synechocystis* 6803 cells. Phycobilins are shown as red areas within the cell and chlorophyll *a* (in PSII) appears green. In most cells the green and red overlap; zones of one colour reflect variation in the concentration of PSII and phycobilisomes in the thylakoid membranes. Image provided by C. Mullineaux, University College London.

genomes does not apply in cyanobacteria, for example), information can in many cases be extrapolated to eukaryotic systems. There are also reasons to study cyanobacteria in their own right, as they are thought to be the origin of the chloroplast and possess features such as the phycobilisomes and PSI trimers that can only be studied in these species.

1.6 State transitions

Photosynthetic organisms are subject to changing light intensity and quality, which can have an impact on their photosynthetic function and, in turn, on their growth. It is possible for organisms to respond to such changes in the environmental conditions by altering the relative levels of biosynthesis of the photosynthetic apparatus. However, protein synthesis is relatively slow and is not a viable means of responding to conditions that may be changing rapidly and frequently.

Cyanobacteria, plants and algae have systems by which they can alter the distribution of energy between the PSI and PSII reaction centre populations without *de novo* protein synthesis. When light favoured by one of the photosystems is encountered, the light-harvesting apparatus is adjusted to favour the other photosystem, thus maintaining a balance. This type of regulation, termed the state transition, occurs on a short time scale (seconds-minutes), allowing rapid adaptation to changes in illumination. This is useful as it quickly optimises the performance of the photosystems.

1.6.1 State transitions in eukaryotes

In plants and green algae, the LHCII apparatus binds either to PSI or PSII complexes, depending on the light conditions. The process of changing between state 1 (in which LHCII are bound to PSII) and state 2 (LHCII bound to PSI) is controlled by an LHCII protein kinase in the thylakoid membrane (reviewed by Haldrup *et al* 2001). In plants the N-terminal region of the LHCII is stromally exposed and can be reversibly phosphorylated; a subsequent conformational change to the complex is thought to cause dissociation of the LHCII during state transitions (Allen 1992). Lunde *et al*

(2003) found that plants can compensate for defective state transitions by increasing the PSI:PSII ratio, and that this is adequate to counteract effects caused by an inability to rapidly adapt to changing light.

1.6.2 State transitions in cyanobacteria

1.6.2.1 Phycobilisomes

Cyanobacteria do not have LHCII but possess equivalent light-harvesting apparatus in the form of phycobilisomes. Phycobilisomes are large, soluble, highly ordered multi-subunit complexes consisting of phycobiliproteins and linker proteins (Bald *et al* 1996). They act as extrinsic antenna for the photosystem reaction centres.

Structurally, the phycobilisomes consist of a central core of 2-4 'cylinders' and a peripheral arrangement of 'rods'. A schematic diagram of a phycobilisome is shown in Figure 1.1, although they are, in reality, considerably larger in size relative to the photosystems. The core cylinders bind the phycobiliprotein allophycocyanin, with phycocyanin being bound by the peripheral rods. Allophycocyanin and phycocyanin are found in all phycobilisomes, although precise structure and composition varies between species and some may also contain phycoerythrin and phycoerythrocyanin (Bald *et al* 1996). The linker proteins do not bind chromophores but play a role in modulating the absorption of light. The structure of the phycobilisome facilitates transfer of the captured light from the rods to the core.

1.6.2.2 Phycobilisomes transfer energy to both PSII and PSI

The phycobiliproteins allow efficient transfer of energy to reaction centre cores. Phycobilisomes are hydrophilic and are anchored to the cytoplasmic surface of the thylakoid membrane. Being highly mobile, they can directly interact with both PSI and PSII by moving across the surface membrane (Mullineaux 1997, Sarcina *et al* 2001). Earlier it had been suggested that the phycobilisomes bound preferentially to PSII and that any energy transfer to PSI was the result of 'spillover' of excessive energy from PSII. It is now known that phycobilisome energy directly excites PSI as

well as PSII (Mullineaux 1992, Li *et al* 2003). In state 1 the phycobilisomes bind predominantly to PSII and in state 2 they bind mainly to PSI.

1.6.2.3 Mechanism of state transitions

The mechanism causing state transitions in cyanobacteria is not fully understood. The *rpaC* gene, which is thought to be involved with regulating light-harvesting and mediation of state transitions, was identified by Emlyn-Jones *et al* (1999). A lack of the putative membrane protein RpaC leads to an inability to carry out state transitions, although its precise role is not known. Similarly to the mechanism in eukaryotes, the state transition in cyanobacteria is thought to be associated with the redox state of the plastoquinone pool or cytochrome b_6f complex (Mullineaux & Allen 1990).

Despite the comparatively different structural organisation of thylakoid membranes in eukaryotic and prokaryotic organisms, the dynamic movement of light-harvesting machinery in order to optimise photosynthetic performance is a common feature. Studies have demonstrated that PSII is immobile in the thylakoid membrane, while the phycobilisomes move rapidly (Mullineaux *et al* 1997, Sarcina *et al* 2001). One can envisage a situation in which the phycobilisomes couple to PSII reaction centres transiently, then uncouple and move to PSI upon receiving a state transition signal, and vice versa.

1.6.2.4 Oligomerisation of PSI is not required for interaction with phycobilisomes

It has been suggested that trimerisation of PSI is a requirement for the successful docking of phycobilisomes to PSI and consequent efficient transfer of energy to the reaction centre (Kruip *et al* 1994, Bald *et al* 1996). Schluchter *et al* (1996) demonstrated that state transitions did, in fact, occur more rapidly in a cyanobacterial mutant with an entirely monomeric PSI population. Work presented in this thesis confirmed this using a different cyanobacterial species and, furthermore, demonstrates that monomerisation of PSI has intriguing effects on both the rate of movement of phycobilisomes and on the speed at which state transitions can be achieved

(Aspinwall *et al* 2004b). This is interesting because the limiting factor on the rate of phycobilisome diffusion has been postulated to be either the transient binding to reaction centres and/or steric hindrance (Mullineaux 1997). Previous studies have shown that the mobility of phycobilisomes is affected by factors such as phycobilisome size and membrane lipid composition (Sarcina *et al* 2001). We can now add PSI oligomerisation (and perhaps associated changes to membrane organisation) to this list.

1.7 Effects of iron deprivation on photosynthesis

1.7.1 Growth and productivity in aquatic habitats is hindered by iron deficiency

Iron is essential for many of the redox reactions of the electron transfer chain in photosynthetic organisms as well as many cellular processes such as respiration. The concentration of iron in aquatic habitats, such as the open ocean where cyanobacteria and prochlorophytes are ubiquitous, is low, due to the low solubility of Fe^{3+}. The concentration of biologically available iron is often sufficiently low to limit the photosynthetic output and growth of cyanobacteria (Behrenfeld *et al* 1996). Primary productivity is therefore dependent on the ability of these organisms to adapt to iron deprivation. As the ocean-living prokaryotes have a significant impact on the nutrient cycling and atmospheric composition, this area of research is of particular importance.

1.7.2 A lack of iron limits synthesis of components of the photosynthetic apparatus

The level of phycobilisomes present in the cell is rapidly reduced under iron limitation (Guikema & Sherman 1983), leading to a marked reduction in the light-harvesting capacity of the photosystems. Sandström *et* al (2002) found that the decreasing level of phycobilisomes was due to a decreased rate of synthesis rather than an increased rate of degradation. This seems reasonable as the phycobilisomes themselves do not contain iron, but it is required as part of the biosynthetic pathway

of phycobiliproteins. Levels of PSI, the most iron-rich photosynthetic structure, are also decreased, severely hindering photosynthetic function (Ivanov *et al* 2000).

1.7.3 Cyanobacterial responses to iron deficiency

Cyanobacteria encountering an environment with low iron content possess a number of adaptations that can be activated to ensure their survival (reviewed by Ferreira & Straus 1994).

In a severely iron-deficient environment, some cyanobacteria may produce siderophores in order to scavenge iron by binding to and solubilising it before it is actively transported into the cell (Straus 1994). Iron transport systems may be optimised and physiological activities reduced. The synthesis of proteins containing iron (e.g. PSI) will be reduced or halted.

1.7.3.1 The *isiAB* genes

Cyanobacteria in iron-limited conditions express the genes *isiA* and *isiB* (*i*ron *s*tress *i*nduced genes), which are part of the same operon. The operon is up-regulated in conditions of iron stress, salt stress and heat shock (Vinnemeier *et al* 1998). The *isiB* gene encodes flavodoxin, an alternative electron acceptor for PSI. PSI shows a strong preference for ferredoxin over flavodoxin and will reduce ferredoxin first if possible (Meimberg & Mühlenhoff 1999). Flavodoxin can, however, replace the iron-containing ferredoxin as an electron acceptor for PSI if necessary (Hutber *et al* 1977). The protein product IsiA, a chlorophyll *a*-binding protein, is also known as CP43' because it shares significant homology with the CP43 protein of PSII (Burnap *et al* 1993, Falk *et al* 1995). The function of CP43' is discussed below.

1.7.3.2 IdiA

The *idiA* (*i*ron *d*eficiency *i*nduced) gene is up-regulated under iron stress and oxidative stress conditions. The IdiA protein is thought to protect the acceptor side of PSII against oxidative stress under conditions of iron stress, although the mechanism

by which this is achieved is unknown. (Michel & Pistorius 2004). IdiA may have a role in the iron-scavenging systems of open ocean cyanobacteria and can act as a marker of iron stress in such species (Webb *et al* 2001).

1.7.3.3 Ferric uptake regulation

Iron-regulated genes in bacteria are under the control of the *fur* gene (*f*erric *u*ptake *r*egulation). The Fur protein is a DNA-binding repressor protein, which represses iron stress-induced genes when sufficient Fe^{2+} is present. Attempts to delete the *fur* gene in *Synechococcus* 7942 were unsuccessful, indicating that Fur has an essential role in the regulation of genes responding to iron deprivation (Ghassemian & Straus 1996).

1.7.3.4 Maintaining viability

Cyanobacteria respond to iron stress with numerous compensatory processes, continuing to grow and photosynthesise as they adapt. If iron starvation is maintained beyond their capacity for acclimation, cells remain viable even if they cease growth. They can re-commence growth once iron becomes available (Sandström *et al* 2002).

1.7.4 The CP43' protein

The precise role for the CP43' protein (encoded by the *isiA* gene) in conditions of iron deficiency has been debated for several decades in the literature and a brief summary follows. It is now known that oxidative stress, rather than iron stress specifically, induces *isiAB* induction (Jeanjean *et al* 2003).

1.7.4.1 Storage of chlorophyll molecules

CP43' is produced in large amounts under iron stress and can be found in uncoupled chlorophyll *a*-protein complexes within the cell. This prompted the proposal that CP43' could act as a storage depot for chlorophyll molecules, binding and holding them in reserve until iron became available again. It was thought that this chlorophyll store would then be utilised for rapid synthesis of new PSI and PSII complexes, which

would aid recovery of the cell's photosynthetic ability following the stress conditions (Riethman & Sherman 1988). However, Park *et al* (1999) countered this by suggesting that storing chlorophyll in this way would in fact be easily be destroyed by the light that would inevitably be absorbed. Binding free chlorophyll is, however, very important to prevent random excitation resulting in the production of dangerous radicals (Yeremenko *et al* 2004).

1.7.4.2 Functional replacement of CP43

Early on, Pakrasi *et al* (1985)thought that CP43' could act as a light-harvesting element, believing that this would primarily be harnessed by PSII. It was later suggested that the CP43' proteins could work as functional replacements for the CP43 of PSII (Burnap *et al* 1993). However, mutants lacking the *isiA* gene showed no difference in functional absorption of light by PSII either under iron replete or iron deficient conditions, indicating that CP43' is not part of the functional light-harvesting antenna of PSII (Falk *et al* 1995). Additionally, the CP43 protein of PSII is highly conserved, whereas the CP43' protein, although highly homologous to CP43, lacks a large hydrophilic loop and is, as a result, a smaller protein. CP43 and CP43' are conserved in terms of the number of transmembrane helices (six) and the number of conserved histidine residues and they are likely to bind the same number of chlorophyll molecules (Bibby *et al* 2001b).

1.7.4.3 Protection from photoinhibition

Park and co-workers postulated that CP43' could protect PSII from photodamage by dissipating excess excitation energy (Park *et al* 1999). Recently it has been discovered that CP43' does, in fact, form a light-harvesting antenna ring around PSI trimers in cyanobacteria experiencing iron stress (Bibby *et al* 2001a, Boekema *et al* 2001a). As a large amount of free CP43' protein is also present in stressed cells, it has been proposed that there could be several roles for this protein. Sandström *et al* (2002) suggest that CP43' could form the PSI antenna ring and also function as a quencher to protect photosystems from excess light, as proposed in the earlier paper (Park *et al* 1999).

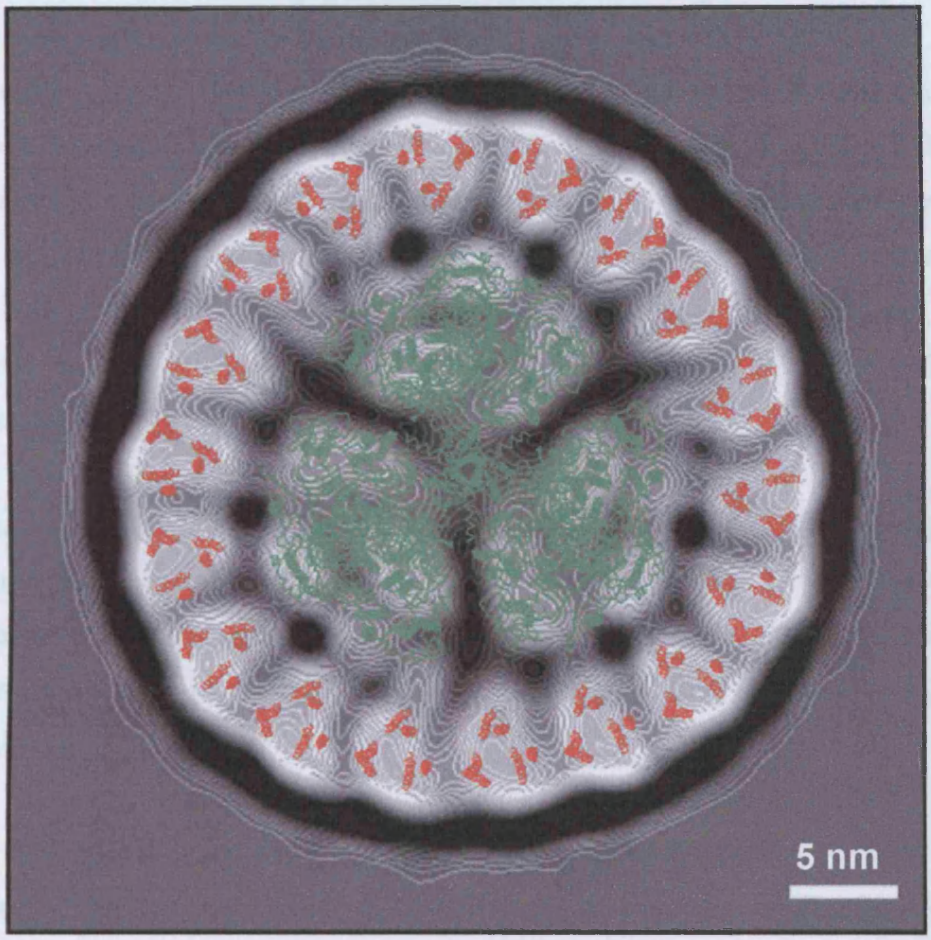

Figure 1.6 Structural of a PSI trimer (green) associated with a ring of 18 CP43' proteins (red) in a supercomplex. The electron micrograph of the supercomplex is overlaid with structural information provided by X-ray crystallography data. Reproduced from Bibby *et al* (2001a).

1.7.5 Iron stress-induced PSI-CP43' supercomplexes

1.7.5.1 CP43' antenna ring dramatically increases PSI light-harvesting capacity

In recent years an iron stress-induced supercomplex consisting of a PSI trimer and CP43' molecules was described (Bibby *et al* 2001a, Boekema *et al* 2001a). Electron microscopy showed that the supercomplex consists of 18 subunits of CP43' arranged in a ring around the PSI trimer. The structure of this supercomplex is shown in Figure 1.6. In response to iron stress, the cyanobacteria induce this additional antenna system to salvage the light-harvesting of PSI at a time when levels of PSI and phycobilisomes are decreasing.

It is probable that each CP43' subunit can bind 12 chlorophyll *a* molecules, by comparison with CP43 of PSII (Zouni *et al* 2001). The 18-mer ring structure may potentially bind 200 chlorophyll *a* molecules and has the capacity to increase the light-harvesting capacity of PSI by 60 - 70% (Bibby *et al* 2001a, Boekema *et al* 2001a).

The chlorophyll molecules of the CP43' ring and the PSI trimer are in sufficiently close proximity to facilitate energy transfer to the reaction centre. The ring appears to act as a rapid and efficient antenna for PSI (Andrizhiyevskaya *et al* 2002). The closest points between antenna and PSI appeared to be near the PsaJ subunit (Bibby *et al* 2001b). Subsequent work using electron cryomicroscopy produced a three-dimensional structural model of the supercomplex, which showed that clusters of chlorophyll molecules associated with the PsaA, PsaB, PsaK and PsaJ subunits of PSI were likely candidates to receive energy from the antenna ring (Nield *et al* 2003). However, a cyanobacterial mutant lacking the PsaJ and PsaF subunits of PSI was found to produce a CP43' antenna ring under iron stress, although it contained only 17 CP43' subunits (Kouřil *et al* 2003).

The discovery of the CP43' antenna ring demonstrates the flexibility of the cyanobacterial light-harvesting systems. The finding of the 17-mer ring in the PsaFJ-

minus mutant provides further evidence of flexibility as each monomer of the PSI trimer must form a different interaction with the antenna ring (Kouřil *et al* 2003).

It is likely that the antenna ring is of great importance in iron stress conditions, as a compensatory mechanism when the levels of iron-rich PSI and also the light-harvesting phycobilisomes decrease. It may also provide a means of increasing the efficiency of PSI at light-limiting intensities, commonly encountered in natural habitats (Bibby *et al* 2001b).

1.7.5.2 Similarity to light-harvesting rings of other organisms

Prochlorophytes, oxygenic prokaryotes that possess chlorophyll *a* and *b*, contain *pcb* genes that encode chlorophyll-binding proteins similar to the CP43' protein. Rings of Pcb proteins that closely resemble the 18-mer CP43' ring of cyanobacteria have been discovered around PSI trimers in prochlorophytes (Bibby *et al* 2001c). As these organisms grow at considerable depth in the ocean, it is likely that the Pcb antenna rings are essential for light-harvesting and increasing reaction centre efficiency. Genes resembling *isiA* and *pcb* genes were found to be expressed in iron-starved *Fischerella*, suggesting that CP43'-like function may be present in heterocystous cyanobacterial strains, despite differences in their genetic arrangement (Geiβ *et al* 2001). Recently, a mutant of *Synechocystis* 6803 that has been engineered to produce chlorophyll *b* (by introduction of the *cao* gene) was subjected to low iron levels; it was found that chlorophyll *b* can also bind to CP43' proteins (Duncan *et al* 2003). This provides additional evidence of the similarity between the Pcb and CP43' proteins.

1.7.5.3 Functional significance of PSI trimerisation

It was proposed that, because the stress-induced antenna rings of both cyanobacteria and prochlorophytes were found to exist around PSI trimers, that the trimeric structure itself was a requirement for the formation of the ring and that this may explain the functional significance of PSI trimerisation in prokaryotes (Bibby *et al* 2001b, 2001c). Work undertaken for this thesis focused on discovering whether this did provide a

satisfactory reason for PSI trimerisation: studies presented here revealed that the CP43' can functionally attach to PSI monomers (Aspinwall *et al* 2004a), which raises interesting questions about the exact nature of the interaction between the antenna ring proteins and the photosystems, as well as leaving open the question regarding the significance of PSI trimerisation.

1.8 Studies included in this work

The main aim of this thesis was to explore the roles played by some of the accessory subunits of PSI. In order to achieve this, a set of cyanobacterial mutants lacking the PsaL and PsaE subunits were constructed (Chapter 3). These mutants were then characterised (Chapter 4). The purpose of PSI trimerisation in cyanobacteria was of particular interest and this was further investigated, using the PsaL-minus mutants, in Chapter 5 in terms of state transitions and phycobilisome interactions and in Chapter 6 in terms of interaction with the iron stress-induced CP43' protein. An EPR analysis of the mutants was used to investigate electron transfer through the altered PSI reaction centres and this is presented in Chapter 7.

CHAPTER TWO

MATERIALS AND METHODS

CHAPTER TWO

MATERIALS AND METHODS

2.1 Bacterial strains, media and growth conditions

2.1.1 Cyanobacterial strains

A glucose-tolerant wild type strain of *Synechocystis* sp. PCC 6803 and wild type *Synechococcus* sp. PCC 7942 from the Pasteur Culture Collection of Cyanobacteria (PCC) were used. Mutants of *Synechocystis* 6803 deficient in PSII, the chlorophyll biosynthesis pathway, PSI subunit PsaL and PSI subunit PsaE, as well as double mutants with combinations of these mutations were also used. A *Synechococcus* 7942 mutant lacking PsaL was constructed for use in FRAP analysis. All cyanobacterial strains used are listed in Table 2.1.

2.1.2 *Escherichia coli* strains

Cloning of DNA was carried out using *E. coli* DH5α cells (Sambrook & Russell 2001).

2.1.3 Growth media and conditions

Cyanobacteria were grown in BG11 medium (Castenholz 1998) supplemented with 0.2 mM Na_2CO_3, 12 mM sodium thiosulphate and 10 mM TES buffer at pH 8.2. Solid BG11 plates were made by adding 1.5% agar (Difco, Maryland, USA). When required, glucose was added at 5 mM. Antibiotics were added to mutant cultures when needed at concentrations described in Table 2.2.

Liquid cultures were grown in liquid culture at 30 °C with orbital shaking at 100 rpm and standard light intensity of approximately 10 $\mu mol.m^{-2}.s^{-1}$. For blue light experiments, a blue filter (Just Blue 079, Lee Filters) and a light intensity of 4

$\mu mol.m^{-2}.s^{-1}$ was used. For state transitions measurements, light intensity of approximately 4 $\mu mol.m^{-2}.s^{-1}$ was achieved by placing filter paper cones over cultures.

Stocks of all cyanobacterial cultures were maintained in liquid culture, on agar plates and as frozen stocks by freezing a dense liquid culture in liquid nitrogen after the addition of 20% (v/v) glycerol.

E. coli cells were grown in Luria Bertani (LB) medium (Sambrook & Russell 2001), supplemented with antibiotics as required. *E. coli* cultures were grown in liquid LB or on LB agar plates at 37 °C and strains were maintained on LB agar plates at 4 °C.

2.2 Molecular biology techniques

2.2.1 Reagents and enzymes

Standard buffers were prepared as described in Sambrook & Russell (2001). Chemicals used were analytical grade reagents purchased from BDH Chemicals (Poole, Dorset, UK) or Sigma Chemicals (St Louis, Missouri, USA) unless otherwise stated. Restriction enzymes and other enzymes used for molecular biology techniques were purchased from New England Biolabs (Beverly, Massachusetts, USA).

Most buffers, solutions and plastic ware used for molecular biology were sterilised by autoclaving at 121 °C for at least 15 minutes. Heat sensitive solutions were sterilised by filtering through a syringe-driven filter unit with a pore size of either 0.45 or 0.22 μm (Millipore, Bedford, USA).

2.2.2 Plasmids

Plasmids used were pBluescript SK+ (Stratagene, La Jolla, California, USA) and pUC4K (Amersham Pharmacia Biotech, New Jersey, USA).

Table 2.1 Strains of cyanobacteria used

Strain	Description	Source	Growth*
Synechocystis 6803 (GT)	Glucose-tolerant wild type	W. Vermaas, Arizona State University	BG11 (with or without 5 mM glucose)
Synechocystis 6803 *psbD$_1$CD$_2$-*	Deficiency in photosystem II	W. Vermaas, Arizona State University (Vermaas *et al* 1990)	BG11 + 5 mM glucose + 25 μM chloramphenicol
Synechocystis 6803 *chlL-*	Deficient in chl biosynthesis pathway	W. Vermaas, Arizona State University (Wu & Vermaas 1995)	BG11 + 50 μM erythromycin
Synechocystis 6803 *psaL-*	Lacks PsaL subunit of PSI	This thesis	BG11 + 50 μM kanamycin
Synechocystis 6803 *psaE-*	Lacks PsaE subunit of PSI	P.R. Chitnis, Iowa State University (Chitnis *et al* 1989a)	BG11 + 50 μM kanamycin
Synechocystis 6803 *chlL- psaL-*	Deficient chl biosynthesis pathway and lacks PsaL subunit of PSI	This thesis	BG11 + 50 μM erythromycin + 50 μM kanamycin
Synechocystis 6803 *chlL- psaE-*	Deficient chl biosynthesis pathway and lacks PsaE subunit of PSI	This thesis	BG11 + 50 μM erythromycin + 50 μM kanamycin
Synechocystis 6803 *psbD$_1$CD$_2$- psaL-*	Deficient in PSII and lacks PsaL subunit of PSI	This thesis	BG11 + 5 mM glucose + 25 μM chloramphenicol + 50 μM kanamycin
Synechocystis 6803 *psbD$_1$CD$_2$- psaE-*	Deficient in PSII and lacks PsaE subunit of PSI	This thesis	BG11 + 5 mM glucose + 25 μM chloramphenicol + 50 μM kanamycin
Synechococcus 7942	Wild type	PCC#	BG11
Synechococcus 7942 *psaL-*	Lacks PsaL subunit of PSI	This thesis	BG11 + 50 μM kanamycin

* For details of growth media see section 2.1.3 # Pasteur Culture Collection

Table 2.2 Antibiotics used to supplement BG11 or LB media

Antibiotic	Source	Concentration
Ampicillin	Sigma, St Louis, Missouri, USA	50 $\mu g.ml^{-1}$
Chloramphenicol	Sigma, St Louis, Missouri, USA	25 $\mu g.ml^{-1}$
Erythromycin	Sigma, St Louis, Missouri, USA	50 $\mu g.ml^{-1}$
Kanamycin	Merck, Darmstadt, Germany	50 $\mu g.ml^{-1}$

2.2.3 Preparation of nucleic acids

2.2.3.1 Extraction of genomic DNA from cyanobacterial cells

Approximately 50 ml of dense cell culture was harvested and resuspended in 400 µl of sterile TSE buffer (5 mM Tris pH 8.5, 50 mM NaCl, 5 mM Na-EDTA). Lysozyme was added to a concentration of 10 $mg.ml^{-1}$ and samples were incubated at 37 °C for 15 minutes with occasional shaking to allow cell wall digestion. Samples were then applied to the Qiagen DNeasy plant mini kit (Qiagen GmbH, Germany) according to the manufacturer's protocol, which causes lysis of the cells followed by extraction and washing of the genomic DNA. DNA was eluted in 10 mM Tris buffer pH 8.0. DNA samples were visualised on 1.2% agarose gels as described in section 2.2.7 and stored at –20 °C until needed.

2.2.3.2 Plasmid DNA from *E. coli*

E. coli strains containing the required plasmid were grown overnight in 10 ml LB medium then harvested by centrifugation. The QIAprep spin miniprep kit (Qiagen GmbH, Germany) was used to extract the plasmid DNA, which was eluted in 10 mM Tris buffer pH 8.0 and stored at –20 °C.

2.2.4 Enzyme reactions

Enzyme reactions were generally carried out using supplied buffers and according to the manufacturers instructions (New England Biolabs, Beverly, Massachusetts, USA).

2.2.4.1 Restriction enzyme digestion

DNA to be cut with a restriction enzyme was suspended in an appropriate buffer supplied by the manufacturer. Usually 1 µl of the enzyme supplied was added to a 30-40 µl reaction volume and incubated at 37 °C for 4 hr. Complete digestion was confirmed by running a small sample on an agarose gel. Incompletely digested reactions were incubated longer.

When two enzymes were used to cut a piece of DNA, a double digest was performed if a suitable common buffer was available. Otherwise the reactions were performed sequentially. From a mixed population of products, the desired fragment was identified from its size on an agarose gel, excised from the gel and purified using the QIAquick gel extraction kit (Qiagen GmbH, Germany).

2.2.4.2 DNA ligation

DNA ligation was performed using T4 DNA ligase (Stratagene, La Jolla, California, USA) in the supplied buffer and in the presence of ATP (also supplied). For sticky ligations a 1:4 ratio of vector to insert was used. Ligase enzyme was added to 1/20 of the reaction volume. Reactions were incubated at 16 °C overnight. For blunt ligation, 1:4 and 1:1 vector to insert ratios were used and 1/10 reaction volume of ligase was added. Reactions were incubated at room temperature for 48-72 hr.

Where appropriate, a negative control, consisting of plasmid with incompatible sticky ends and no insert DNA, was included to confirm that the vector would not re-ligate. A positive control of vector with compatible sticky ends or blunt ends was always included to confirm ligase activity.

When a DNA insert was to be blunt cloned into a vector, the vector was first treated with calf intestinal alkaline phosphatase for 1 hr at 37 °C to prevent the blunt vector ends from re-ligating without insert.

2.2.4.3 Creating blunt ended DNA fragments using mung bean nuclease

DNA fragments and vectors with unsuitable single-strand extensions were blunted using mung bean nuclease (New England Biolabs). DNA at 0.1 $\mu g.ml^{-1}$ was prepared in the buffer supplied with the enzyme. One unit of enzyme was added per µg DNA and the reaction incubated at 30 °C for 30 min. The enzyme was then inactivated by addition of SDS to a concentration of 0.01%. The blunted DNA was recovered by passing through a QIAquick PCR purification kit (Qiagen GmbH, Germany).

2.2.5 Polymerase chain reaction

Particular genes were amplified from genomic DNA using PCR. The PCR was carried out using the Expand High Fidelity PCR System kit (Boehringer Mannheim, Germany). Each PCR reaction of 50 µl total volume contained: 1x buffer containing 1.5 mM $MgCl_2$ (supplied with kit), 200 µM dNTPs, 1.2 µM forward primer, 1.2 µM reverse primer, up to 1 µg template DNA (such as genomic DNA extract), 0.8 µl (equivalent to 2.6 units) enzyme (from kit) and sterile distilled H_2O to the final volume. A negative control tube was included containing water in place of template DNA.

PCR reaction tubes were placed into an automated thermocycler. Typical cycles were: an initial 2 minute denaturation of the DNA template at 94 °C followed by 25 cycles of 30 s at 94 °C, 30 s at 45 °C, 60 s at 72 °C and a final elongation at 72 °C for 7 minutes. The exact cycles used were optimised for each pair of primers (for primer sequences see Chapter 3).

The products of PCR reactions were resolved by agarose gel electrophoresis as described in section 2.2.7. If necessary, a particular band was selected and purified using the QIAquick gel extraction kit (Qiagen GmbH, Germany). If the reaction yielded a single product it was purified using the QIAquick PCR purification kit (Qiagen GmbH, Germany). DNA samples were then stored at –20 °C.

2.2.6 DNA sequencing

DNA sequencing was performed by Laura W. Wood (University College London) using automated cycle sequencing (Perkin-Elmer ABI Prism 377 DNA sequencer).

2.2.7 Agarose gel electrophoresis

To visualise and separate DNA fragments according to their size, agarose gel electrophoresis was performed. Agarose was dissolved in TAE buffer (40 mM Tris-acetate, 1 mM EDTA pH 8.0) by heating. The percentage of agarose used depended

on the approximate size of DNA to be resolved but typically a 1% agarose gel was used. To allow visualisation of the DNA under UV light, ethidium bromide was added to the gel at a concentration of 0.5 $\mu g.ml^{-1}$ before setting.

DNA samples were prepared by adding 6x DNA loading buffer (0.25% bromophenol blue, 15% Ficoll type 400-DL) at a suitable ratio. A sample of DNA size markers (1 kb ladder, New England Biolabs) was also prepared in loading buffer. This ladder gave reference bands with sizes: 10.0, 8.0, 6.0, 5.0, 4.0, 3.0, 2.0, 1.5, 1.0 and 0.5 kb. Gels were run in tanks of TAE buffer at 50–100 volts until the dye front had advanced sufficiently. DNA bands were observed by UV illumination (UV transilluminator, UVP) and photographed (DOC-IT gel documentation system, UVP, with Video graphic printer, Sony).

To separate a particular fragment of DNA from a mixed population, the fragments were resolved by gel electrophoresis and the desired band excised from the gel and purified using the QIAquick gel extraction kit (Qiagen GmbH, Germany).

2.2.8 Preparation of competent *Escherichia coli* DH5α cells

A single colony of *E. coli* DH5α cells was inoculated into 10 ml LB liquid medium and incubated overnight at 37 °C with vigorous shaking until stationary phase was reached. A dilution of 1 ml of culture into 10 ml fresh LB was incubated for a further 3 hours. Cells were pelleted by centrifugation at 4 °C, resuspended in 10 ml ice cold 100 mM $MgCl_2$ and cooled on ice for 5 minutes. Cells were pelleted as before and resuspended in 1 ml ice cold 100 mM $CaCl_2$. Competent cells were stored at 4 °C overnight before use in transformation reactions.

2.2.9 Transformation of competent *Escherichia coli* DH5α cells

Aliquots of 100 µl of competent DH5α cells (prepared as described in section 2.2.8) were added to 5 µl of ligation reaction or control DNA on ice. After chilling on ice for 30 minutes, cells were heat shocked by transfer to 42 °C for one minute, followed by cooling on ice for a further 10 minutes. Each transformation reaction was added to

1ml of LB liquid medium pre-warmed to 37 °C and incubated with shaking at 37 °C for 1-2 hours. Samples of 100 µl of each reaction, as well as 10x concentrated samples (obtained by microfuging and resuspending cells in LB), were plated out onto LB agar with appropriate antibiotic selection. Usually a positive transformation control, such as a routine re-transformation of pBluescript, was included to check for cell competency, as well as a sample of untransformed competent cells to confirm cell viability.

2.2.10 Transformation of cyanobacterial cells

A cell culture was grown in BG11 medium at 30 °C until the optical density at 750 nm (OD_{750}) had reached 0.5. The culture was then diluted with 1 volume of fresh medium and grown overnight. Cell density was estimated as described in section 2.3.3. A small sample of culture (1-2 ml) was harvested by microfuging at maximum speed for 15 minutes. Cells were resuspended to adjust concentration to 4 x 10^8 cells per ml. Aliquots of 100 µl of cells were used for each transformation. The DNA to be transformed was added in 10 µl TE buffer. Transformed cells were incubated at 30 °C for four hours and then spread onto BG11 agar plates. Cells were allowed to recover for 3-4 days before antibiotic selection was applied. This was done by overlaying the transformation plate with 2ml of cooled 0.6 % agar containing sufficient antibiotic to give the required concentration after allowing for diffusion throughout the plate. Surviving colonies were subsequently streaked onto selection agar containing the antibiotic.

2.3 Biochemical techniques

2.3.1 Growth rate measurement

Flasks containing 100 or 200 ml cells were inoculated from an exponentially growing starter culture to give an OD_{750} of approximately 0.1, determined using Unicam UV/Vis Spectrometer (Thermo Electron Corporation, Cambridge, UK). Each culture was set up in triplicate and the results for the set were averaged. Flasks were

incubated and 1 ml samples taken at regular intervals for A_{750} measurement. The A_{750} was plotted against time to give a growth curve.

SigmaPlot 5.0 software (Jandel Scientific) was used to produce a semilog plot of the data in order to identify the exponential part of the growth curve. The software was then used to fit an exponential growth rise against each growth curve according to the equation:

$y=A.\exp^{kx}$,

where y is A_{750}, x is time in hr, A is the initial A_{750} and k is the growth rate.

The value of k was used to give an estimate of the doubling time for the culture using the equation:

$dt = \ln 2/k$, where dt is doubling time in hr.

2.3.2 Estimation of chlorophyll *a* concentration

2.3.2.1 Chlorophyll *a* in whole cells

In order to estimate the chlorophyll concentration of whole cells, a 1 ml sample was microfuged for 15 minutes at maximum speed and the supernatant discarded. The cell pellet was resuspended in 1 ml of methanol and centrifuged again. The A_{666} and A_{750} of the supernatant were measured using a Unicam UV/Vis Spectrometer (Thermo Electron Corporation, Cambridge, UK) against a reference cuvette of methanol. The chlorophyll concentration was calculated using the equations below (which were adapted from Porra *et al* 1989, by setting the chlorophyll *b* concentration to zero):

$(OD_{666} - OD_{750}) \times 12.6 = [\text{chl}]$ in $\mu g.ml^{-1}$

or $(OD_{666} - OD_{750}) \times 14.0 = [\text{chl}]$ in μM.

2.3.2.2 Chlorophyll *a* in thylakoid membranes

To estimate the chlorophyll concentration of thylakoid membranes, a 1/200 or 1/100 dilution of membranes in methanol was prepared. The concentration was then measured as for whole cell methanol extracts (section 2.3.2.1).

2.3.3 Estimation of cell density

2.3.3.1 Use of absorbance to measure cell scattering

To estimate cell density, the OD_{750} of a 1 ml sample of cells or a suitable dilution was measured. For the Unicam UV/Vis spectrophotometer, the cell density can be estimated as follows:

$$OD_{750} \times 1.52 \times 10^8 = \text{cells per ml.}$$

The spectrophotometric estimation had previously been calibrated for this spectrophotometer using a haemocytometer cell counting method.

2.3.3.2 Cell counting

Cell density was estimated by counting cells in a haemocytometer. A drop of cells was applied to the haemocytometer slide and an optically flat coverslip placed on top. The number of cells within the haemocytometer grid was counted under a light microscope at 40x magnification. The number of cells in the grid x 10^4 gave an estimate of the number of cells per ml.

2.3.4 Preparation of thylakoid membranes from cyanobacterial cells

A large culture (2-16 l) of dense cells was harvested by centrifugation at 10,000 *g* for 10 minutes at 4 °C. When very large volumes were to be used, a cell harvester (with Pellicon 0.45 μm membrane cassette; Millipore, USA) was first used to concentrate the cells. Cells were resuspended in a small volume of French press buffer (25% v/v glycerol, 10 mM $MgCl_2$, 50 mM HEPES pH 7.5). Cells were broken by passing twice

through a French pressure cell (Aminco) at 15,000 psi or twice through a One-shot cell disrupter (Constant Systems Ltd, UK) at 13,500 psi. Samples were centrifuged for 10 minutes at 9000 *g* at 4 °C. The pellet of cell debris was discarded and the supernatant centrifuged for 1 hour at 160,000 *g* at 4 °C. The supernatant of phycobilisomes and cytoplasm was discarded. The pellet of thylakoid membranes was resuspended in French press buffer to wash and centrifuged for a further hour. Membranes were then resuspended either in EPR buffer (20 mM Tris pH 8.0, 0.1 M NaCl) (for samples to be used for EPR) or French press buffer (for samples to be used for photosystem isolation) and frozen in liquid nitrogen for storage.

2.3.5 Isolation of photosystems from thylakoid membranes

Thylakoid membranes were diluted to 1 $mg.ml^{-1}$ chl in solubilisation buffer (20 mM Tricine-NaOH pH8.0, 10 mM $CaCl_2$, 10 mM $MgCl_2$). Membrane samples were stirred at 4 °C in the dark as β-dodecylmaltoside was added to 2% w/v. After 30 minutes stirring, the solubilised membrane samples were loaded onto continuous sucrose density gradients in ultracentrifuge tubes. The gradients were prepared from sucrose dissolved in gradient buffer (0.5M mannitol, 20 mM Tricine-NaOH pH8.0, 10 mM $CaCl_2$, 10 mM $MgCl_2$, 0.04% w/v β-dodecylmaltoside) at 10% and 50% sucrose w/v. The two sucrose concentrations were continuously blended with a gradient mixer to produce a gradient from 50% at the tube base to 10% at the top. After loading, gradients were centrifuged at 150,000 *g* for 16 hours at 4 °C.

Bands separated by these gradients were recovered by inserting a needle and drawing up the band into a syringe. For wild type cells, an orange band of carotenoids formed near the top of the tube, a green band of PSI monomers and PSII dimers in the centre and a further green band of PSI trimers toward the bottom. The composition of the bands was confirmed by 77K fluorescence emission spectroscopy (see section 2.4.2). Photosystem samples were stored in liquid nitrogen.

2.3.6 Removal of manganese from thylakoid membranes

When thylakoid membranes were to be used for EPR samples they were first washed to remove excess manganese. The chlorophyll concentration was estimated as described in section 2.3.2. Samples were diluted 10x in EPR buffer containing 0.3M NaCl and mixed by gentle rotation for 15 minutes at 4 °C. The same volume of EPR buffer containing 2 mM Na-EDTA was then added and mixed for a further 15 minutes. Membranes were recovered by centrifuging for 1 hour at 160,000 *g* and resuspended to their original chlorophyll concentration in EPR buffer.

2.3.7 Oxygen evolution measurements

Oxygen evolution and uptake measurements were taken using an oxygen electrode (Hansatech, Kings Lynn, Norfolk, UK) according to the manufacturer's instructions. Measurements were made at 30 °C using whole cells at 10 μM chlorophyll. Oxygen evolution was measured while applying a light source and oxygen uptake was measured in the dark.

2.4 Biophysical techniques

2.4.1 Absorption spectroscopy

Room temperature optical absorption spectra were recorded using either an Aminco DW2000 spectrophotometer (SLM Instruments, Illinois, USA) or a Unicam UV/Vis spectrophotometer (Thermo Electron Corporation, Cambridge, UK). The light path was 1 cm. Usually the absorption was measured from 400 to 750 nm.

2.4.2 77K fluorescence emission spectroscopy

Samples of whole cells were adjusted to a chlorophyll concentration of 5 $\mu g.ml^{-1}$ in BG11 medium and injected into 4 mm external diameter silica tubes. To obtain samples with cells in state 2, samples were dark adapted for 5 minutes before freezing in liquid nitrogen. To obtain state 1, samples were adapted to red light (provided by

using a Schott RG665 glass filter and a light source with an intensity of 20 $\mu E.m^{-2}.s^{-1}$) prior to freezing.

Samples of photosystems from sucrose density gradient bands (as described in section 2.3.5) were placed in tubes and frozen as described for whole cells.

Fluorescence emission spectra were recorded at 77 K using a Perkin-Elmer LS50 luminescence spectrometer (Perkin-Elmer, Maryland, USA) fitted with a sample holder containing liquid nitrogen. Samples were excited using a wavelength of 435 nm for chlorophyll excitation or 600 nm for phycocyanin excitation. The fluorescence emission was measured from 620 to 750 nm. Excitation and emission slit widths were 5 nm.

The spectra for chlorophyll excitation showed peaks at 685 and 695 nm representing PSII and a peak at around 720 nm representing PSI. For phycocyanin excitation spectra, the peaks at 655 and 720 nm represent phycocyanin and PSI respectively. The shoulder at 695 nm represents PSII. The peak at 685 nm is due to a combination of fluorescence from PSII and phycobilisome core long wavelength pigments (terminal emitters).

2.4.3 Room temperature fluorescence induction transients

The kinetics of the state 2 to state 1 transition in whole cells was measured using room temperature fluorescence induction transients in a manner similar to that described by Schluchter *et al* (1996).

A laboratory-built spectrofluorimeter was used (Glynn Laboratory of Bioenergetics, UCL). After growth in dim light, cell cultures were adjusted to a chlorophyll concentration of 3 $\mu g.ml^{-1}$ in BG11 medium. Fluorescence cuvettes containing 3 ml samples of cells were dark adapted for 5-10 minutes in the presence of 20 μM DCMU in order to drive cells into state 2. A phycobilisome-absorbed light source (from light passing through a Schott RG610 and an Ealing 660 nm short-pass filter) at an intensity of 100 $\mu E.m^{-2}.s^{-1}$ was then applied. The illumination was controlled by an

electronic shutter with an opening time of 1 ms. The fluorescence from the sample was detected by a photomultiplier screened by a Schott RG695 glass filter. The level of fluorescence was recorded over 60 s and showed a rise attributed to transition from state 2 to state 1. The experiment was repeated several times using different cell cultures to ensure reproducibility. Exponential curves were fitted to these traces using SigmaPlot 5.0 software (Jandel Scientific) and used to calculate the t½ for the state transition.

2.4.4 Fluorescence Recovery After Photobleaching (FRAP)

Cells to be used for FRAP were grown overnight in a culture supplemented with 0.5% (v/v) DMSO in order to cause cell elongation. Samples of cells were spotted onto BG11 agar and allowed to dry so that the cells were adsorbed onto the agar. Samples were then excised from the agar plate and sealed into a custom-made sample holder with a glass coverslip and maintained at 30 °C by circulating water around the sample holder.

FRAP experiments were carried out as described in Aspinwall *et al* (2004b) using a Nikon PCM2000 laser-scanning confocal microscope. Excitation light was provided by a 20 mW red HeNe laser (to give 633 nm) through a 50 μm pinhole and a 60X objective lens. Fluorescence emission was defined by a 650 nm long-pass filter. The confocal spot was scanned for 2-3 s across the cell to photobleach the phycobilisomes in that area (as described in Chapter 5). Images of the recovering cell were recorded every 3 s by scanning the confocal spot across the cell. Fluorescence bleaching profiles were extracted using Optimas 5.0 software and fitted to Gaussian curves using SigmaPlot software 5.0 (Jandel Scientific) as described in Chapter 5. Diffusion coefficients for the phycobilisomes were calculated as described by Mullineaux *et al* (1997).

2.4.5 Electron Paramagnetic Resonance (EPR)

2.4.5.1 Preparation of ascorbate reduced EPR samples

Thylakoid membranes or isolated photosystems suspended in EPR buffer were injected into quartz EPR tubes. Samples had a chl concentration of 1 $mg.ml^{-1}$ or higher and each tube received 300 µl. The tubes were cooled on ice and dark adapted for at least 30 minutes.

To reduce the samples, sodium ascorbate was added using a Hamilton syringe fitted with a long needle to give a final concentration of 30 mM and mixed. Samples were then incubated in complete darkness for 1 hour on ice before freezing in liquid nitrogen in the dark.

When phenazine methosulphate was required in addition to the sodium ascorbate, it was added to a concentration of 0.1 mM and the samples incubated and frozen as described above.

2.4.5.2 Preparation of dithionite reduced EPR samples

Samples were injected into tubes and dark-adapted. A flask of 0.1M Tris pH 9.0 buffer was made anaerobic by bubbling argon gas through via a solution of 0.1M Tris pH 9.0 with 10 $mg.l^{-1}$ methyl viologen and 2 % w/v sodium dithionite. A solution of 2% w/v sodium dithionite was then prepared in the anaerobic buffer. Each EPR sample received 30 µl of this solution to give a final concentration of 0.2 % sodium dithionite. Samples were incubated on ice in the dark under a stream of argon gas prior to freezing in liquid nitrogen.

2.4.5.3 CW-EPR

EPR spectra were recorded using a Jeol RE1X spectrometer (Kyoto, Japan) fitted with a helium cryostat (Oxford Instruments, Abingdon, Oxfordshire, UK). Illumination was with a 150 W light source. Measurements were recorded in dark and light.

2.4.5.4 Pulsed EPR

Kinetic pulsed EPR spectra and kinetics were measured using a Bruker ESP380 X-band spectrometer with a variable Q dielectric resonator (Bruker model 1052 DLQ-H8907) fitted with an Oxford Instruments CF935 cryostat cooled with liquid nitrogen. Actinic illumination was supplied by an Nd-YAG laser (Spectra Physics DCR-11) with 10 ns pulse duration.

2.4.6 Electron microscopy and image analysis of PSI particles

Electron microscopy and image processing of isolated PSI particles was carried out in collaboration with Jim Barber, James Duncan and Tom Bibby at Imperial College London, UK.

Samples of isolated particles, prepared as described in section 2.3.5, were negatively stained using 2% uranyl acetate on glow discharged carbon evaporated grids and imaged using a Philips CM 100 electron microscope at 80 kV. Electron micrographs were digitised and single particle data sets obtained by selecting all possible particles. Data were processed using IMAGIC-5 software as described in van Heel *et al* 1996, 2000 and in Sherman *et al* 1998.

CHAPTER THREE

CREATING CYANOBACTERIAL MUTANTS LACKING ACCESSORY SUBUNITS OF PHOTOSYSTEM I

CHAPTER THREE

CREATING CYANOBACTERIAL MUTANTS LACKING ACCESSORY SUBUNITS OF PHOTOSYSTEM I

3.1 Introduction

The PsaA and PsaB subunits constitute the core of photosystem I, binding the reaction centre, other pigments and most of the electron transfer cofactors. These subunits are essential for photosynthetic function. The remaining accessory subunits, of relatively low molecular mass, play various other roles. The function of some accessory subunits remains undetermined or unclear but molecular genetic studies of mutants in several model organisms are increasing our knowledge of these subunits. This thesis contains experiments conducted to clarify the roles played by two of these subunits – PsaL and PsaE – in cyanobacteria. The PsaL subunit is known to form the trimerisation domain of the photosystem in cyanobacteria (Chitnis & Chitnis 1993), although the advantage of trimerisation is not known. PsaE has been implicated in several processes including facilitating ferredoxin reduction on the stromal side of PSI (Weber & Strotmann 1993, Sonoike *et al* 1993) and cyclic electron transport (Yu *et al* 1990, Zhao *et al* 1993), although many of these are mostly speculative roles. Details of previous work on each of these accessory subunits is provided in Chapter 1.

In order to determine the functions of these subunits, a range of mutants lacking these polypeptides from PSI were created. PsaL-minus and PsaE-minus mutants were created in *Synechocystis* 6803, a commonly used model organism for this type of study. In addition a PsaL-minus mutant of *Synechococcus* 7942 was made, as this organism is useful for studying phycobilisome mobility by FRAP analysis and detecting effects on state transitions (as described in Chapter 5).

Double mutants were also made in *Synechocystis* 6803 *chlL*- and PSII- backgrounds. The *chlL*- cells (a kind gift from W. Vermaas) are deficient in the light-independent chlorophyll biosynthesis pathway (Wu & Vermaas 1995). Cyanobacteria are normally capable of manufacturing chlorophyll with or without light via two different branches

of the chlorophyll biosynthesis pathway. The deletion of the *chlL* gene has provided a mutant lacking the light-independent protochlorophyllide reduction branch (Wu & Vermaas 1995). The cells can be grown in the dark to deplete chlorophyll, while cell growth continues. The photosystems are gradually lost from the cells. The absence of chlorophyll decreases the stability of chlorophyll-binding proteins. Upon return to light conditions, greening occurs, with initial reduction of accumulated protochlorophyllide followed by synthesis of chlorophyll *a* and production of functional photosystems. The double mutants can be used to investigate PSI stability when particular accessory subunits are not present.

The double mutants in the PSII- background, also a gift from W. Vermaas, simplify preparation of photosystem I particles and biochemical protocols. In particular, when looking for different arrangements of PSI on a sucrose gradient, it is convenient to eliminate PSII so that it does not interfere with interpretation. This was put to particularly good use when studying PSI-CP43' particles as described in Chapter 6.

This chapter describes the molecular biology strategies employed to produce the set of cyanobacterial mutants described above.

3.2 PsaL-minus mutants of *Synechocystis* 6803

The *Synechocystis* 6803 genome contains a single copy of the *psaL* gene, which is adjacent to the *psaI* gene, as shown in Figure 3.1. A strategy to disrupt this gene, thereby eliminating production of the PsaL polypeptide, by inserting an antibiotic resistance marker was devised.

Genomic DNA from wild type cells of *Synechocystis* 6803 was extracted as described in Chapter 2 and used as template DNA in a PCR reaction using primers PsaL6803/1f and PsaL6803/1r (see Table 3.1). These primers were designed to amplify a 936 bp fragment of DNA including the entire *psaL* gene and some flanking DNA. The PCR product was extracted and purified from an agarose gel.

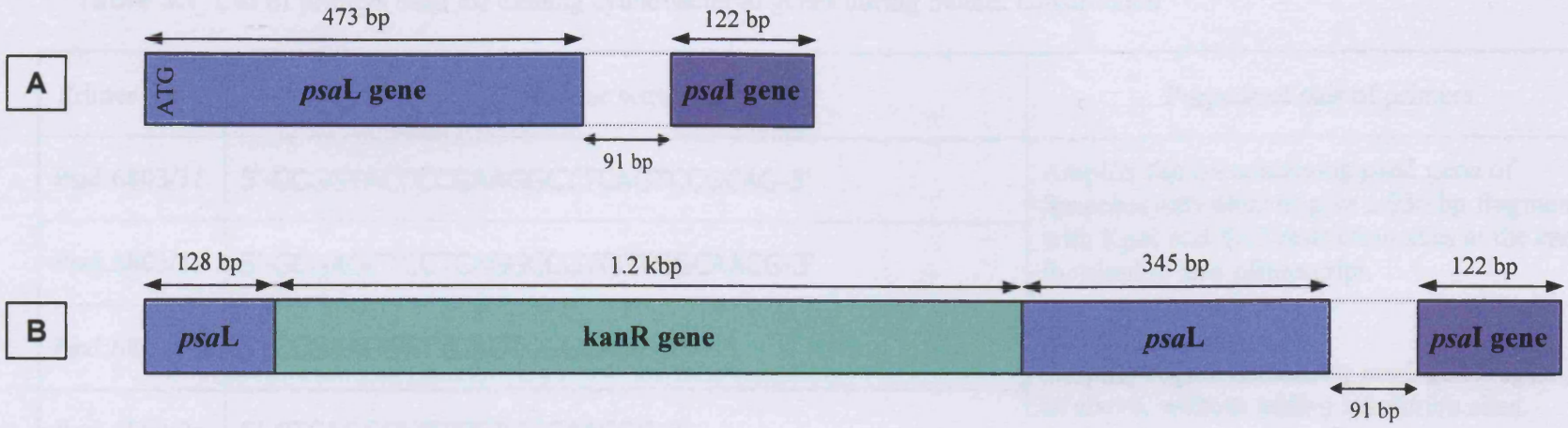

Figure 3.1 Mutation of the *psaL* gene of *Synechocystis* 6803. The arrangement of the *psaL* gene and the adjacent *psaI* gene in the wild type genome is represented in **A**. After cloning the *psaL* gene, the kanamycin resistance gene (kanR) was inserted into the gene, as described in this chapter, resulting in a mutant with the genetic arrangement shown in **B**. The *psaL* gene was disrupted by the kanR addition, resulting in a mutant that does not synthesise the PsaL polypeptide.

Table 3.1 List of primers used for cloning cyanobacterial genes during mutant construction

Primer name	Primer sequence	Purpose of pair of primers
PsaL6803/1f	5′-CCGGTACCCCGAAGGCTTCAGTCCGCAG-3′	Amplify region containing *psaL* gene of *Synechocystis* 6803 to give a 936 bp fragment with KpnI and SacI restriction sites at the ends for cloning into pBluescript.
PsaL6803/1r	5′-GCGAGCTCCTCAGGCCGTCGTGGCAACG-3′	
PsaL6803/2f	5′-CCGAAGGCTTCAGTCCGCACC-3′	Amplify region containing *psaL* gene region, as above, without adding restriction sites.
PsaL6803/2r	5′-CTCAGGCCGTCGTGGCAACGG-3′	
PsaE6803/3f	5′-GGGGTACCCGTGACGCCGGAACTGTACATGGGC-3′	Amplify region containing *PsaE* gene region of *Synechocystis* 6803 to give a 3024 bp fragment with KpnI and SacI sites at the ends.
PsaE6803/3r	5′-GGGAGCTCCCTGACCCCATACTGATCCGGTGC-3′	
PsaL7942/1r	5′-TCGAAGCCACCTAGAAGGCG-3′	Amplify region containing the 3' end of the *psaL* gene of *Synechococcus* 7942 to give 250 bp product.
PsaL7942/1f	5′-GGCCCTCTGCGCAATACCGA-3′	
PsaL7942/2f	5′-CTGCCGATCTATCGTCGCGG-3′	When used with PsaL7942/1r, to amplify region containing whole *psaL* gene from *Synechococcus* 7942.

The primers used had been designed to incorporate recognition sites for the restriction enzymes KpnI and SacI at the ends of the DNA fragments. The PCR product and an aliquot of the plasmid vector pBluescript SK+ were double digested with the enzymes SacI and Asp718 (which has the same recognition site as KpnI) in order to create compatible sticky ends on the fragment and vector. Fully digested DNA samples were purified as described in Chapter 2 and ligated using T4 DNA ligase in a reaction with a 1:4 ratio of vector:fragment at 16 °C overnight.

E. coli cells made competent for DNA transformation by $MgCl_2/CaCl_2$ treatment were transformed with the ligation mixture and plated onto LB agar plates containing ampicillin at 50 $\mu g.ml^{-1}$ to select for the ampicillin resistance gene on pBluescript and IPTG and X-gal for blue-white colony selection (as explained in Sambrook & Russell 2001). Control plates with untransformed competent cells (to confirm cell viability by the appearance of a lawn of cells), an undigested pBluescript transformation (to confirm transformation competence by the appearance of numerous blue colonies) and a digested vector only transformation (to confirm that the vector could not re-ligate in the absence of fragment by a lack of colonies of these plates) were included.

Transformants (white colonies) were picked off the plates and streaked out onto LB plates containing ampicillin, to create a renewable stock of plasmid, and also grown up in liquid culture for preparation of plasmid DNA. The resulting plasmids were digested with the enzyme StuI, which had a unique recognition site within the cloned *psaL* gene, to linearise, and their size (4.1 kb) was verified by running on an agarose gel. The plasmids were also double digested with SacI and Asp718 to confirm that the fragment and vector could be regained.

The plasmid pUC4K was digested with the enzyme HincII to yield three products. The 1.2 kb band was excised from agarose gels as this contains the kanamycin resistance gene (aminoglycoside 3'-phosphotransferase) carried on the plasmid.

One of the pBluescript-psaL constructs was digested with the enzyme StuI , which cut once in the middle of the *psaL* gene to give blunt ends. The construct was then treated with CIAP (calf intestinal alkaline phosphatase) to prevent the blunt ends from

re-ligating. The kanamycin resistance gene taken from pUC4K was blunt ligated into the construct at room temperature for 72 hours. Competent *E. coli* cells were transformed with the ligation, along with the controls described previously, and resulting white colonies were streaked out onto fresh plates and grown in liquid culture for plasmid preparation. The pBluescript-psaL-kanR constructs were digested with SacI enzyme to verify their size (5.3 kb) on an agarose gel.

The finished construct, containing the *psaL* gene, now interrupted by the kanamycin resistance gene, was transformed into wild type cells of *Synechocystis* 6803 as described in Chapter 2. Transformed cells were then spread onto BG11 agar plates and incubated at 30 °C for several days. Soft agar (0.6 % w/v) containing sufficient kanamycin to diffuse throughout the agar plate was overlayed onto the transformation plates. After several weeks incubation, small green colonies of transformants appeared. Cells of the *Synechocystis* 6803 *chlL-* and *Synechocystis* 6803 PSII- mutant, described in Section 3.1, were also transformed with the construct in the same way in order to create double mutants. When transformant colonies appeared they were repeatedly re-streaked to single colonies on BG11 agar containing appropriate antibiotic selection (see Table 3.2).

After several generations of transformants had been streaked, liquid cultures were started and genomic DNA was extracted. This DNA was used in PCR reactions with primers PsaL6803/2f and PsaL6803/2r. These primers were similar to those used to originally clone the *psaL* gene region but were completely homologous to the DNA sequence (as they did not have additional restriction sites). The PCR products were run on agarose gels to confirm that only the interrupted version of the *psaL* gene still existed in the mutants and that they had therefore fully segregated and now had the mutant version of the genetic arrangement shown in Figure 3.1. Figure 3.2 shows the agarose gel with wild type *psaL* gene being amplified as a 930 bp product from genomic DNA of wild type cells and also the PSII- mutant. The three samples from the *psaL-* mutant and the *chlL- psaL-* and PSII- *psaL-* double mutants yield only the larger 2130 bp fragment i.e. the *psaL* gene interrupted by the kanamycin resistance gene.

Table 3.2 Antibiotic selection for mutant strains of cyanobacteria

Mutant strain	Genes mutated	Antibiotic selection*
Synechocystis 6803 PSII-	***psbD*$_1$, *psbD*$_2$, *psbC***	25 μM **chloramphenicol**
Synechocystis 6803 *chlL-*	***chlL***	50 μM **erythromycin**
Synechocystis 6803 *psaL-*	***psaL***	50 μM **kanamycin**
Synechocystis 6803 *psaE-*	***psaE***	50 μM **kanamycin**
Synechocystis 6803 *chlL- psaL-*	***chlL*, *psaL***	50 μM **erythromycin** 50 μM **kanamycin**
Synechocystis 6803 *chlL- psaE-*	***chlL*, *psaE***	50 μM **erythromycin** 50 μM **kanamycin**
Synechocystis 6803 PSII- *psaL-*	***psbD*$_1$, *psbD*$_2$, *psbC*, *psaL***	25 μM **chloramphenicol** 50 μM **kanamycin**
Synechocystis 6803 PSII- *psaE-*	***psbD*$_1$, *psbD*$_2$, *psbC*, *psaE***	25 μM **chloramphenicol** 50 μM **kanamycin**
Synechococcus 7942 *psaL-*	***psaL***	50 μM **kanamycin**

* Strains lacking PSII also required 5 mM glucose

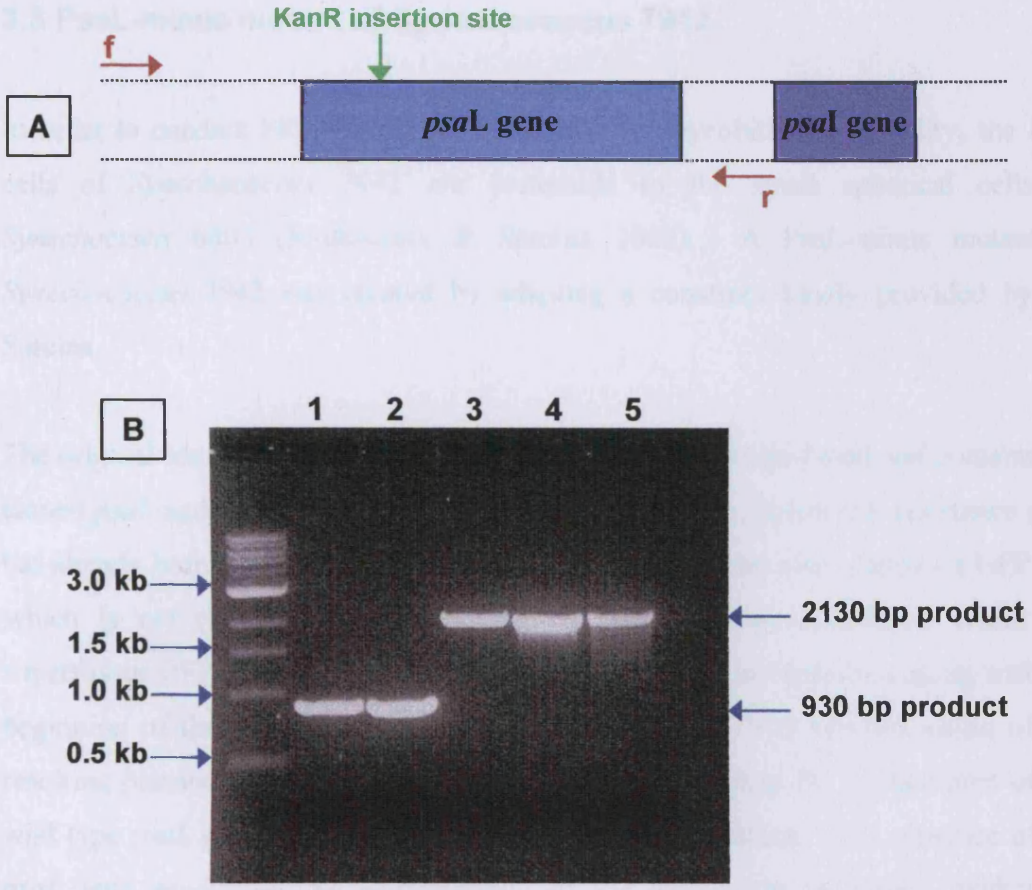

Figure 3.2 PCR to demonstrate deletion of *psaL* in *Synechocystis* 6803 strains.

A shows the annealing positions of the primers (PsaL6803/2f and/2r), which are designed to amplify the *psaL* gene region (not to scale). **B** shows an agarose gel showing the PCR products. The PCR reactions shown in lanes 1 and 2 used DNA from wild type cells (1) and cells with the PSII- background (2). Each of these samples gave rise to a 930 bp product, representing the *psaL* gene. Lanes 3, 4 and 5 show PCR products from reactions using DNA from the *Synechocystis* 6803 *psaL*- mutant, the *chlL- psaL-* double mutant and the PSII- *psaL-* double mutant, respectively. These PCR reactions yielded a 2130 bp product, demonstrating the insertion of the 1.2 kb kanamycin resistance gene into the *psaL* gene site.

3.3 PsaL-minus mutant of *Synechococcus* 7942

In order to conduct FRAP experiments to look at phycobilisome mobility, the long cells of *Synechococcus* 7942 are preferable to the small spherical cells of *Synechocystis* 6803 (Mullineaux & Sarcina 2002). A PsaL-minus mutant of *Synechococcus* 7942 was created by adapting a construct kindly provided by M. Sarcina.

The original construct is shown in Figure 3.3. It is pBluescript-based and contains the cloned *psaL* and *psaI* genes of *Synechococcus* 7942. The kanamycin resistance gene has already been added as a selectable marker. The construct also contains a GFP tag, which is not required for this mutant. A strategy was devised in which the superfluous GFP tag would be excised by restriction enzyme digestion along with the beginning of the *psaL* gene, including the start codon. The transformation of the resulting plasmid into *Synechococcus* 7942 would then cause the replacement of the wild type *psaL* gene with the truncated non-functional version. The presence of the *psaI* gene would aid the incorporation of the kanamycin resistance marker by homologous recombination into the correct site in the genome. The wild type arrangement of these genes and also the eventual mutant arrangement are shown in Figure 3.4.

The construct was double digested with the restriction enzymes SacII and SpeI, which excised the region marked out by red arrows in Figure 3.3. The 848 bp region containing the GFP tag and the beginning of the *psaL* gene was discarded. The remaining 5033 bp linearised constructs were treated with mung bean nuclease to create blunt ends. The modified construct was then self-ligated and transformed into competent *E. coli* cells with ampicillin and kanamycin selection. The resulting transformants were grown in liquid culture and used for plasmid preparation. The 'new' plasmids (called pL7942A) were checked to ensure that they were the correct size of 5 kb and sequenced to ensure that it had the expected DNA arrangement. Wild type *Synechococcus* 7942 cells were transformed with pL7942A and plated onto BG11 agar plates containing kanamycin.

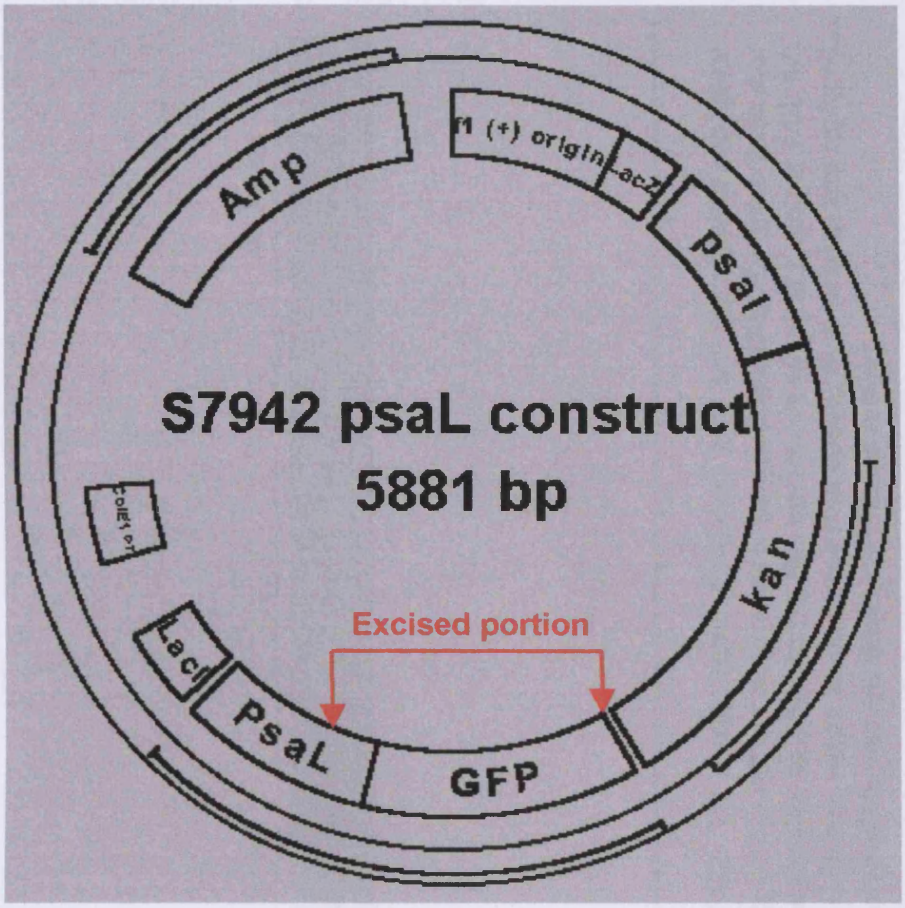

Figure 3.3 A pBluescript-based construct containing the *psaL* gene of *Synechococcus* 7942 (provided by M. Sarcina). The construct contains the cloned *psaL* and *psaI* genes of *Synechococcus* 7942 as well as the kanamycin resistance gene from the plasmid pUC4K and a GFP tag. The construct was adapted by excision of the GFP tag and the beginning of the *psaL* gene, including the start site, as indicated by the red arrows, to create a construct that could be used to produce a PsaL-minus mutant of *Synechococcus* 7942.

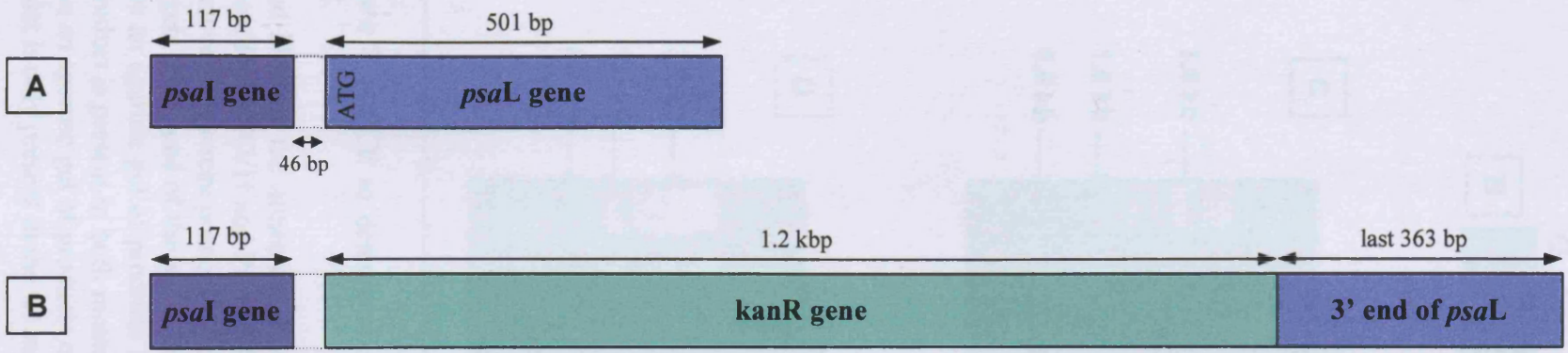

Figure 3.4 Mutation of the *psaL* gene of *Synechococcus* 7942. The arrangement of the *psaL* gene and the adjacent *psaI* gene in the wild type genome is represented in **A**. After cloning of this area of the genome, partial deletion of the *psaL* gene and addition of selectable marker, the kanamycin resistance gene (kanR), as described in this chapter, resulted in a mutant with the genetic arrangement shown in **B**. The end of the *psaL* gene (138 bp), which included the start codon, were deleted and replaced with the kanamycin resistance gene. As a result, the PsaL polypeptide was not synthesised in the mutant.

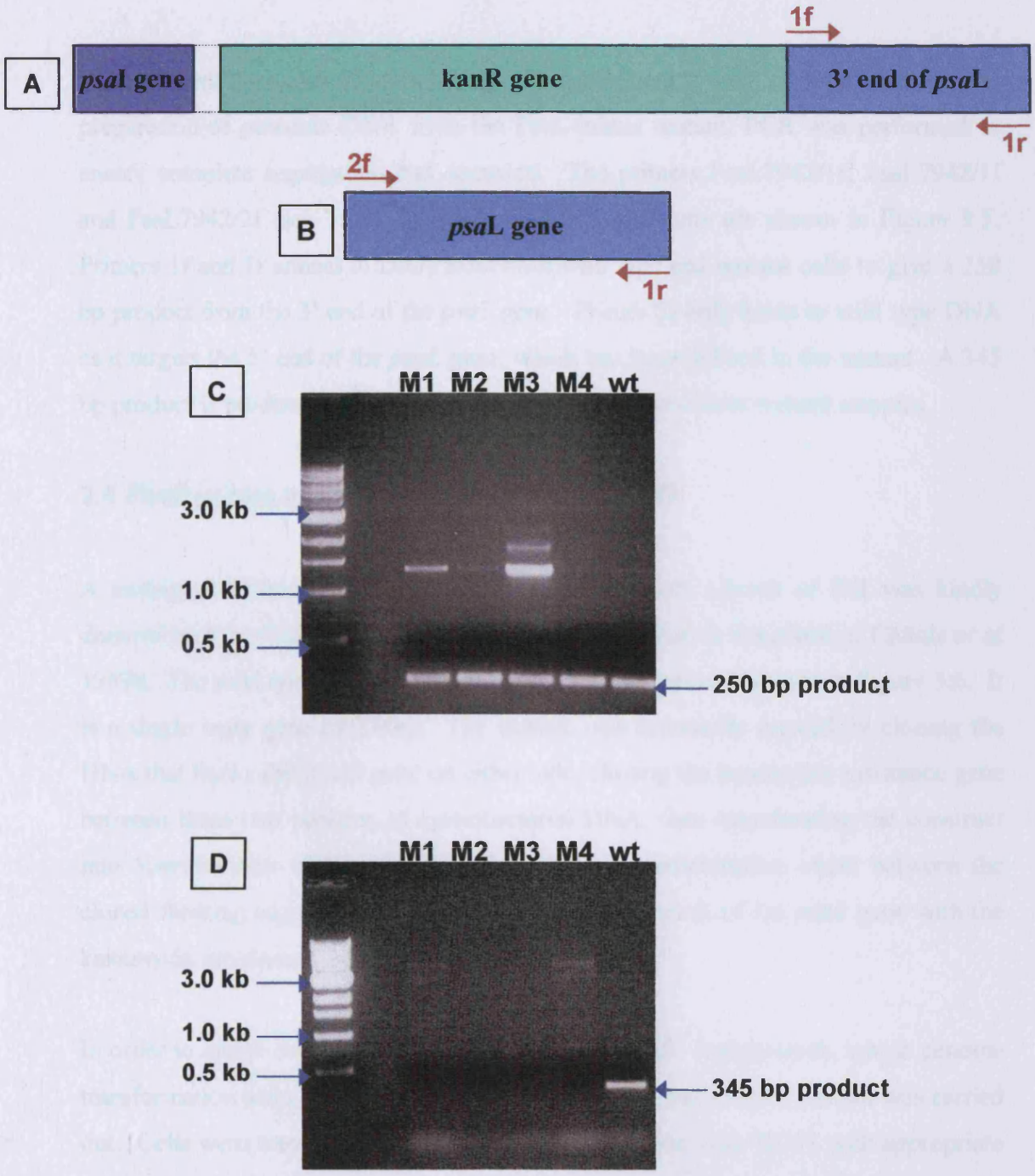

Figure 3.5 PCR to demonstrate partial deletion of *psaL* in *Synechococcus* 7942.

A and **B** show the annealing sites for the PCR primers used (not to scale). Primers PsaL7942/1f and PsaL79421r anneal to DNA from both wild type and mutant cells, whereas primer PsaL942/2f should only bind to wild type DNA as it targets the 5' end of the *psaL* gene, which has been deleted in the mutant. **C** shows an agarose gel of products from PCR using primers 1f and 1r. The 250 bp product is present in both mutant (M1 – M4) and wild type (wt) samples. **D** shows an agarose gel of products obtained using primers 2f and 1r. The 345 bp product is only present in the wt sample and none of the mutants.

After numerous rounds of re-streaking and subsequent growth of liquid culture and preparation of genomic DNA from the PsaL-minus mutant, PCR was performed to ensure complete segregation had occurred. The primers PsaL7942/1r, PsaL7942/1f and PsaL7942/2f (see Table 3.1) were used. The results are shown in Figure 3.5. Primers 1f and 1r anneal to DNA from both wild type and mutant cells to give a 250 bp product from the 3' end of the *psaL* gene. Primer 2f only binds to wild type DNA as it targets the 5' end of the *psaL* gene, which has been deleted in the mutant. A 345 bp product is produced only from wild type DNA and not from mutant samples.

3.4 PsaE-minus mutants of *Synechocystis* 6803

A mutant of *Synechocystis* 6803 deficient in the PsaE subunit of PSI was kindly donated by P.R. Chitnis. The construction of this mutant is described in Chitnis *et al* 1989a. The wild type arrangement of the *psaE* gene region is shown in Figure 3.6. It is a single copy gene of 224bp. The mutant was essentially created by cloning the DNA that flanks this small gene on either side, cloning the kanamycin resistance gene between these two portions of cyanobacterial DNA, then transforming the construct into *Synechocystis* 6803 cells. The homologous recombination event between the cloned flanking segments of DNA caused the replacement of the *psaE* gene with the kanamycin resistance marker.

In order to create double mutants in the *chlL*- and PSII- backgrounds, whole genome transformation using genomic DNA isolated from the PsaE-minus mutant was carried out. Cells were transformed in the usual way and plated onto BG11 with appropriate antibiotic selection including kanamycin (see Table 3.2 for the antibiotics used for each strain). After numerous rounds of re-streaking, the putative mutants were grown in liquid culture and DNA extracted.

PCR reactions using the primers PsaE6803/3f and PsaE6803/3r were used to amplify the region of the genome around the missing *psaE* gene. These primers gave a 3 kb product only with wild type genomic DNA. No product was obtained from the PsaE-minus mutant, as expected, as this area had been deleted and replaced with the kanamycin resistance marker. In order to ensure that the mutant DNA was viable,

PCR using primers for other unrelated and intact genes were used in simultaneous PCR reactions (the PsaL primers, for example, and also primers to amplify the kanamycin resistance cassette) and gave the expected products, showing that the mutant DNA had been successfully prepared and was normal in other photosynthetic genes (data not shown). Figure 3.7 shows the agarose gel of the PCR products comparing wild type and the PsaE-minus mutant DNA. The results for the double mutants were identical and have therefore not been shown.

3.5 Discussion

The set of mutants described in Section 3.1 were successfully created and maintained on solid media and liquid culture. The PsaL-minus mutants were used to investigate the role of trimerisation of PSI in cyanobacteria, leading to interesting observations regarding phycobilisome movement, state transition rates and interaction of the photosystem with light-harvesting apparatus. The PsaE-minus mutants were used for spectroscopic analysis and compared to wild type in an attempt to clarify the importance of this subunit.

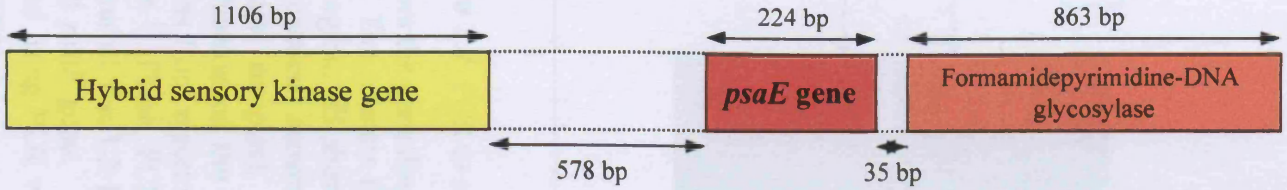

Figure 3.6 Mutation of the *psaE* gene of *Synechocystis* 6803. The arrangement of the *psaE* gene and adjacent genes in the wild type genome is shown. A mutant deficient in the PsaE polypeptide was kindly donated by P. R. Chitnis (Chitnis *et al* 1989a). This was created by deleting the *psaE* gene and inserting a kanamycin resistance gene in its place.

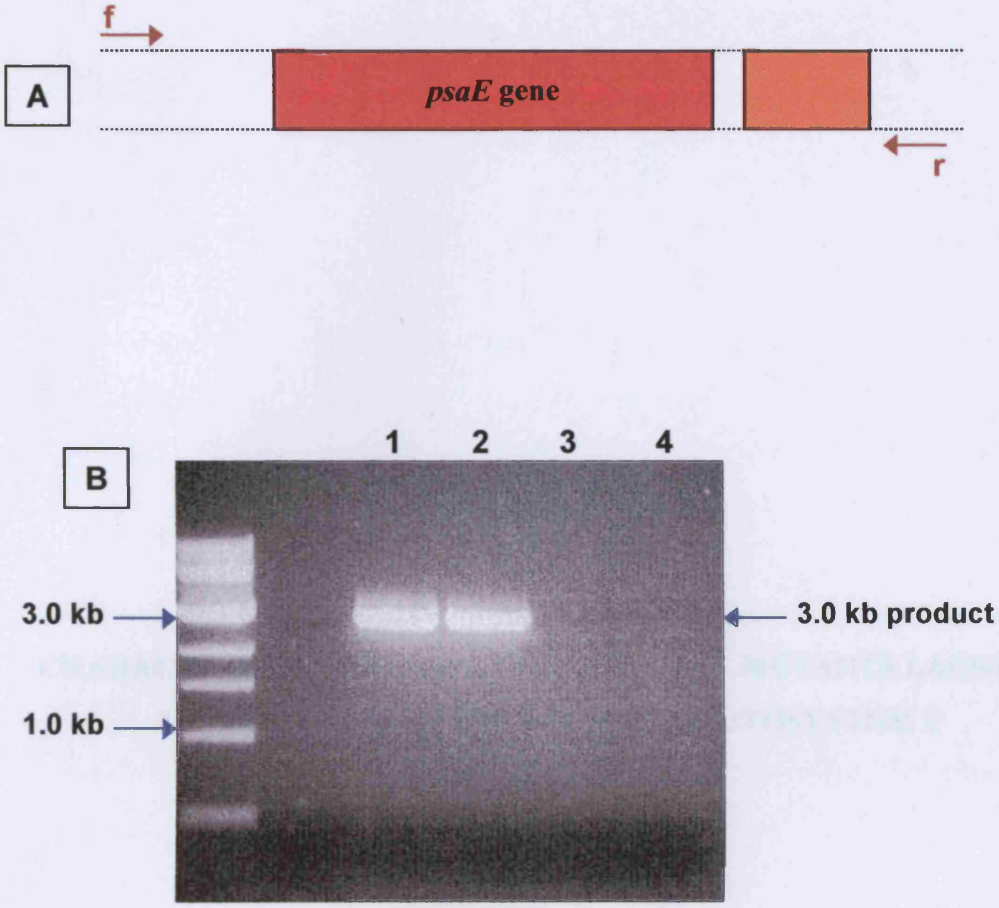

Figure 3.7 PCR to confirm deletion of *psaE* in *Synechocystis* 6803.

A shows the annealing positions of the primers to wild type DNA (not to scale). The primers (PsaE/3f and /3r) are designed to amplify the *psaE* gene region. **B** shows an agarose gel showing the PCR products. The PCR reactions shown in lanes 1 and 2 used DNA from wild type cell (duplicate samples). These gave a 3.0 kb product, representing the amplification of the *psaE* gene region. Lanes 3 and 4 show PCR products from reactions using DNA from the *Synechocystis* 6803 *psaE*-mutant. These PCR reactions give no product, demonstrating the insertion of the 1.2 kb kanamycin resistance gene into the site of the deleted *psaE* gene. The quality of the DNA from these samples was checked using PCR with primer to amplify other unaffected genes (data not shown).

CHAPTER FOUR

CHARACTERISATION OF CYANOBACTERIAL MUTANTS LACKING THE PsaL AND PsaE SUBUNITS OF PHOTOSYSTEM I

CHAPTER FOUR

CHARACTERISATION OF CYANOBACTERIAL MUTANTS LACKING THE PsaL AND PsaE SUBUNITS OF PHOTOSYSTEM I

4.1 Introduction

The PSI complex is composed of multiple subunits, which are transcribed from genes dispersed around the cyanobacterial genome; some are cotranscribed (Schwabe & Kruip 2000). The core subunits PsaA and PsaB form a core upon which the other subunits are assembled. A detailed description of the individual subunits is provided in Chapter 1.

4.1.1 The PsaL subunit

In cyanobacteria, PSI forms trimeric structures, although a population of monomers is also present, with the trimer:monomer ratio being influenced by a variety of factors such as ionic strength (*in vitro*) (Schwabe & Kruip 2000). It is, however, difficult to assess the effect of these factors on the *in vivo* ratio. The subunit PsaL is essential for PSI trimerisation (Chitnis *et al* 1993). As trimeric PSI has never been observed in plant or algal chloroplasts, despite the presence of the PsaL subunit in these organisms, it is presumed that the PsaL subunit may have alternative or additional roles.

4.1.2 The PsaE subunit

A number of different roles have been suggested for the PsaE subunit, including facilitation of ferredoxin docking on the stromal side of PSI and a role in cyclic electron transport (Chitnis *et al* 1995). Mutants lacking the PsaE subunit exhibited reduced PSI function, implying that this subunit does have some important specific function (Chitnis *et al* 1989a). PsaE is also highly conserved between different species (Rousseau *et al* 1993).

4.2 Characterisation of PsaL-minus mutants under normal growth conditions

When the functional role of the PsaL subunit of PSI was first investigated, Chitnis *et al* (1993) determined that it is dispensable for photosynthesis in cyanobacteria. A mutant lacking PsaL showed wild type rates of electron transfer through PSI. The primary effect of losing the PsaL subunit was that PSI no longer formed trimeric structures. It was discovered that PsaL is the structural component of PSI that forms the trimerisation domain (Chitnis & Chitnis 1993).

4.2.1 The PsaL-minus mutant grows at wild type rate under normal conditions

The growth rates of wild type *Synechocystis* 6803 cells and the PsaL-minus mutant were compared by monitoring the increase in OD_{750} as described in Chapter 2. Under normal laboratory conditions (30 °C and white light at an intensity of approximately 10 $\mu mol.m^{-2}.s^{-1}$), both strains grew at the same rate. The growth curves are shown in Figure 4.1. The doubling times for each strain were calculated from the initial exponential growth and were found to be approximately 20 hours for both strains. The lack of trimeric PSI is no disadvantage to the mutant in terms of photosynthetic growth under normal conditions.

4.2.2 Spectroscopic analysis of PsaL-minus mutants

Absorption spectra were recorded at room temperature for wild type and PsaL-minus mutants in order to establish whether there is any alteration to the pigment composition resulting from altered membrane organisation in the mutant. The spectra for the *Synechococcus* 7942 strains are shown in Figure 4.2. Both spectra are of similar shape, showing that the pigment composition is similar in both wild type and mutant cells. Absorption spectra using the *Synechocystis* 6803 strains also demonstrated this (data not shown as it is identical).

Fluorescence emission spectra at 77K were recorded to investigate the PSI:PSII ratio in the mutant. Figure 4.3 shows a pair of spectra with excitation at 435 nm (absorbed

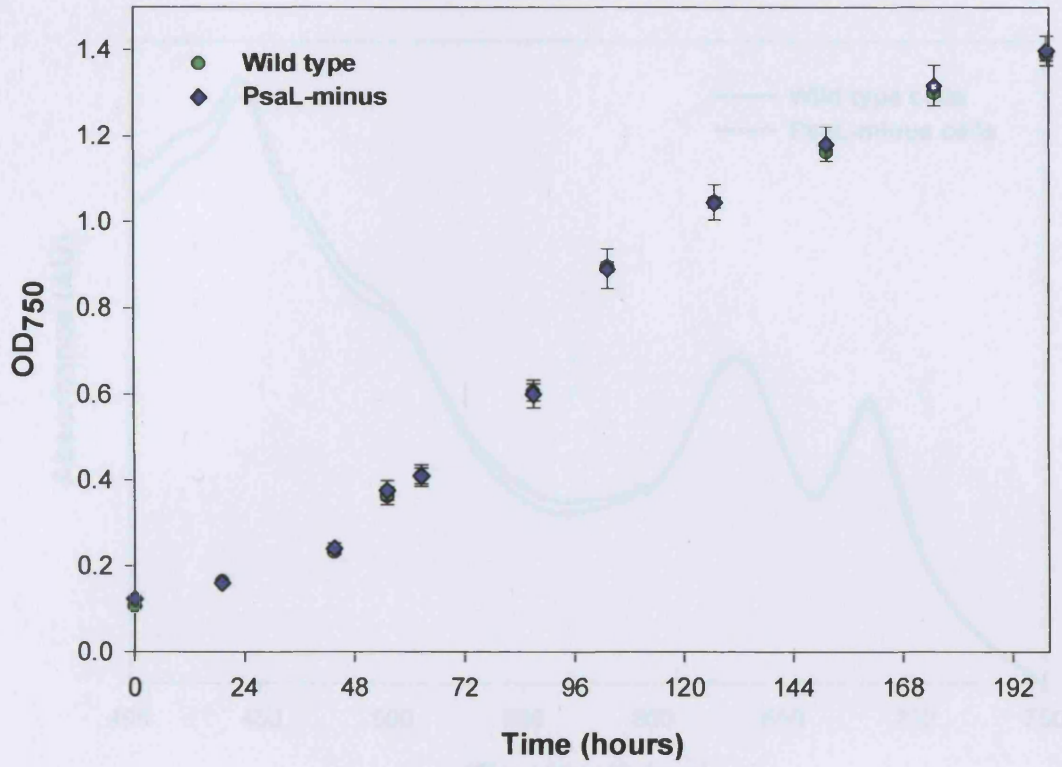

Figure 4.1 Growth curves for *Synechocystis* 6803 wild type and PsaL-minus cells grown in normal laboratory conditions (at 30 °C) and under standard illumination of 10 $\mu mol.m^{-2}.s^{-1}$. Cells were added to flasks of growth medium to give an initial OD_{750} of 0.1. The increase in OD_{750} was measured in at least triplicate for each strain and averaged to produce the plots shown. Curves were fitted to the exponentially rising part of each plot, as described in Chapter 2, and used to calculate doubling times. The doubling times for both wild type and PsaL-minus cells were found to be approximately 20 hours.

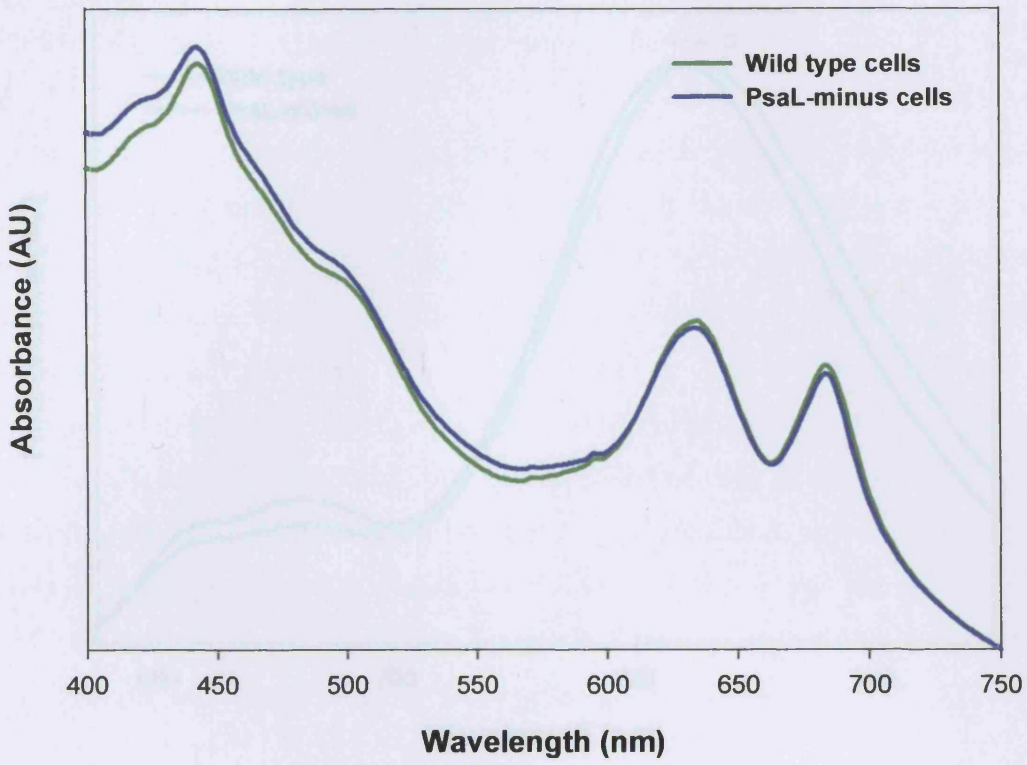

Figure 4.2 Absorption spectra at room temperature for *Synechococcus* 7942 wild type and PsaL-minus cells. Spectra are normalised at 680 nm (chlorophyll *a*-absorbed light). There is no significant difference between the wild type and mutant spectra.

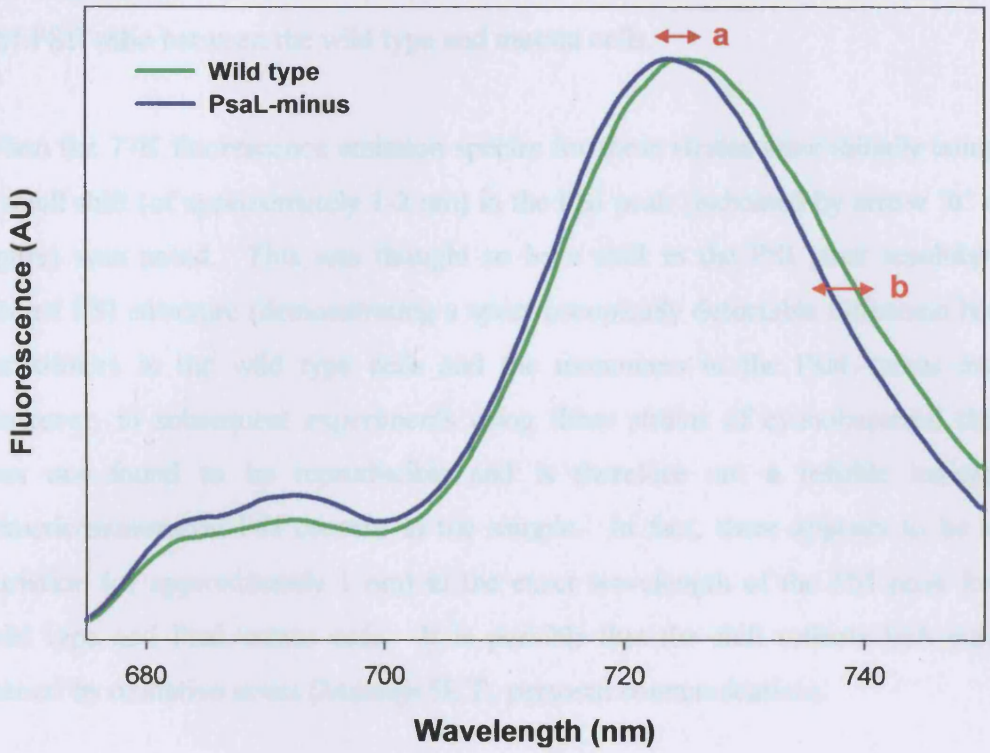

Figure 4.3 Fluorescence emission spectra at 77K with excitation at 435nm (chlorophyll-absorbed light) for samples of *Synechocystis* 6803 wild type and PsaL-minus cells. Cells at 5 μM chlorophyll were dark-adapted prior to freezing. The spectra are normalised to the PSI peak at around 722 nm. PSII is represented by the peaks at 685 and 695 nm. When comparing the two spectra, a small shift of approximately 1 nm in the PSI peak can be seen (arrow **a**). The wild type PSI peak appears broader than the PsaL-minus PSI peak (arrow **b**).

by chlorophyll) for *Synechocystis* 6803 wild type and PsaL-minus. Both spectra are of similar shape and show a peak at approximately 720 nm, representing PSI, and peaks at 685 and 695 nm, which represent PSII. Spectra of this type were measured on numerous occasions for this thesis and no consistent difference was found in the PSI:PSII ratio between the wild type and mutant cells.

When the 77K fluorescence emission spectra for these strains were initially compared, a small shift (of approximately 1-2 nm) in the PSI peak (indicated by arrow 'a' on the figure) was noted. This was thought to be a shift in the PSI peak resulting from altered PSI structure (demonstrating a spectroscopically detectable difference between the trimers in the wild type cells and the monomers in the PsaL-minus mutant). However, in subsequent experiments using these strains of cyanobacteria, the shift was not found to be reproducible and is therefore not a reliable indicator of trimeric/monomeric PSI content in the sample. In fact, there appears to be a little variation (of approximately 1 nm) in the exact wavelength of the PSI peak for both wild type and PsaL-minus cells. It is possible that the shift reflects IsiA induction caused by oxidative stress (Matthijs HCP, personal communication).

There also seems to be a difference in the breadth of the PSI peak (shown by arrow 'b' on the figure). The PSI peak for wild type cells appeared broader and this was thought to be an indicator that this peak was comprised of fluorescence from a mixed PSI population consisting of both trimers and monomers, whereas the narrower PsaL-minus PSI peak resulted only from monomers.

The equivalent spectra for the *Synechococcus* 7942 strains are shown in Figure 4.4 in order to demonstrate that the PSI:PSII ratio is the same in this strain and that the altered membrane arrangements that must result from a wholly monomeric PSI population in the mutant have not had an effect on this ratio.

Fluorescence emission spectra at 77K with excitation at 600 nm (phycocyanin-absorbed light) were also recorded and are shown in Figure 4.5. The spectra for wild type and PsaL-minus cells are similar shapes, which implies that energy from the excited phycobilisomes is being successfully transferred to both PSII and PSI reaction

centres. Further experiments to investigate the interaction of photosystems with phycobilisomes in these cells are presented in Chapter 5.

4.2.3 Sucrose density gradients confirm that no PSI trimers exist in PsaL-minus cells

Thylakoid membranes from wild type and PsaL-minus mutants were prepared and solubilised as described in Chapter 2. The solubilised components of the thylakoids were separated according to their size by loading onto sucrose density gradients followed by ultracentrifugation. Figure 4.6 shows an example of the gradient profiles obtained from *Synechococcus* 7942 wild type and PsaL-minus cells. In both samples there are orange bands containing carotenoids at the top of the gradient, followed by a series of green bands containing the photosystems. Unusually, a thin band could be seen in between the two thick green bands. Usually there are only two green bands, with the upper band containing a mixture of PSI monomers and PSII dimers and the lower band containing PSI trimers. Samples of each band were extracted for further analysis. The lack of a low green band in the PsaL-minus profile confirms the lack of trimeric PSI in these mutants. It is also unusual to see a blue band such as the lowest band in the PsaL-minus profile. This contains phycobilisomes that were not removed during the preparation procedure and it is likely that a blue band is also present in the wild type gradient, although obscured by the PSI trimer band.

Figure 4.7 shows a 77K fluorescence emission analysis of the bands from the gradients. The main green bands of photosystems (labelled A, C, D) were found to contain PSI plus PSII (in A and D) and just PSI in C. The thin green bands (labelled B or E) contained PSII. It is unusual to separate a PSII sample this cleanly from PSI monomers. In experiments that required pure PSI, a PSII-minus background mutation was employed as described in Section 4.6 below.

An example of a sucrose density gradient demonstrating the absence of PSI trimers in the *Synechocystis* 6803 PsaL-minus strains is featured in Figure 4.14.

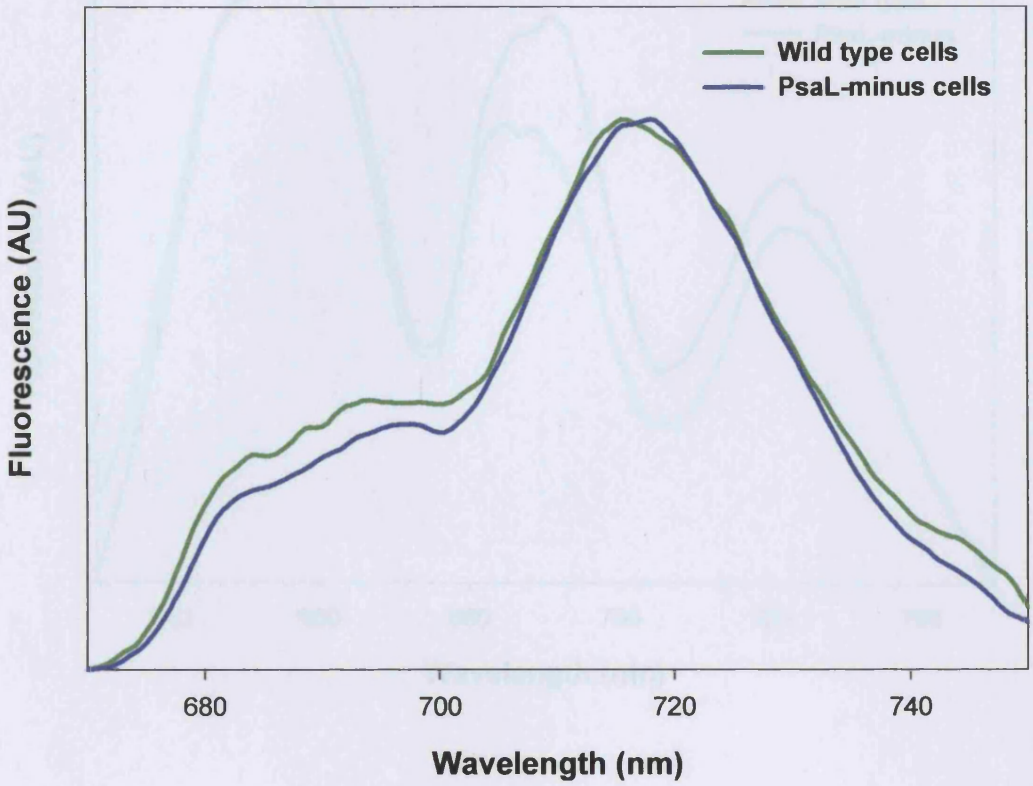

Figure 4.4 Fluorescence emission spectra at 77K with excitation at 435 nm (chlorophyll-absorbed light). Samples of *Synechococcus* 7942 wild type and PsaL-minus cells at 5 μM chlorophyll were dark-adapted prior to freezing. The spectra are normalised to the PSI peak at 715 nm. PSII is represented by peaks at 685 and 695 nm. The ratio of PSI:PSII for the two cell types are similar.

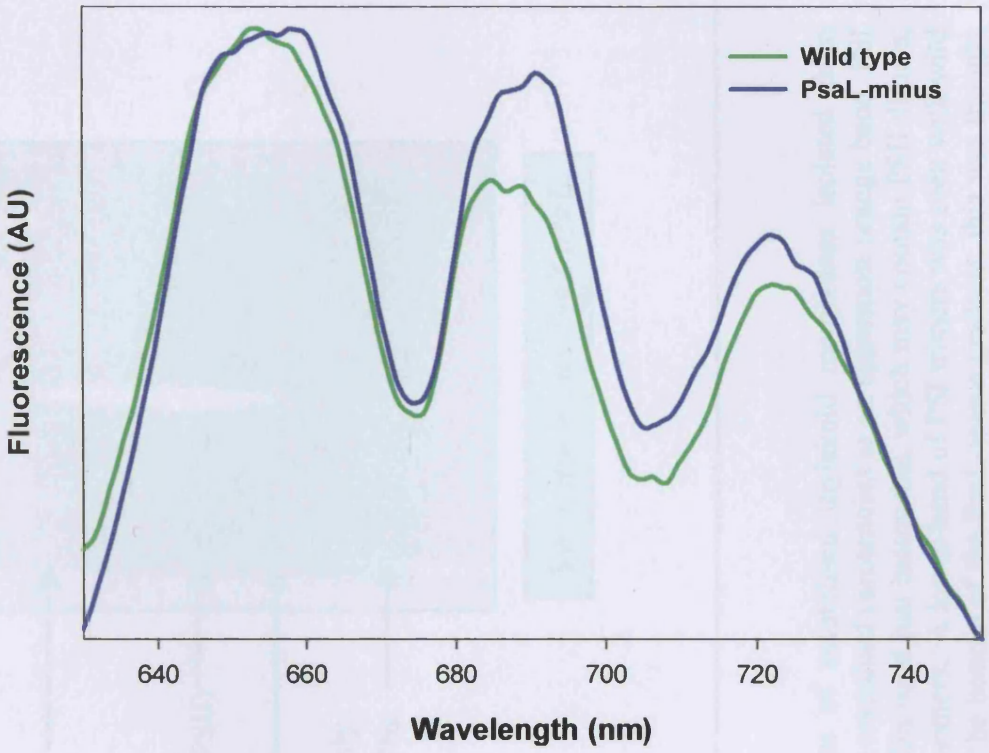

Figure 4.5 Fluorescence emission spectra at 77K with excitation at 600nm (phycocyanin-absorbed light). Samples of *Synechocystis* 6803 wild type and PsaL-minus cells at 5 μM chlorophyll were dark-adapted prior to freezing. The spectra are normalised to the phycocyanin peak at 653 nm. The presence of peaks representing PSI (at 722 nm) and PSII (at 695 nm) imply that energy from the excited phycobilisomes is being successfully transferred to these reaction centres.

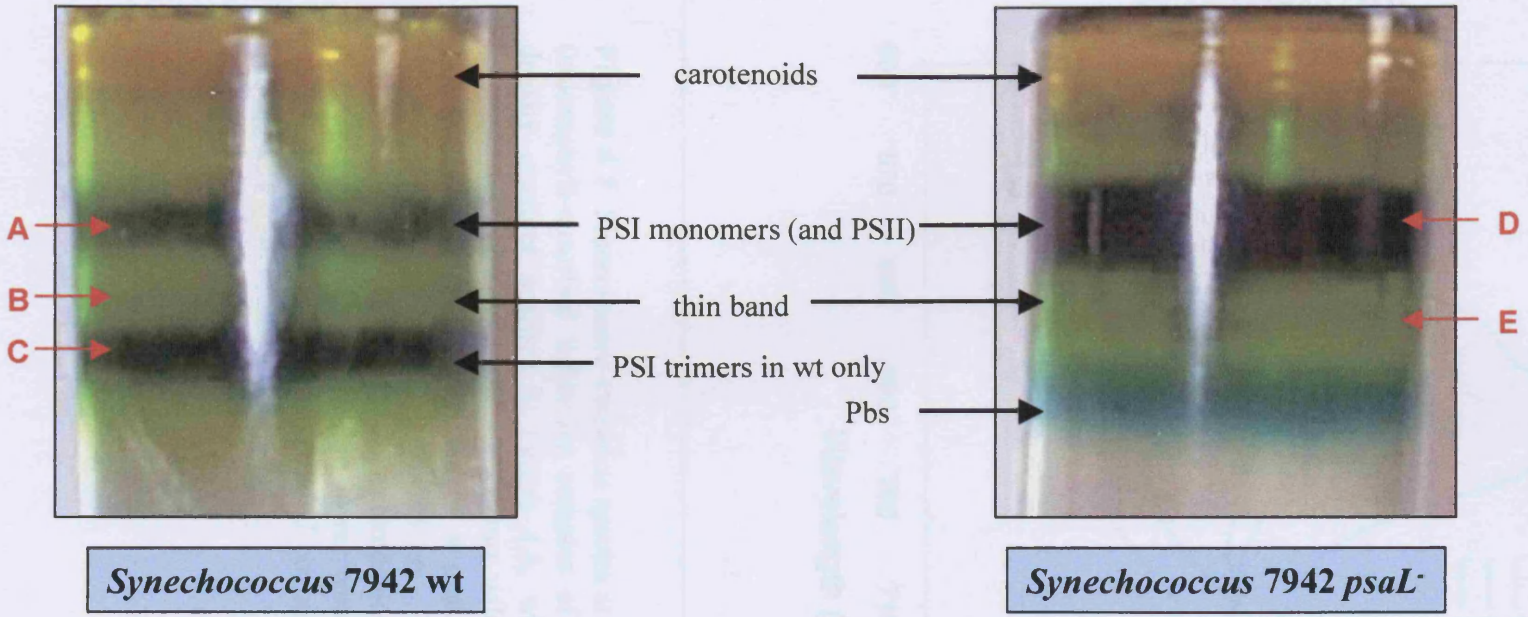

Figure 4.6 Sucrose density gradients to separate components of solubilised thylakoid membranes isolated from *Synechococcus* 7942 wild type and PsaL-minus cells. Both samples contained carotenoids as an uppermost orange band, PSI monomers as a thick green band towards the top of the tube and a thin band just below this, which may contain PSII dimers, although these usually separate out in the same band as the PSI monomers. A lower band of PSI trimers was seen with wild type only, as expected. Unusually, a pale blue band was visible at the bottom of the PsaL-minus gradient; this was thought to contain phycobilisomes (Pbs) that had not been removed in the washing stages of the preparation. Samples were extracted from the bands indicated by red letters for analysis by 77K fluorescence spectroscopy as shown in Figure 7.

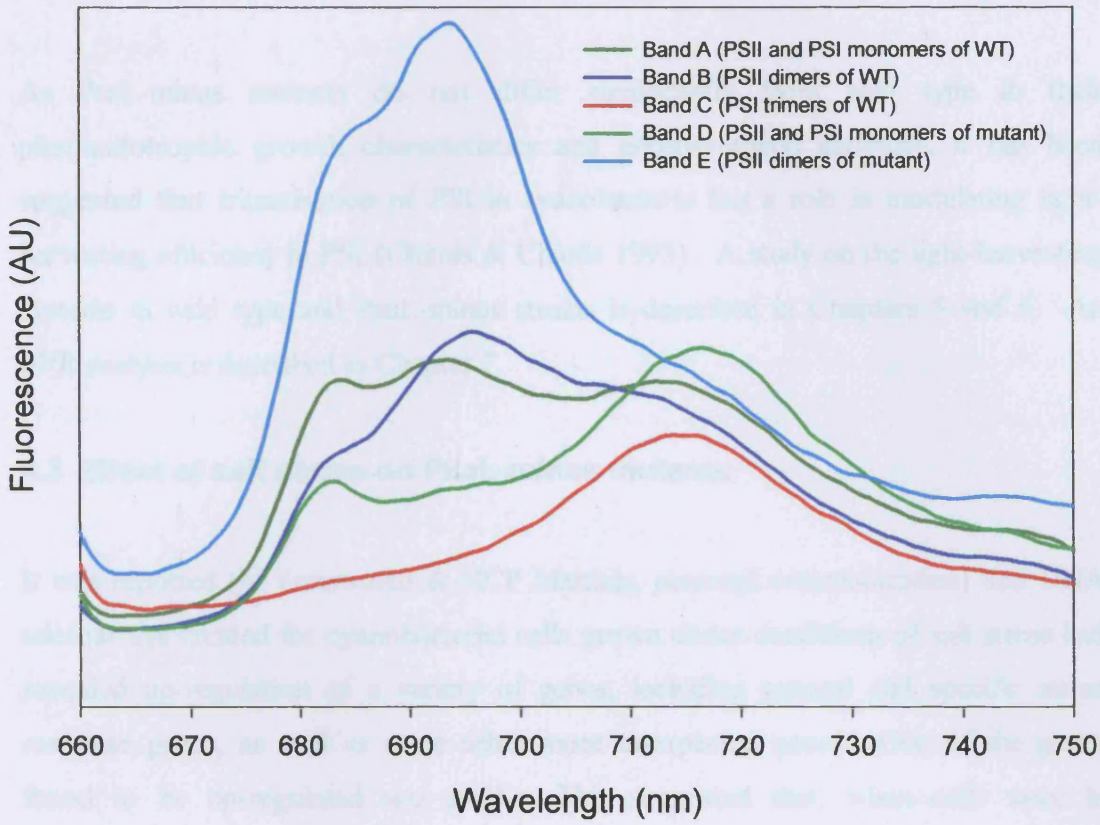

Figure 4.7 Fluorescence emission spectra at 77K with excitation at 435nm (chlorophyll-absorbed light) for samples of bands separated on sucrose density gradient profiles in Figure 4.6, which were derived from the solubilised thylakoids of *Synechococcus* wild type and PsaL-minus cells. The presence of PSI is indicated by a peak at around 720 nm. PSII is represented by peaks at 685 and 695 nm. The spectra confirm that PSI monomers were present in the upper bands in each gradient (bands A and D) along with some PSII. The thin lower band in each gradient (B and E) appears to contain PSII only. Band C contains PSI trimers and was found only in wild type.

4.2.4 Further analyses of PsaL-minus mutants

As PsaL-minus mutants do not differ significantly from wild type in their photoautotrophic growth characteristics and photosynthetic activities, it has been suggested that trimerisation of PSI in cyanobacteria has a role in modulating light-harvesting efficiency in PSI (Chitnis & Chitnis 1993). A study on the light-harvesting systems in wild type and PsaL-minus strains is described in Chapters 5 and 6. An EPR analysis is described in Chapter 7.

4.3 Effect of salt stress on PsaL-minus mutants

It was reported (N Yeremenko & HCP Matthijs, personal communication) that DNA microarrays created for cyanobacterial cells grown under conditions of salt stress had revealed up-regulation of a variety of genes, including general and specific stress response genes, as well as some other more unexpected genes. One of the genes found to be up-regulated was *psaL*. This suggested that, when cells were in conditions of salt stress, the trimeric structure of PSI was favoured over monomers, and that more PsaL subunit was synthesised so that the level of trimerisation was maximised under these conditions. We investigated the effects of salt stress on our PsaL-minus mutants.

4.3.1 The PsaL-minus mutant is not disadvantaged in salt stress conditions

When the *Synechocystis* 6803 PsaL-minus mutant and wild type cells were grown under salt stress conditions (by the addition of 0.5 M NaCl to the growth medium), there was no detectable disadvantage to the PsaL-minus strain despite the fact that it could only produce entirely monomeric PSI. The growth curves shown in Figure 4.8 compare the growth of the two strains in normal BG11 medium and in medium supplemented with salt. The initial exponential growth phase for both strains in both conditions was similar (with doubling times of 30-35 hours). Although the growth curves appear to diverge after several days of growth, the difference in OD_{750} between the stressed and unstressed flasks for each strain were the same. The salt-stressed

cultures of each strain grew slightly slower towards the end of the experiment. The PsaL-minus mutant did not appear to be adversely affected by the presence of elevated salt levels in the growth medium or at least not more than wild type.

4.3.2 The proportion of PSI in trimeric conformation does not alter with increased salt in the growth medium

In order to establish whether growth in salt stress conditions would actually result in an increased proportion of trimerised PSI, a series of sucrose density gradients were produced as shown in Figure 4.9. Wild type *Synechocystis* 6803 cells were used so that both trimeric and monomeric populations of PSI would be present in the cells. Gradient A in this figure was produced from solubilised photosystems from wild type cells grown for 7 days under normal conditions (standard BG11 medium). Gradient B was produced from photosystems of wild type cells that were grown in identical conditions to A but with the addition of 0.5M NaCl for the entire 7 day growth period and gradient C from cells that were grown in normal BG11 for 3 days then with added NaCl for the final 4 days (to 'salt shock' an established cell culture). Samples of solubilised photosystems from each culture with identical chlorophyll concentrations were loaded onto each gradient. There does not appear to be an increase in the proportion of trimerised PSI particles in the salt stress samples, as might be expected if the purpose of up-regulation of the *psaL* gene under salt stress was to increase the level of trimerisation. Indeed, if there is any difference in trimer:monomer ratio then there is a slight decrease in trimerisation under salt conditions.

4.4 Effect of growth in blue light on PsaL-minus mutants

It has been suggested that growth of cyanobacteria under dim blue light results in an increase in the amount of PSI produced (a higher PSI:PSII ratio) and that the PSI produced is strongly trimeric (a higher trimer:monomer ratio) (Petra Fromme, personal communication). This would suggest that dim blue light induces cells to produce large amounts of strongly trimeric PSI in order to better adapt themselves to these conditions. If this is true then it is possible that the PsaL-minus mutant would be disadvantaged as it cannot produce any trimeric PSI.

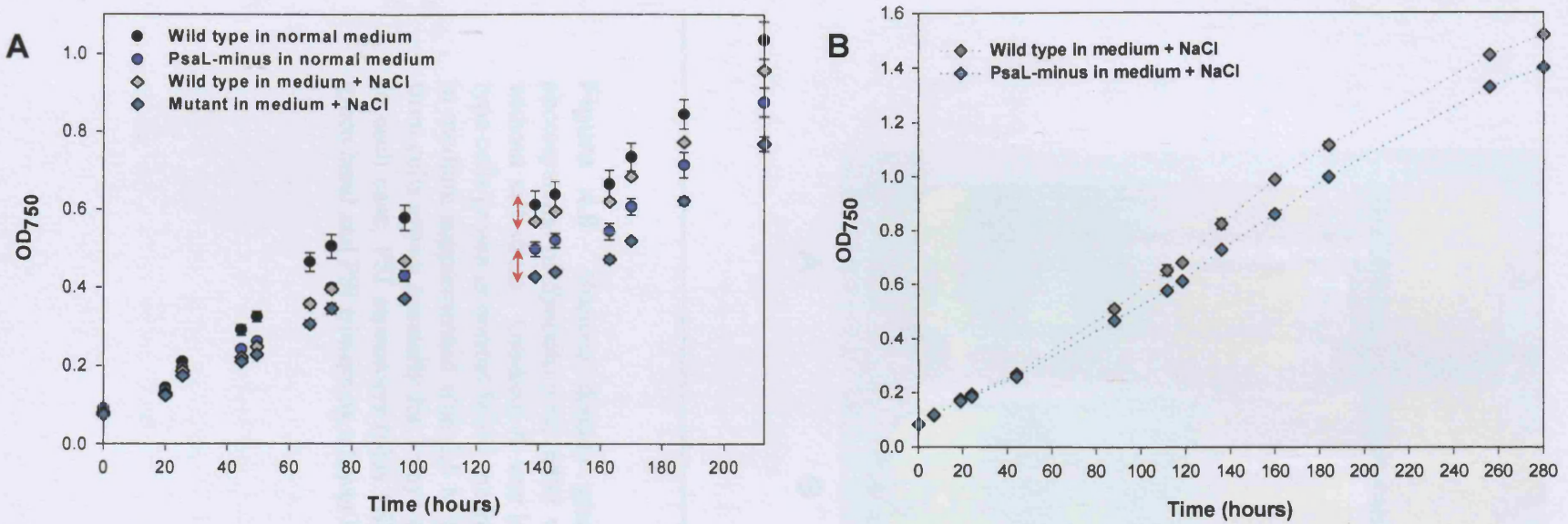

Figure 4.8 Growth curves for *Synechocystis* 6803 wild type and PsaL-minus cells grown in normal BG11 medium and BG11 supplemented with 0.5 M NaCl (**A**). The OD_{750} for each culture was measured (triplicate flasks for each of the growth conditions/strains) regularly for 200 hours. In the initial 60 hours of the experiment no difference in growth rate for any of the cultures was noticed with all cultures giving a doubling time of 30 to 35 hours. After 60 hours, the growth rates appear to diverge. The difference in OD_{750} between stressed and unstressed cultures of each strain were similar (indicated by red arrows). The experiment was later repeated for wild type and mutant cells grown in medium supplemented with 0.5 M NaCl (**B**) with similar results.

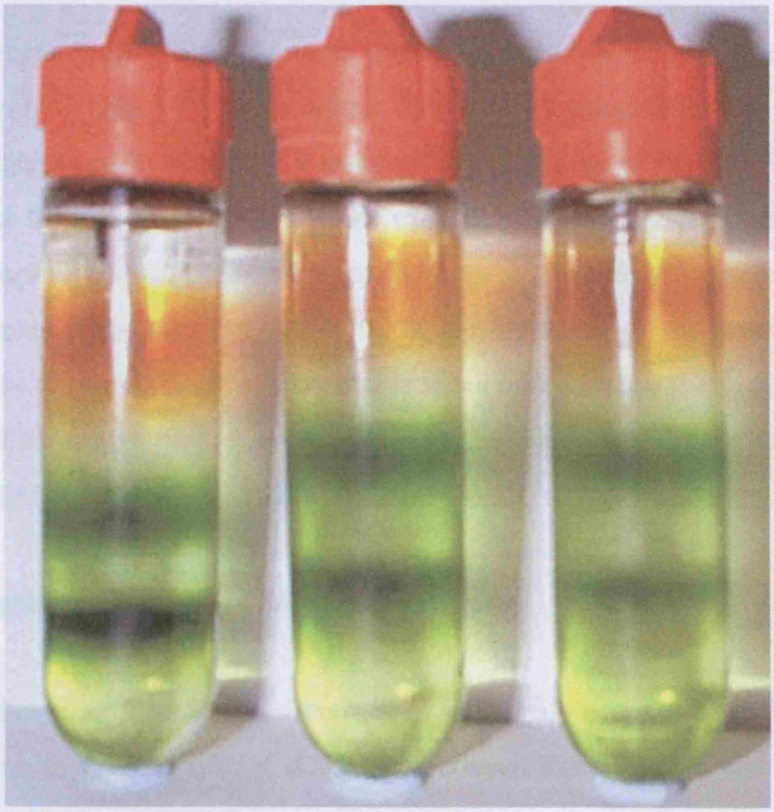

Figure 4.9 Sucrose density gradients to separate solubilised photosystems of *Synechocystis* 6803 wild type cells grown with and without salt stress. Gradient **A** was loaded with a sample from wild type cells grown in normal BG11 medium, gradient **B** from cells grown in medium supplemented with 0.5 M NaCl for 7 days and gradient **C** from cells grown normally for 3 days and then 0.5 M NaCl for 4 days. In each case, PSI monomers (plus PSII) are represented by an upper green band and PSI trimers by a lower band.

4.4.1 Blue light increases the trimer:monomer ratio of PSI

Wild type *Synechocystis* 6803 cells were grown in normal laboratory conditions and also under dim blue light. The cells in blue light grew considerably more slowly than usual as the light intensity was only 4 $\mu mol.m^{-2}.s^{-1}$. Samples of thylakoid membranes were extracted from the cells grown under each light source and solubilised samples of equal chlorophyll concentration were loaded onto sucrose density gradients. A pair of these gradients is shown in Figure 4.10. It can be seen that the lower band (PSI trimers) is more dense in the blue light sample when compared to the upper band (PSI monomers). This shows that growth under dim blue light does appear to cause cells to produce a higher proportion of trimeric PSI.

4.4.2 Blue light increases the PSI:PSII ratio

Figure 4.11 shows an absorbance spectrum of cells grown under blue light. There does not appear to be a significant difference between the wild type and PsaL-minus cells. Figure 4.12 shows 77K fluorescence emission spectra for the same cells after 4 days and 11 days growth under blue light. In both wild type and PsaL-minus cells, the PSI:PSII ratio increases after the cells have spent longer in blue light, adding weight to the argument that these light conditions induce PSI synthesis.

4.4.3 PsaL-minus mutants are disadvantaged under blue light conditions

Wild type and PsaL-minus strains of *Synechocystis* 6803 were grown under dim blue light and their growth rate was monitored. The experiment had to be conducted over the course of a month as the cells grow very slowly under such dim light. Several pairs of flasks for each strain were grown on separate occasions to ensure that the rates were reproducible. The average initial doubling times were found to be 33 hours for wild type and 49 hours for PsaL-minus cells. Growth curves are shown in Figure 4.13; the wild type cells grow significantly faster under the blue light conditions, demonstrating that the mutant is indeed disadvantaged in some way.

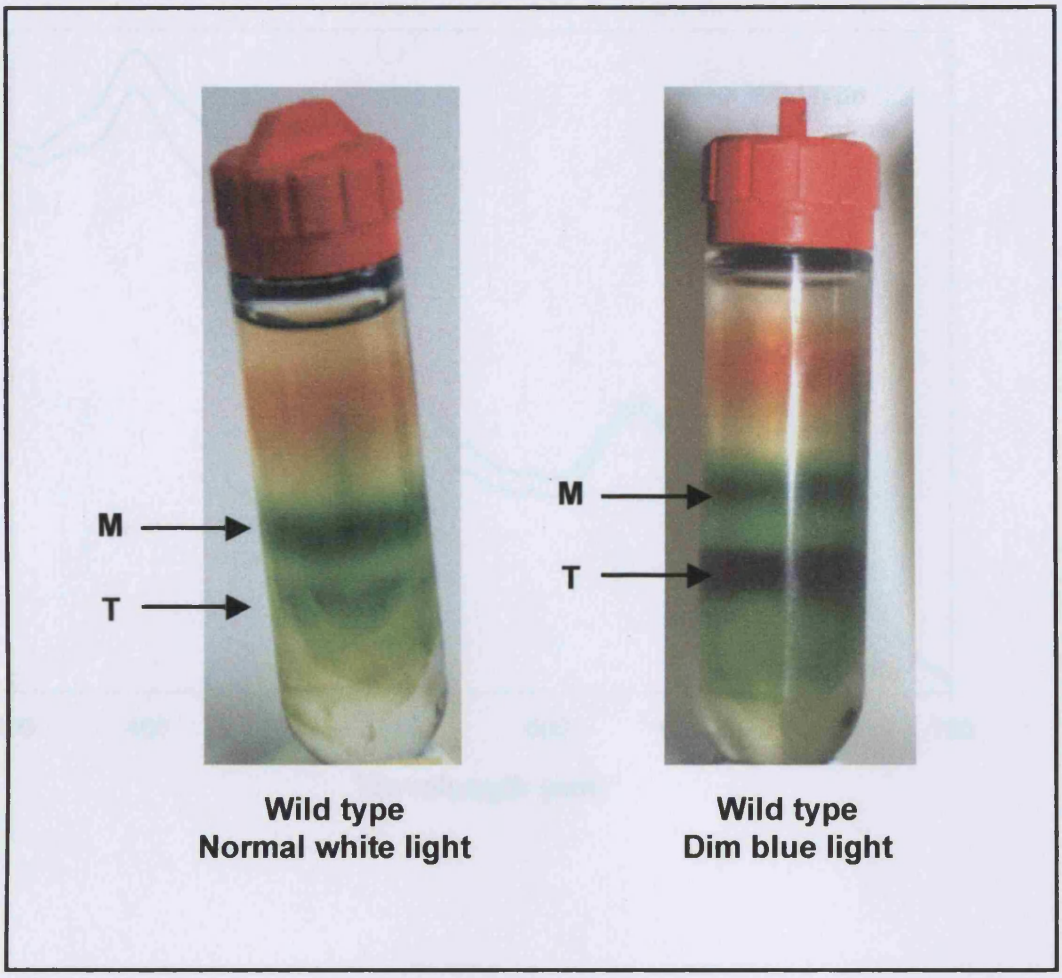

Figure 4.10 Sucrose density gradients for samples of photosystems isolated from *Synechocystis* 6803 wild type cells grown under normal white light laboratory conditions or dim blue light conditions. Samples of solubilised photosystems with equal chlorophyll concentrations were loaded onto each gradient and centrifuged overnight, resulting in the separation of monomeric PSI (**M**) and trimeric PSI (**T**). The blue light growth conditions result in a higher ratio of trimeric to monomeric PSI.

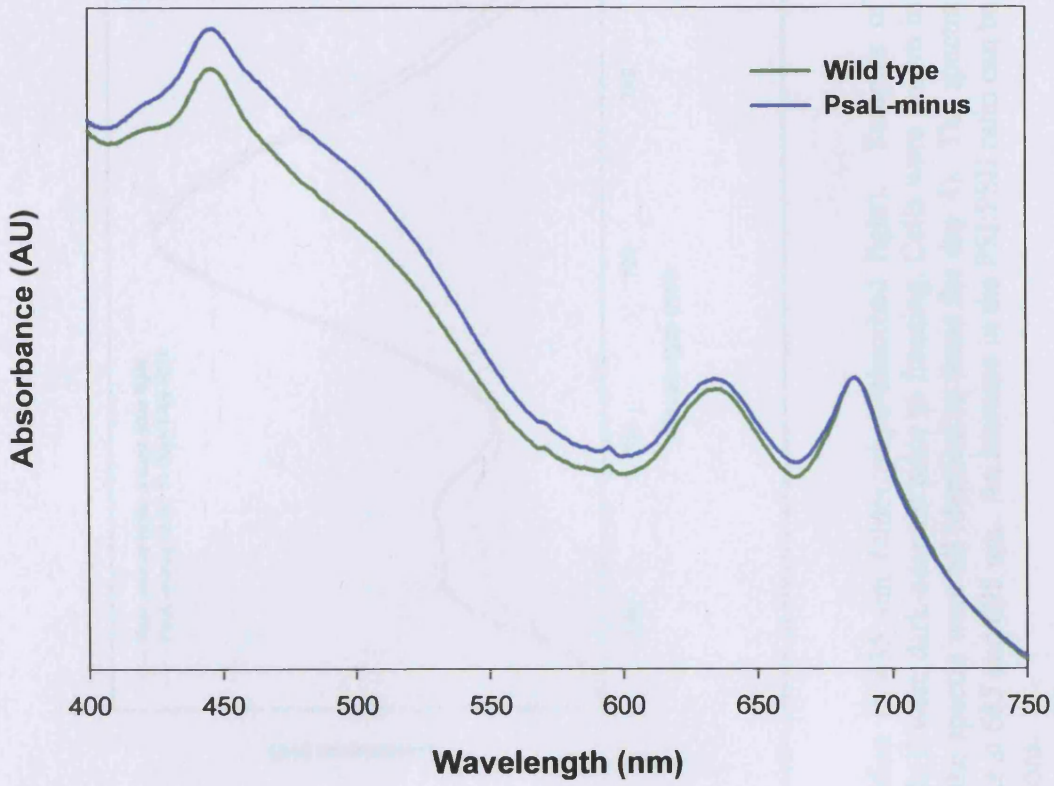

Figure 4.11 Absorption spectra at room temperature for *Synechocystis* 6803 wild type and PsaL-minus cells grown under blue light conditions. Spectra are normalised at 685 nm (chlorophyll *a*-absorbed light). The blue region of the spectrum (400-550 nm) reflects the absorbance from chlorophyll *a* and the carotenoids. The relative amount of absorbance in this region is higher for the PsaL-minus cells than for the wild type cells, suggesting an increased level of carotenoids.

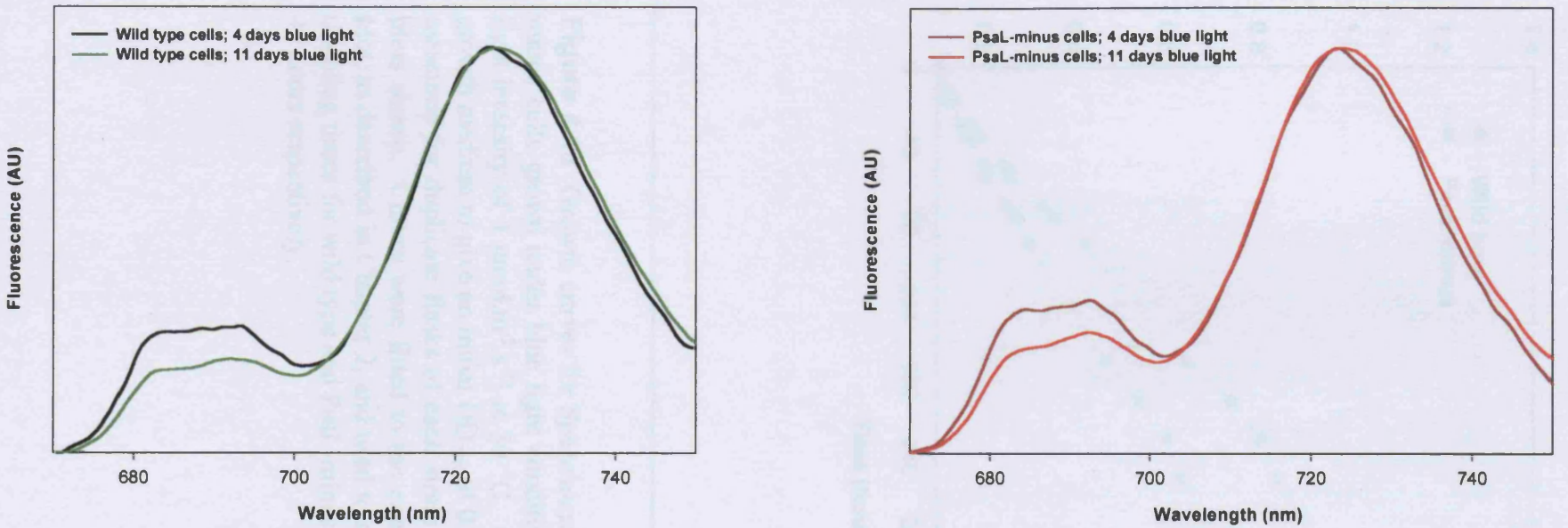

Figure 4.12 Fluorescence emission spectra at 77K with excitation at 435 nm (chlorophyll-absorbed light). Samples of *Synechocystis* 6803 wild type and PsaL-minus cells at 5 μM chlorophyll were dark-adapted prior to freezing. Cells were grown in dim blue light for 4 or 11 days before samples were taken (at day 0 the spectra were all identical to those for day 4). The spectra are normalised to the PSI peak at 715 nm. PSII is represented by peaks at 685 and 695 nm. An increase in the PSI:PSII ratio can be seen for each cell type after cells were left longer in blue light conditions.

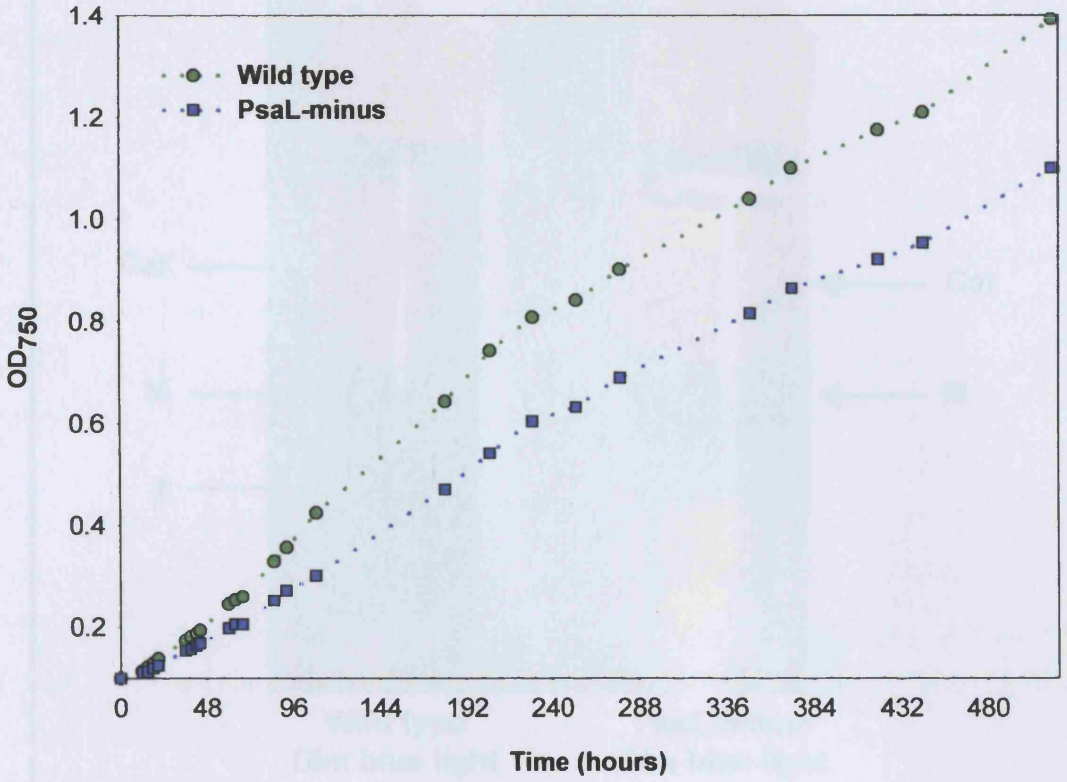

Figure 4.13 Growth curves for *Synechocystis* 6803 wild type and PsaL-minus cells grown under blue light conditions (Just Blue 079 filter and light intensity of 4 $\mu mol.m^{-2}.s^{-1}$) at 30 °C. Cells were added to flasks of growth medium to give an initial OD_{750} of 0.1. The increase in OD_{750} was measured for duplicate flasks of each strain and averaged to produce the plots shown. Curves were fitted to the exponentially rising part of each plot, as described in Chapter 2, and used to calculate doubling times. The doubling times for wild type and PsaL-minus cells were found to be 33 and 49 hours respectively.

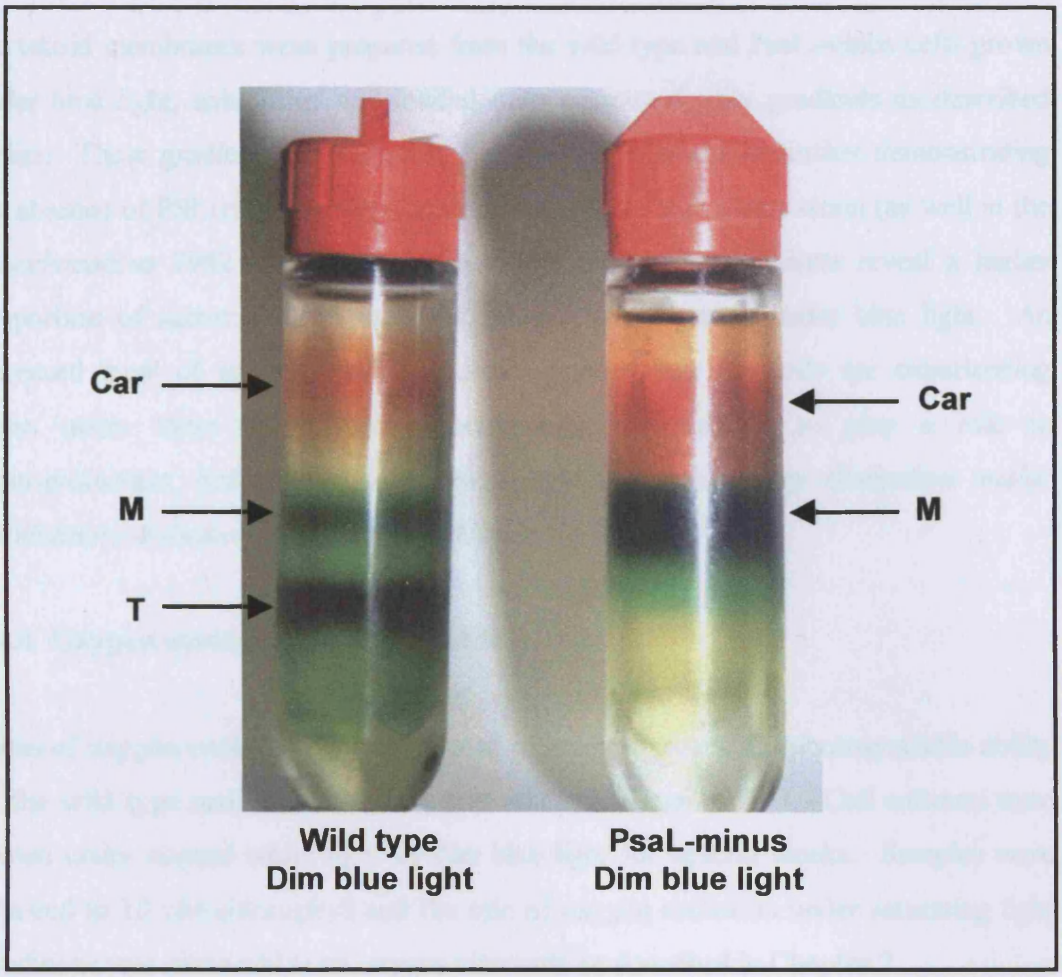

Figure 4.14 Sucrose density gradients for samples of photosystems isolated from *Synechocystis* 6803 wild type and PsaL-minus cells grown under dim blue light conditions. Samples of solubilised photosystems with equal chlorophyll concentrations were loaded onto each gradient and centrifuged overnight, resulting in the separation of monomeric PSI (**M**) and trimeric PSI (**T**). The carotenoids (**Car**) can be seen at the top of the gradients, with a higher percentage of the PsaL-minus sample consisting of carotenoids, indicating stress.

Thylakoid membranes were prepared from the wild type and PsaL-minus cells grown under blue light, solubilised and loaded onto sucrose density gradients as described earlier. These gradients are shown in Figure 4.14. As well as further demonstrating the absence of PSI trimers in the *Synechocystis* 6803 PsaL-minus strain (as well in the *Synechococcus* 7942 mutant shown in Figure 4.6), these gradients reveal a higher proportion of carotenoids in the PsaL-minus mutant grown under blue light. An increased level of synthesis of carotenoids implies that the cells are experiencing stress under these conditions as carotenoids are thought to play a role in photoprotection, defence against singlet oxygen, excess energy dissipation and/or stabilisation of photosystems (Frank & Cogdell 1995).

4.4.4 Oxygen electrode measurements

Rates of oxygen evolution were measured in order to assess the photosynthetic ability of the wild type and PsaL-minus mutant of *Synechocystis* 6803. Cell cultures were grown under normal white light or dim blue light for several weeks. Samples were adjusted to 10 μM chlorophyll and the rate of oxygen evolution under saturating light conditions was measured in an oxygen electrode as described in Chapter 2.

4.4.4.1 Oxygen evolution under saturating light

Figure 4.15 shows that, under saturating light conditions, the rate of oxygen evolution (per chlorophyll) was higher for both the wild type and mutant cells that had been grown under white light. (Although it is possible that the difference in rate could be influenced by a difference in photosystem ratio.) This suggests that photosynthetic efficiency was reduced in both strains by growth in the blue light conditions, although there was no additional evidence that the PsaL-minus mutant was at a disadvantage compared to wild type. The measurements were repeated on several occasions. On some occasions, it was observed that the PsaL-mutant did not appear to respire in the dark (i.e. there was no noticeable oxygen uptake before the light was switched on to induce oxygen evolution). This led us to postulate that the monomeric PSI in the thylakoid membrane had somehow disrupted the organisation of the membrane components, leading to a defective respiratory chain, despite the fact that

photosynthetic function was maintained. Another explanation would be that the PsaL-minus cells were unable to accumulate respiratory substrates, thus preventing respiration in the dark. However, this result was found not to be reproducible and the mutant respired normally on other occasions.

4.4.4.2 Oxygen evolution under blue light

The oxygen evolution of cells grown for a week under white or blue light conditions was measured with a 480 nm short pass filter to create blue light in the oxygen electrode chamber. Figure 4.16 shows the results of this experiment (it was not repeated sufficient times to allow error bars to be added). This experiment revealed that, with 50 $\mu mol.m^{-2}.s^{-1}$ blue light to induce oxygen evolution, the cells that had been grown under blue light conditions produced more oxygen than those that had been grown under normal white light. This is presumably because the blue-grown cells were better adapted to functioning under blue light. In this instance, the PsaL-minus mutant appears to be at a slight disadvantage when compared to wild type, although without error bars it is difficult to say whether this is true.

4.5 Characterisation of PsaE-minus mutants

4.5.1 Growth rate is slightly reduced in PsaE-minus mutants

Initial characterisation of the PsaE-minus mutant included comparing growth rate with that of wild type cells. Growth curves are shown in Figure 4.17. The growth rate was measured both by monitoring OD_{750} and by manual counting of cell samples. Cell counting was used as an additional method since the mutant cells tended to form small clumps in liquid culture. Rapid orbital shaking of growth flasks eliminated the clumping, which is presumed to be due to a high level of exopolysaccarhide production. With both methods, the PsaE-minus mutant grew at a reduced rate compared to wild type cells, suggesting that it was in some way disadvantaged under normal laboratory conditions. During the exponential growth phase of the OD_{750}-based experiment, the doubling times were found to be 34 hours for wild type cells and 46 hours for PsaE cells.

Absorbance and 77K fluorescence emission spectra for the PsaE-minus cells were identical to wild type spectra and are not shown.

4.5.2 PSI electron transfer may be altered in the PsaE-minus mutant

When the PsaE subunit was first characterised (Chitnis *et al* 1989a), it was reported that a *Synechocystis* 6803 PsaE-minus mutant had been created and that loss of the PsaE subunit had only minor phenotypic effects. One of the effects noted was a decrease in PSI activity to 70% of wild type levels (Chitnis *et al* 1989a). Rousseau *et al* (1993) suggested a role for PsaE in the interaction of ferredoxin with PSI, as PsaE-minus mutants showed a decrease in the rate of ferredoxin reduction. Many papers describing studies on PsaE have been published over the last decade (reviewed in Chapter 1) and a variety of roles for this subunit have been proposed but no definitive function has yet been determined. For this thesis it was decided that an EPR-based analysis of this mutant would be conducted, in an attempt to determine whether a lack of PsaE does have an effect on PSI electron transfer. The results of the EPR analysis of the PsaE-minus cells are described in Chapter 7.

4.6 The PSII-minus mutant background

The PSII-minus mutant lacks the PsbC and PsbD (C, D1 and D2) subunits of PSII (Vermaas *et al* 1990). No PSII is assembled in these cells and for this reason they require glucose for growth. Figure 4.18 shows 77K fluorescence emission spectra for *Synechocystis* 6803 wild type cells and the PSII-minus mutant cells. When the cells were excited with light of 435 nm, to excite chlorophyll, the spectrum for each strain included a large peak at around 720 nm, demonstrating the presence of PSI. The wild type strain also gave peaks at 685 and 695 nm, representing PSII. When the same samples were excited with light at 600 nm, absorbed by phycocyanin, the wild type cells gave a typical spectrum with peaks to present fluorescence by phycocyanin

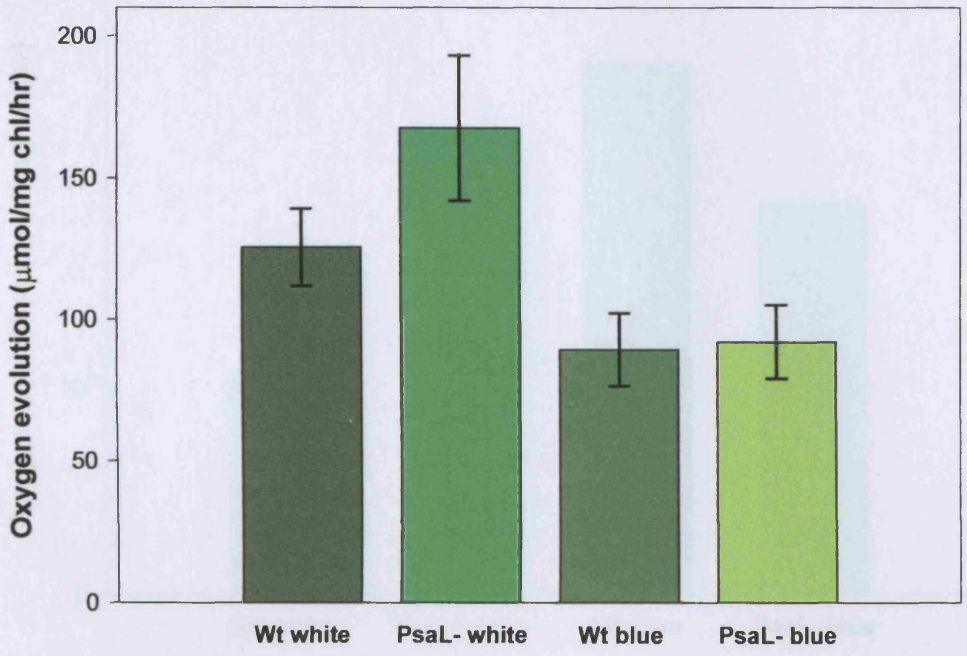

Figure 4.15 Oxygen evolution from wild type and PsaL-minus cells of *Synechocystis* 6803 under saturating light conditions (at least 400 $\mu mol.m^{-2}.s^{-1}$). Cultures were grown either under normal white light or dim blue light as indicated. Each bar shows the average oxygen evolution taken from at least seven measurements with different cultures and at different times.

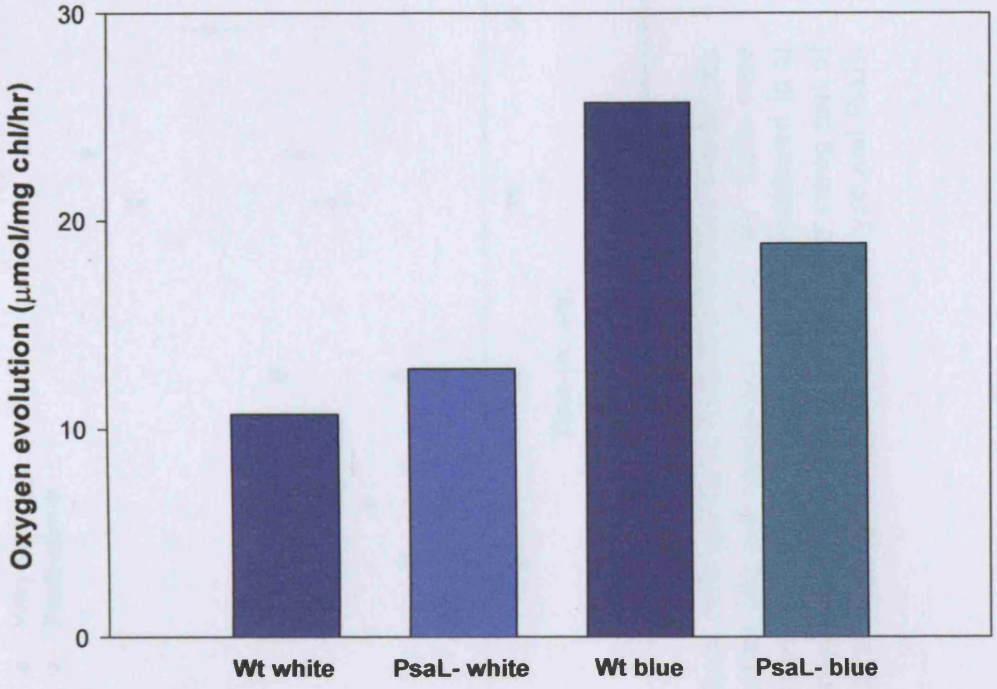

Figure 4.16 Oxygen evolution from wild type and PsaL-minus cells of *Synechocystis* 6803 measured under 50 µmol.m^{-2}.s^{-1} blue light. Cultures were first grown either under normal white light or dim blue light as indicated.

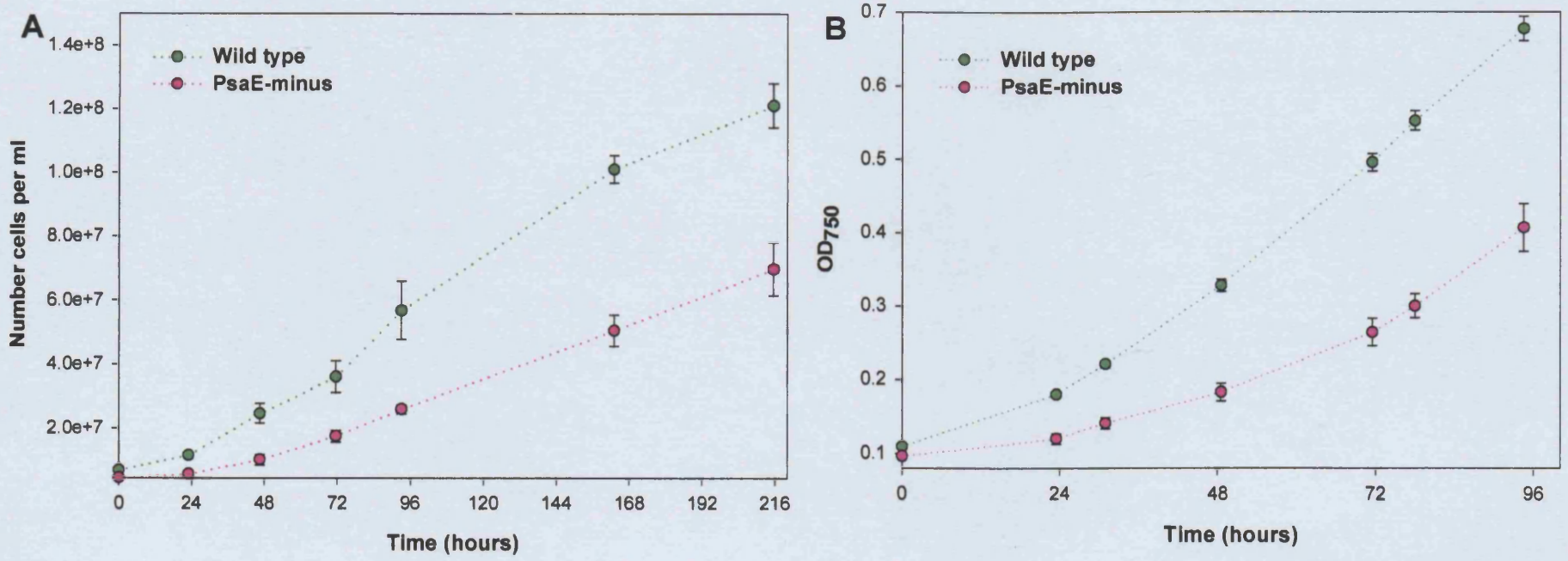

Figure 4.17 Growth curves for *Synechocystis* 6803 wild type and PsaE-minus cells grown in normal laboratory conditions. Two methods for estimating cell density were employed: manual cell counting (**A**) and monitoring OD_{750} (**B**) Cells were added to flasks of growth medium to give an initial OD_{750} of 0.1. The increase in cell number or OD_{750} was measured in at least triplicate for each strain and averaged to produce the plots shown. Curves were fitted to the exponentially rising part of each plot in **B**, as described in Chapter 2, and used to calculate doubling times. The doubling times for wild type and PsaE-minus cells were found to be 34 and 46 hours respectively.

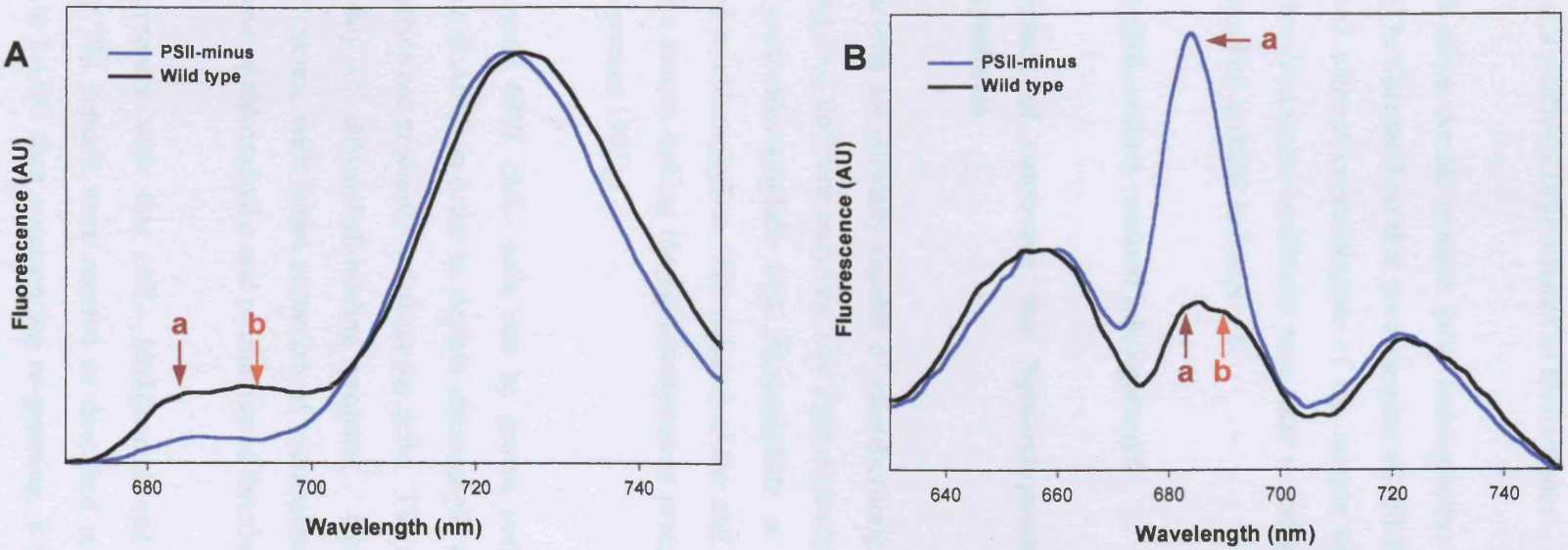

Figure 4.18 Fluorescence emission spectra with excitation at 435 nm (**A**) and 600 nm (**B**) for *Synechocystis* 6803 wild type and PSII-minus cells. Cells at 5 μM chlorophyll were dark adapted prior to freezing. Peaks at around 720 nm represent PSI, which is present in both strains. The wild type samples also contain PSII, which is represented by peaks at 685 nm (arrow **a**) and 695 nm (arrow **b**). The PSII-minus samples lack the 695 nm peak representing PSII. The apparently very large 685 nm peak seen for PSII-minus cells when excited at 600 nm (panel **B**) is due to uncoupled phycobilisomes generating a relatively large amount of fluorescence.

(653 nm), PSII (685 and 695 nm) and PSI (720 nm). The very large peak at 685 nm on the spectrum for the PSII-minus mutant is due to uncoupled phycobilisomes generating a relatively large amount of fluorescence.

The PSII-minus double mutants (also lacking either PsaL or PsaE) were created as described in Chapter 3 so that pure samples of PSI from each of these mutants could be isolated without contamination of the sample with PSII. This was particularly useful when iron stress conditions were used to induce the CP43' antenna system and this is described in detail in Chapter 6.

4.7 The *chl*L-minus mutant background

4.7.1 Effect of removing the light-independent pathway of chlorophyll synthesis

Cyanobacteria are normally capable of manufacturing chlorophyll in the light or in the dark using two different enzymes, one light-dependent and one light-independent, to convert protochlorophyllide into chlorophyllide *a*. The chlorophyllide *a* is then converted to chlorophyll *a*. The deletion of the *chlL* gene in *Synechocystis* 6803 has provided a mutant lacking the light-independent protochlorophyllide reduction branch (Wu & Vermaas 1995).

Synechocystis 6803 *chlL-* cells can be grown under light-activated heterotrophic conditions (LAHC) in order to deplete chlorophyll, while cell growth continues. The photosystems are gradually lost from the cells. The absence of chlorophyll decreases the stability of chlorophyll-binding proteins. Upon return to light conditions, greening occurs, with initial reduction of accumulated protochlorophyllide followed by synthesis of chlorophyll *a* and production of functional photosystems.

Double mutants with this *chlL-* background and the additional deletion of an accessory PSI subunit were created as described in Chapter 3. By growing these mutants in LAHC then commencing re-greening, it was hoped that the assembly of PSI and any effect of the missing polypeptides on this could be observed.

4.7.2 Bleaching and re-greening of *chlL*-minus cells

Cultures of *Synechocystis* 6803 wild type and *chlL*-minus cells were grown either under full illumination or in LAHC (complete darkness except for 10-20 minutes light per day). Glucose was added to the medium to support growth in the absence of photosynthesis for cells under LAHC. After 9 days under LAHC, the *chlL*-minus cells were entirely depleted of chlorophyll and were returned to full light conditions to attempt re-greening. The wild type cells under LAHC did not survive but the *chlL*- cells were visibly green after several days growth in full light.

Figure 4.19 shows absorbance spectra recorded at various points during the experiment. At the start of the experiment the spectra for all the cells were similar, with peaks representing phycobilins at about 630 nm and for chlorophyll *a* at 690 nm (data not shown). After 7 days growth the spectra for the *chlL*- cells grown under LAHC show a flattening of the chlorophyll peak. Some decrease in the chlorophyll peak was often seen after only 24 hours in the dark (data not shown). The wild type cells under LAHC continued to manufacture chlorophyll using the alternative enzymatic pathway using the light-independent enzyme. After complete chlorophyll depletion (assessed visibly after 9 days of LAHC), followed by a return to growth in full light, the reappearance of the peak for chlorophyll was seen (panel C of Figure 4.19). The cells were visibly green after several days in full light.

Fluorescence emission spectra at 77 K with excitation at 435 nm after 24 hours growth in either full light or LAHC are shown in Figure 4.20. After only 24 hours the *chlL*-minus cells under LAHC have already started to lose PSI, as indicated by the flattening of the PSI peak. The spectra for the cells grown under full light remain the same throughout the experiment, reflecting the normal rates of photosystem synthesis and turnover in these cells.

The *chlL*-minus cells can be bleached and re-greened as described above, providing an opportunity to study the assembly of photosystem I after complete depletion. It is hoped that this will be a useful tool in assessing the role of subunits of photosystem I in the biosynthetic pathway. Several attempts to grow the double mutants (*chlL*-

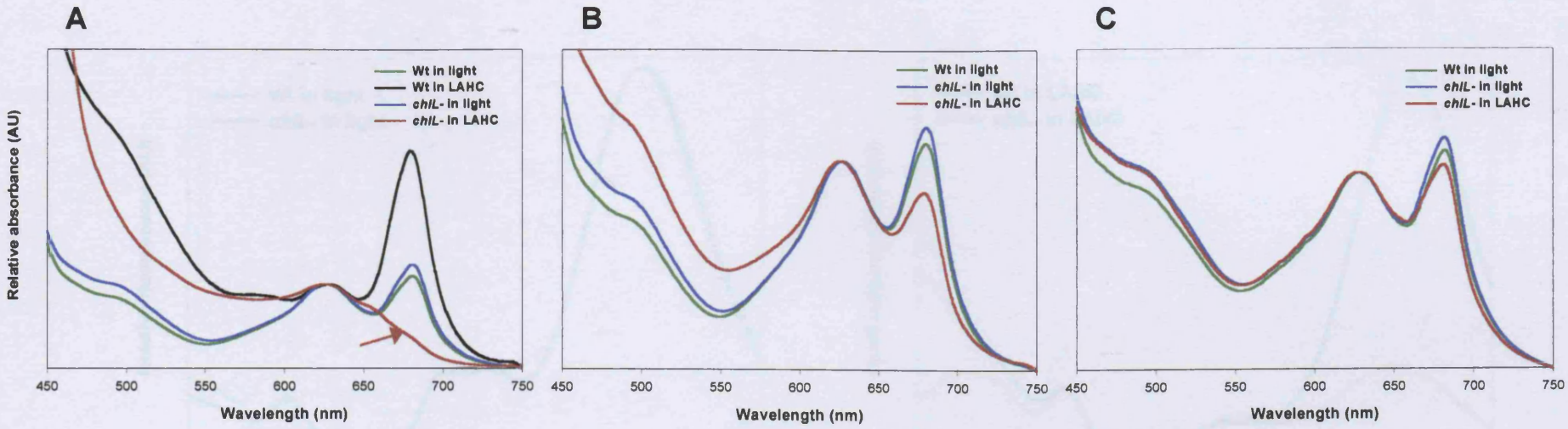

Figure 4.19 Absorbance spectra at room temperature to show the decreasing level of chlorophyll in *Synechocystis* 6803 *chlL*-minus cells during bleaching and the increasing chlorophyll level during re-greening. Spectra were recorded for both wild type cells and the *chlL*- mutant after growing either under white light or in LAHC (light-activated heterotrophic conditions) as indicated. After 7 days growth in these conditions (panel **A**) a decrease in the level of chlorophyll in the *chlL*- cells can be seen (red arrow). The bleached cells were then returned to the light and re-greening occurred to the bleached *chlL*- culture (panel **B**). The wild type cells in LAHC did not survive. After several weeks under full light conditions, the level of chlorophyll in the *chlL*- cells had returned to normal (panel **C**) and re-greening was complete.

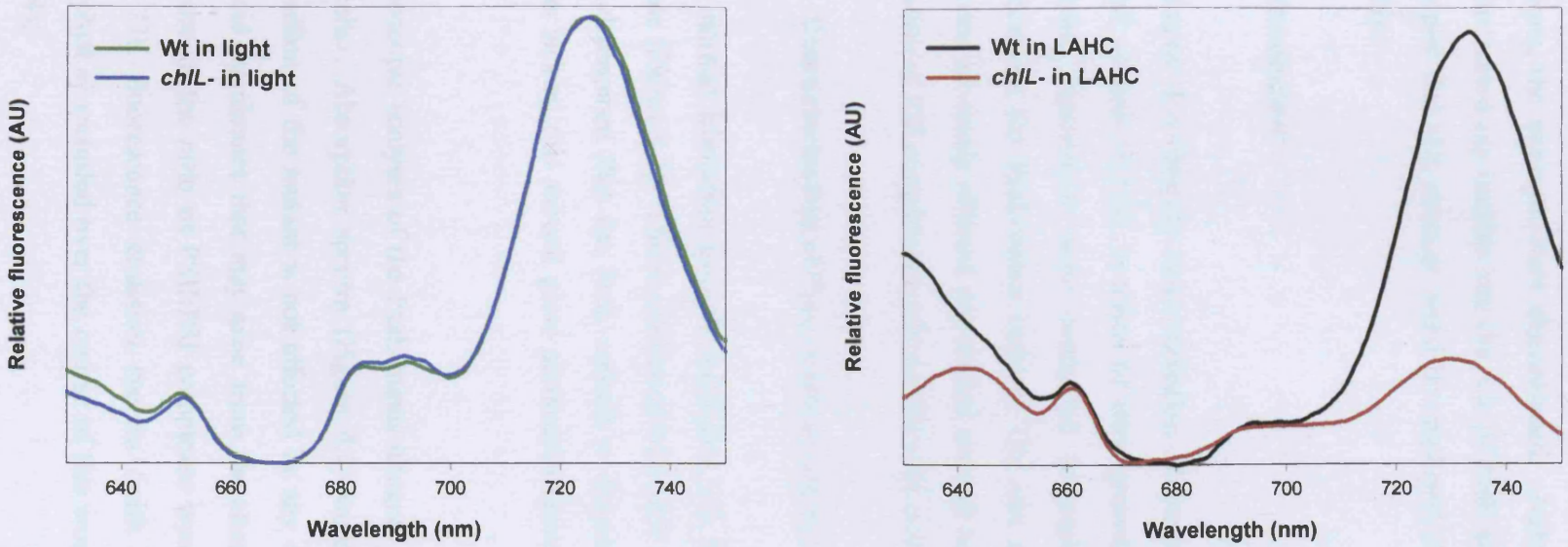

Figure 4.20 Fluorescence emission spectra at 77 K to show the decreasing level of PSI in *Synechocystis* 6803 *chlL*-minus cells during bleaching. Spectra were recorded for both wild type cells and the *chlL*- mutant after growing either under white light or in LAHC (light-activated heterotrophic conditions) as indicated. After 24 hours growth in these conditions, a decrease in the level of PSI was seen in the *chlL*- cells grown in LAHC.

psaE- and *chlL- psaL-*) under LAHC were unsuccessful. Unfortunately, primarily due to time constraints and difficulties maintaining viable cultures under these growth conditions, the attempts were discontinued. Although the double mutants did not therefore reveal any insights into the role of PsaE and PsaL in the biosynthesis of PSI, it is hoped that this strategy could be employed in the future to study photosystem assembly.

4.8 Discussion

This chapter describes the characterisation of cyanobacterial mutants lacking the PsaL or PsaE subunit of PSI, in terms of their growth rate and spectroscopic features. Additional experiments were conducted to explore the effect of various stress conditions on the PsaL-minus mutant. The aim was to find whether any of these conditions adversely affected this mutant enough to suggest that a wholly monomeric population of PSI complexes could put the cells at a disadvantage.

4.8.1 Characterisation of PsaL-minus mutants

Under normal laboratory growth conditions, the PsaL-minus mutants grew at wild type rate (Figure 4.1). This is consistent with early studies using PsaL-minus mutants, which determined that the PsaL subunit is dispensable for photosynthesis and that mutants lacking this subunit grew photoautotrophically at normal rates (Chitnis *et al* 1993).

Spectroscopic analyses of the PsaL-minus mutants were comparable to those of wild type cells. Absorption spectra (Figure 4.2) were used to show that the pigment composition of the mutant is not affected by any changes to the organisation of the thylakoid membranes that may arise from the altered PSI population. Similarly, no difference in the ratio of PSII:PSI complexes was observed from inspection of the many 77K fluorescence emission spectra (with excitation at 435 nm to excite chlorophyll *a*) recorded over the course of this work (examples shown in Figures 4.3 and 4.4).

The transfer of energy from the light-harvesting phycobilisomes to the photosystem reaction centres was examined using 77K fluorescence emission spectra with excitation at 600 nm (Figure 4.5). Again, the spectra recorded for the PsaL-minus mutant and wild type cells were similar, showing that energy could be transferred from the phycobilisomes to both PSII and to PSI, whether it is trimeric or monomeric. This shows that phycobilisomes are capable of successfully docking with monomeric PSI and, therefore, that the physiological reason for trimerisation is not to permit the association with the light-harvesting apparatus. The interaction of the phycobilisomes with PSI was investigated in greater detail in experiments described in Chapter 5.

The absence of trimeric PSI was confirmed using sucrose density gradients to separate the photosystems by molecular mass. An example of one of these gradients is shown (Figure 4.6) and spectroscopic analysis of the bands extracted from this gradient is presented (Figure 4.7). Although it is well documented that PsaL forms the trimerisation domain of cyanobacterial PSI (Chitnis & Chitnis 1993, Jordan *et al* 2001), this tells us what the polypeptide physically does, but it does not suggest why this is physiologically useful. As PSI is found in monomeric form in eukaryotic photosynthetic organisms, it seems reasonable to assume that the trimerisation seen in cyanobacteria is of some importance to these organisms, i.e. that trimerisation of PSI confers some advantage to the cyanobacterium. Much of the work presented in this thesis is aimed at discovering whether this is the case.

4.8.2 PsaL-minus mutants are not disadvantaged under salt stress

DNA microarray analysis designed to reveal cyanobacterial genes with up-regulated gene expression under salt stress showed, perhaps surprisingly, that transcription of the *psaL* gene was increased under salt stress (N Yeremenko & HCP Matthijs, personal communication). However, the PsaL-minus mutant did not appear to be adversely affected by growth in high salt medium, or at least to no greater extent than wild type cells (Figure 4.8). Sucrose density gradients to examine the photosystem populations of wild type cells grown under salt stress were produced (Figure 4.9). These did not reveal an increase in the proportion of trimerised PSI, as one might predict if the level of PsaL polypeptide being synthesised has been increased. These

experiments showed that growth in high salt conditions did not reveal any advantage in having the ability to trimerise PSI, nor did they show that trimerisation was increased at all as a result of salt stress. Kanesaki *et al* (2002) carried out DNA microarray analysis on *Synechocystis* 6803 cells under salt stress and found that the growth rate of stressed cells was decreased by 50%. The results presented here show some decrease in growth rate for salt stressed cells, although not such a marked reduction in growth rate. Kanesaki *et al* (2002) did not report an up-regulation of the *psaL* gene in salt stressed cells.

4.8.3 PsaL-minus mutants are disadvantaged under dim blue light conditions

It has been proposed that growth of cyanobacteria under dim blue light results in a shift in the trimer:monomer ratio of PSI in favour of the trimer and causes cells to produce large amounts of mostly trimeric PSI (P Fromme, personal communication). This intriguing suggestion prompted growth experiments in which PsaL-minus cells were placed under dim blue light, in order to establish whether their inability to carry out this shift toward trimerisation would place them at a disadvantage. Sucrose density gradients using wild type cells were produced and showed that there was indeed an increase in the proportion of trimeric PSI in cells grown in blue light (Figure 4.10). Furthermore, spectroscopic analysis of both wild type and PsaL-minus grown in blue light demonstrated a gradual change in the PSI:PSII ratio that appeared to confirm that PSI synthesis was increased. The PsaL-minus mutant grew significantly more slowly than wild type under the dim blue light conditions. These experiments provided growth conditions in which the PsaL-minus mutant was at a disadvantage because of its inability to produce trimeric PSI. Sucrose gradients derived from mutant cells grown under the blue light regime showed an increased proportion of carotenoids, suggesting that the cells were under stress.

Although the discovery of growth conditions that place the PsaL-minus mutant at a disadvantage indicate that there may indeed be some physiological reason for PSI trimerisation in cyanobacteria, the reason for the blue light effect is not clear. Further experiments using oxygen evolution measurements were carried out (see Section 4.4.4) in order to establish whether photosynthetic function was perturbed. A

lower rate of oxygen evolution was measured for both wild type and PsaL-minus cells grown under blue light (compared to those grown under standard laboratory conditions in white light). The oxygen evolution measurements did not, however, provide supporting evidence to show that the mutant was disadvantaged compared to wild type.

Initially it appeared that the PsaL-minus mutant, although able to photosynthesise normally when illuminated, did not respire in the dark. This led us to consider that the respiratory electron transfer chain had been disrupted in some way by the alteration to the thylakoid membrane arrangement. However, in subsequent repetition of the oxygen electrode experiments, the mutant respired normally. The reason behind the interesting effect found when using dim blue light to demonstrate the advantage of trimeric PSI remains unknown. We can speculate that the large number of monomeric PSI complexes being synthesised by the mutant cells are more difficult to pack into the membrane than the predominantly trimeric PSI in the wild type cells and that this has an adverse effect on the mutant cells capacity to thrive.

4.8.4 Characterisation of the PsaE-minus mutant

The PsaE-minus mutant was found to grow at a slightly reduced rate compared to wild type cells (Figure 4.17). No differences in the spectroscopic properties of the PsaE-minus mutant were found. Early reports on the PsaE subunit stated that PSI activity was reduced in the mutant (Chitnis *et al* 1989a). It was decided to use EPR analysis of PSI function to determine whether loss of either the PsaE or PsaL subunits had an effect on electron transfer through the PSI reaction centre core; the results are presented in Chapter 7.

4.8.5 The *chlL*-minus cells

It was anticipated that use of double mutants made using the *chlL*-minus background would give insights into the effect of losing accessory subunits on PSI assembly. Initial studies on the *chlL*-minus mutant showed that use of LAHC did lead to loss of almost all pigment and a reduction in the level of photosystems, as described by Wu

& Vermaas (1995). However, the LAHC make it difficult to maintain viable cultures and cells often cannot be re-greened after full chlorosis. This means that, although it is relatively straightforward to remove all chlorophyll, the most interesting and instructive stage of the experiment, involving the biosynthesis of new photosystems, is often not reached. Attempts to conduct experiments on the double mutants were abandoned due to time constraints.

CHAPTER FIVE

THE EFFECTS OF PSI MONOMERISATION ON STATE TRANSITIONS AND PHYCOBILISOME MOBILITY

CHAPTER FIVE

THE EFFECTS OF PSI MONOMERISATION ON STATE TRANSITIONS AND PHYCOBILISOME MOBILITY

5.1 Introduction

Green plants have LHCII light-harvesting antennae, which are integral parts of the photosystem structure and act to channel energy into the reaction centres. Cyanobacteria lack the LHCII structures but possess the functionally comparable extrinsic phycobilisomes. Phycobilisomes are large, soluble, highly ordered complexes consisting of phycobiliproteins and linker proteins (Bald *et al* 1996). They are present on the cytoplasmic surface of the thylakoid membrane. Their structure consists of a core with rods radiating outward. The phycobiliprotein composition varies between species. *Synechocystis* 6803 phycobilisomes consist of a core of allophycocyanin with phycocyanin rods. The phycobiliproteins allow efficient transfer of energy down the rod pigments to the core and then on to the chlorophyll antennae of the photosystem reaction centres. Phycobilisomes are highly mobile and can directly interact with both PSI and PSII (Mullineaux 1997, Sarcina *et al* 2001).

Different light conditions favour light absorption by different photosystem populations. It may be necessary for cells to make rapid adjustments to the balance of light absorption by PSI or PSII. Adjusting the PSI:PSII ratio by protein synthesis can take hours or days. A rapid method of adjustment is achieved when cells undergo state transitions, which can occur on a second to minute timescale. In cyanobacteria state transitions are achieved by reorganisation of the phycobilisomes, which can move quickly across the thylakoid membrane surface in order to redistribute their energy to either PSI or PSII as needed. Cells are in state 1 when the phycobilisomes are predominantly coupled to PSII and in state 2 when they are associated primarily with PSI. In plants a similar state transition occurs, with the LHCII being mostly associated with PSII in the thylakoid grana in state 1 and with stromal PSI in state 2. In both systems the light-harvesting antennae are required to be able to travel relatively far and to be able to couple transiently to both photosystem populations.

In this chapter the light harvesting by phycobilisomes in PsaL-minus cells, which contain entirely monomeric PSI, is investigated. Initial studies showed that the association of phycobilisomes to monomeric PSI could occur and that their energy transfer to the reaction centre was unhindered. Further investigation into the kinetics of the state transition and FRAP experiments to determine the effects on phycobilisome mobility in this altered membrane environment were conducted. This study was conducted using the wild type and PsaL-minus mutant cells of *Synechococcus* 7942. The thylakoid membranes of this cyanobacterium have a very regular arrangement of concentric cylinders along the long axis of the cell, making them ideal for FRAP measurements (Mullineaux & Sarcina 2002). The data presented in this chapter were recently published in Aspinwall *et al* (2004b).

5.2 Energy transfer from phycobilisomes to photosystem reaction centres

The thylakoid membranes of wild type cyanobacteria contain dimeric PSII and both monomeric and trimeric forms of PSI, whereas in PsaL-minus mutants the thylakoids contain only monomeric PSI along with PSII. Although this is likely to result in a difference in the structural arrangement of the membranes, there appears to be little effect on either the pigment composition of the cells or the PSII to PSI ratio (see Chapter 4). The mobile light-harvesting phycobilisomes move across the surface of the membrane, channelling energy into the reaction centres of both PSII and PSI complexes. To determine whether the different membrane organisation found in PsaL-minus mutants affected phycobilisome function, the interaction with the photosystems was characterised.

The transfer of energy from phycobilisomes to the photosystem reaction centres can be observed by measuring fluorescence emission at 77K for whole cells excited at 600 nm. In Figure 5.1, spectra for *Synechococcus* 7942 wild type and PsaL-minus cells are compared and shown to be of similar shape. The transfer of energy from the phycobilisomes to PSI (indicated by the peak at 715 nm) and PSII (indicated by the shoulder at 695 nm) reaction centres is therefore unimpaired in cells lacking the PsaL

subunit of PSI. Phycobilisomes can interact effectively with PSI either in its monomeric or trimeric form.

5.3 State transitions occur normally in PsaL-minus cells

In order to further examine the interaction of phycobilisomes with monomeric PSI, the ability of PsaL-minus cells to perform state transitions was examined. This can be monitored by comparing the 77K fluorescence emission spectra of cells adapted to either state 1 using a red light source or to state 2 by incubation in darkness. When excited at 435 nm (chlorophyll excitation) or 600 nm (phycocyanin excitation), a difference in the relative emission of PSII to PSI indicates that a state transition can occur. The PSII emission (at 685 and 695 nm) is lower relative to that of PSI (at 715 nm) and phycocyanin (at 654 nm) when cells are adapted to state 2. This decrease in PSII emission when the phycobilisomes are excited can be explained by movement of the phycobilisomes from PSII to PSI during the state transition. The decrease in PSII emission when chlorophyll is excited is not understood. In fact it has been shown that state transitions can cause only one of these two spectral changes rather than both (Emlyn-Jones *et al* 1999).

In this study using both *Synechocystis* 6803 and *Synechococcus* 7942 species, state transitions can be detected for both wild type and PsaL-minus mutant cells. Figure 5.2 shows a typical set of spectra for *Synechococcus* 7942 cells. The reduced emission from PSII for cells in state 2 as compared to cells in state 1 is clear for both wild type and mutant cells and at both excitation wavelengths. There is no difference in the sets of spectra for wild type and mutant cells, showing that state transitions can occur in either type of membrane arrangement. A similar set of spectra can be obtained for *Synechocystis* 6803 cells treated in the same way (data not shown), although the alteration to the PSII emission is less pronounced.

5.4 The rate of state transitions is increased in cells lacking PsaL

Previous work by Schluchter *et al* (1996) with *Synechococcus* 7002 cells followed the state 2 to state 1 transition by inducing the transition then recording the resulting

fluorescence transient. They found that state transition kinetics were faster in a PsaL-minus mutant when compared to wild type. A similar strategy was employed to study the kinetics of state transitions in the *Synechococcus* 7942 mutant for this thesis.

Cells with equivalent chlorophyll concentrations in fresh growth medium were dark-adapted to induce state 2. DCMU was added in order to block the flow of electrons from PSII to the PQ pool. Upon illumination of the adapted cell samples with phycobilin-absorbed light, the mobile electron carriers of the thylakoid membranes become oxidised and cells are driven into state 1. The PSII reaction centres are closed (due to the presence of DCMU) and the phycobilisomes shift from PSI complexes to couple with PSII in an attempt to amplify their light-harvesting capacity. By monitoring the induced rise in fluorescence, the kinetics of this transition can be measured.

There is a sharp initial increase in fluorescence (lasting 1 ms) when the illumination is initially applied, as the application of a light source causes fluorescence emission. This initial rise also represents the closure of PSII traps. This sharp rise can be subtracted from each trace, leaving the fluorescence rise attributed to the state transition (occurring on a second to minute time scale). Figure 5.3 shows typical original traces for *Synechococcus* 7942 wild type and PsaL-minus mutant cells, along with traces with an exponential rise fitted as described in Chapter 2. After several repetitions, average rates for each cell type were calculated.

Figure 5.4 shows a typical fluorescence trace for each cell type overlaid and normalised such that the eventual maximal fluorescence would be the same for each trace. The kinetics of the state transition are visibly faster for the mutant cells. Table 5.1 presents the half-times for the fitted exponential rises for each cell type. The wild type cells had an average half-life of 23.9 ± 4.5 s and the mutant an average of 13.0 ± 2.1 s. This difference in rate was shown to be significant by an unpaired T-test, which gave a P value of 6×10^{-6}. Overall the rate of state transition was approximately 1.8 times faster with PsaL-minus cells than with wild type.

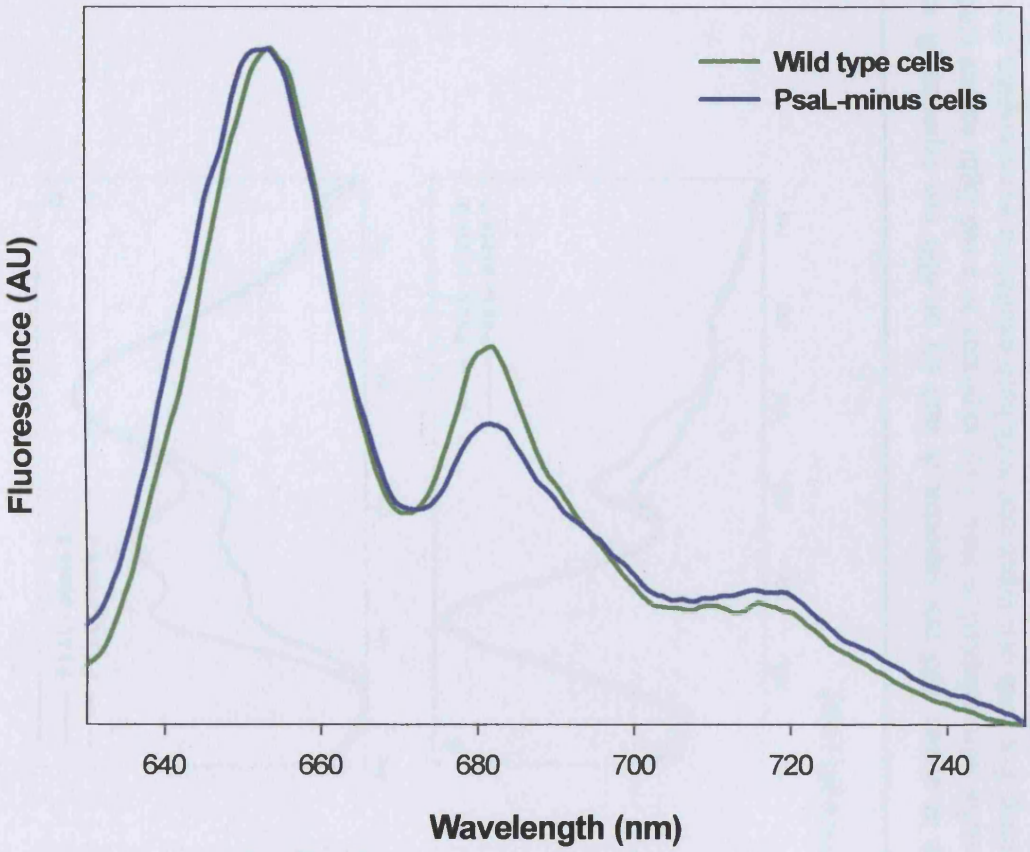

Figure 5.1 Fluorescence emission spectra at 77K with excitation at 600nm (phycocyanin-absorbed light). Samples of *Synechococcus* 7942 wild type and PsaL-minus cells at 5 μM chlorophyll were dark-adapted prior to freezing. The spectra are normalised to the phycocyanin peak at 653 nm. The presence of peaks representing PSI (at 715 nm) and PSII (at 695 nm) imply that energy from the excited phycobilisomes is being successfully transferred to these reaction centres.

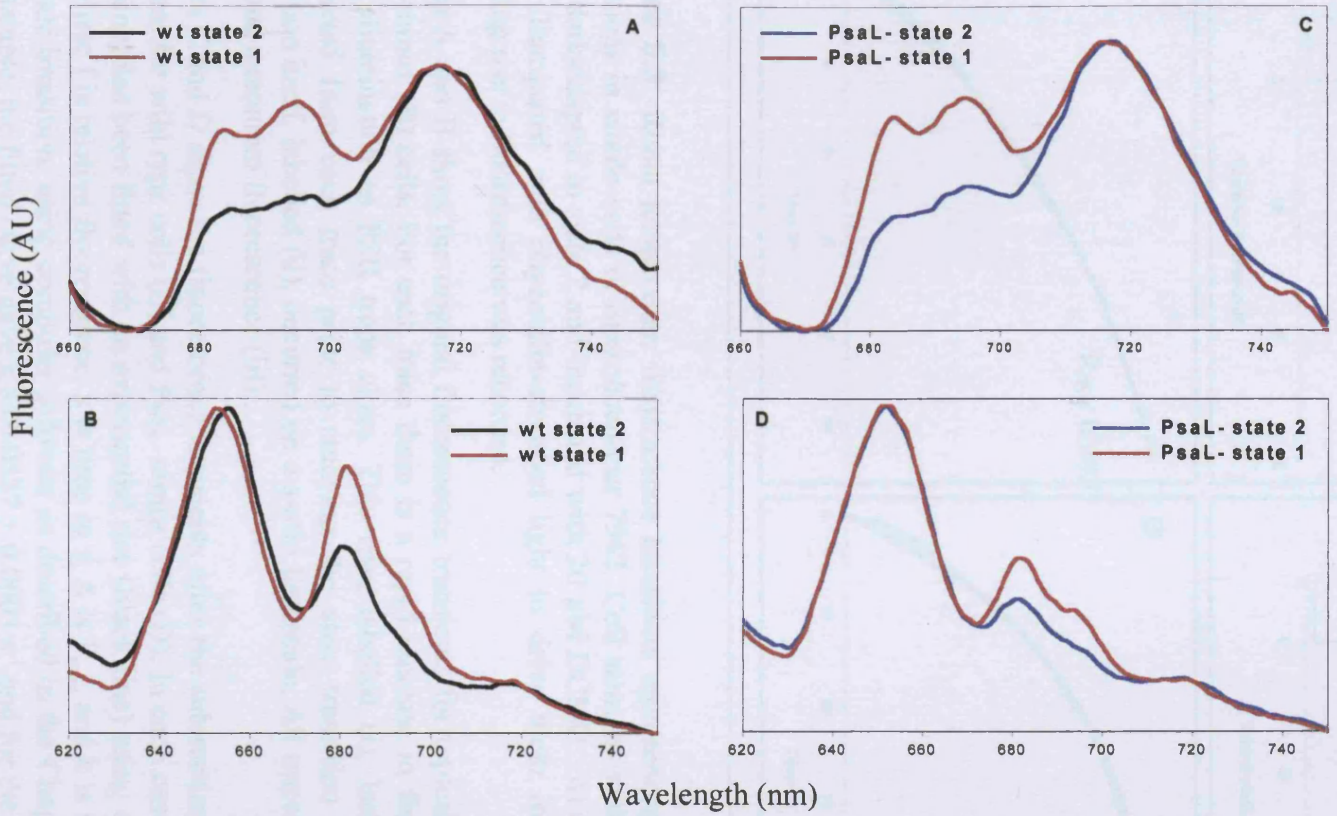

Figure 5.2 Fluorescence emission spectra at 77K with excitation at either 435 nm (spectra A and C) or 600 nm (spectra B and D). *Synechococcus* 7942 wild type (A and B) and PsaL-minus (C and D) cells were adapted to state 1 by exposure to a red light source (red lines) or to state 2 by incubation in darkness (black or blue lines) before freezing. For both cell types and with both excitation wavelengths, the state 2 spectra exhibit lower PSII fluorescence (at 685 and 695 nm) relative to that of PSI (at 715 nm). This is indicative of the ability to adapt to the different light conditions by performing state transitions.

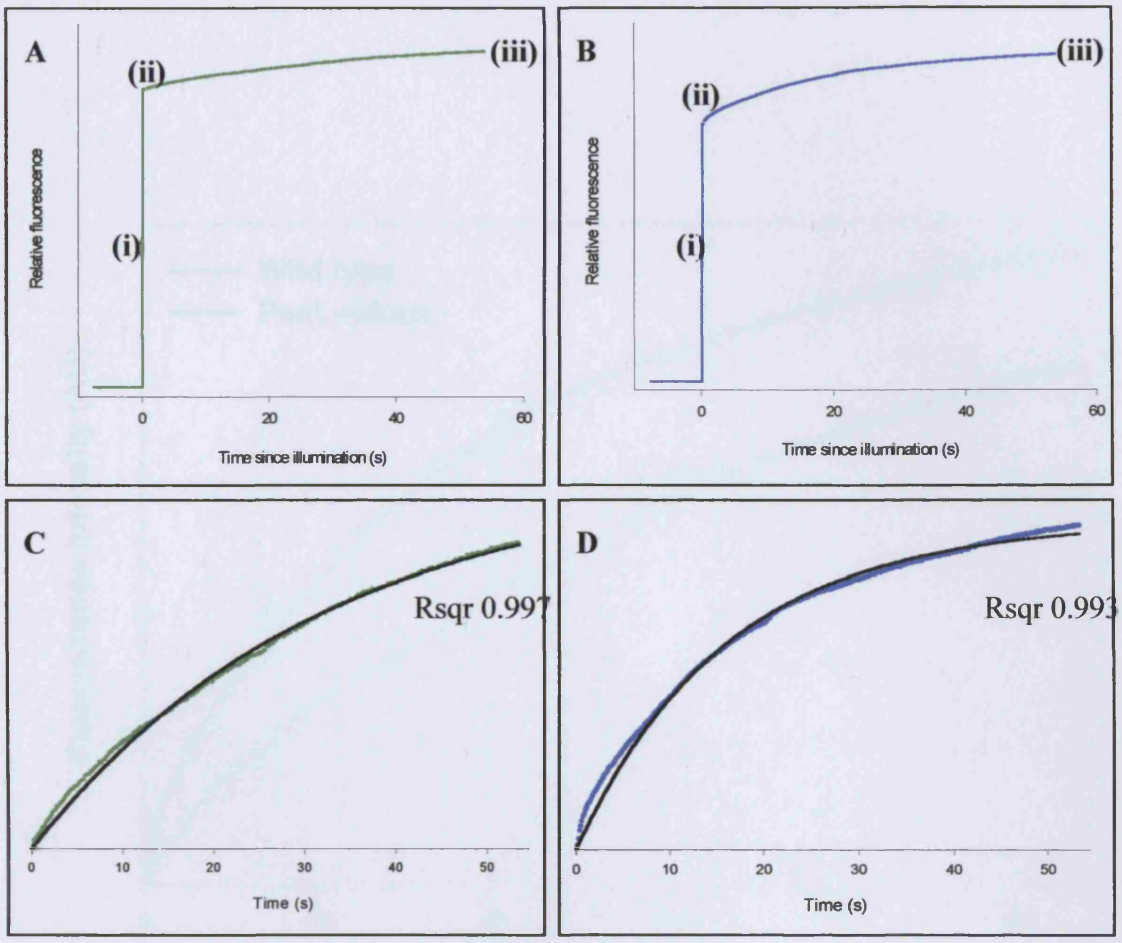

Figure 5.3 Room temperature fluorescence transients representing state 2 to state 1 transitions in whole cells of *Synechococcus* 7942. Cell samples with 3 μM chlorophyll were dark-adapted to state 2 and incubated with 20 μM DCMU. At time = 0 s, the cells were illuminated with phycobilin-absorbed light to drive them into state 1 and the resulting rise in fluorescence was recorded.

Traces A and B show the original fluorescence transients for typical wild type (A) and PsaL-minus (B) cells. For each trace there is a rapid increase in fluorescence intensity upon illumination as PSII traps close. This rise, labelled (i), lasted 1 ms and was subtracted from each trace prior to studying the state transition kinetics. The state transition itself, labelled (ii), occurred on a s-min timescale. All traces tended towards an eventual maximum fluorescence (iii).

Traces C and D show the fluorescence transients after the subtraction of the initial rapid increase for wild type cells (C) and PsaL-minus cells (D). In each case the trace (green or blue line) has been fitted with an exponential rise (black line) using equation $f=A(1-\exp^{-kx})$, where f is relative fluorescence, x is time in s, A is F_{max} and k is the rate constant for the state transition, using computer software as described in the Chapter 2. For this wild type sample, the fitted curve gave k as $0.0327 \pm 0.0003\ s^{-1}$ and for the PsaL-minus mutant sample k is $0.0624 \pm 0.0005\ s^{-1}$. Values for repeat experiments with different cell samples are listed in Table 5.1.

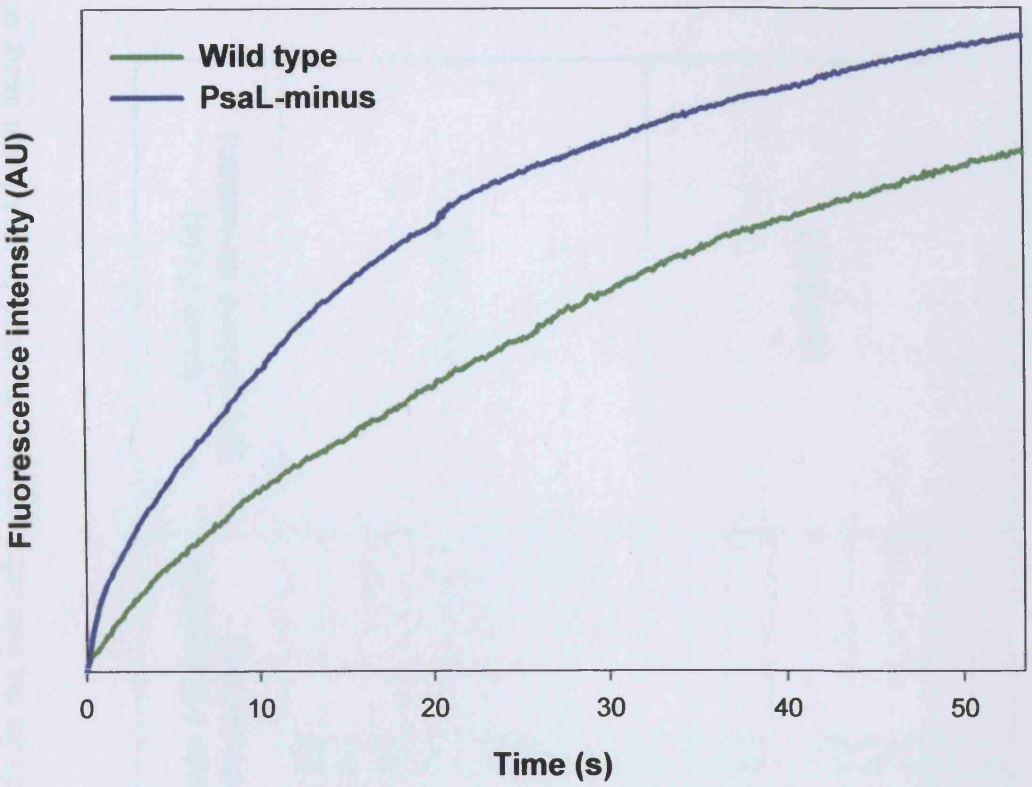

Figure 5.4 Room temperature fluorescence transient traces, representing the transition from state 2 to state 1 in *Synechococcus* 7942 cells. Cell samples with 3 μM chlorophyll were dark-adapted to state 2 and incubated with 20 μM DCMU. At time 0 s the cells were illuminated with phycobilin-absorbed light to drive them into state 1 and the resulting rise in fluorescence was recorded.

Typical traces for wild type (green line) and mutant (blue line) cells are shown after subtraction of the immediate, dramatic fluorescence rise (lasting 1 ms) and with normalisation to equivalent eventual maximum fluorescence. The traces shown have half-times of 23 s for wild type cells and 11 s for mutant cells.

Table 5.1 Values for t½ for state 2 to state 1 transitions in *Synechococcus* 7942 wild type and PsaL-minus cells as measured by room temperature fluorescence transients. The difference in the mean t½ for the two cell types was found to be significant using an unpaired student T-test, which gave P as 5.6×10^{-6}.

Cell type		Mean t½ (s) for state 1 transition [± standard deviation]	Mean t½ (s) [± standard deviation]
Wild type	1	27.4 ± 0.6	23.9 ± 4.5
	2	17.9 ± 0.2	
	3	23.5 ± 0.4	
	4	22.1 ± 0.1	
	5	22.6 ± 0.2	
	6	21.2 ± 0.2	
	7	30.9 ± 0.7	
	8	29.9 ± 0.3	
	9	20.0 ± 0.2	
PsaL-minus	1	13.8 ± 0.1	13.0 ± 2.1
	2	15.1 ± 0.1	
	3	16.8 ± 0.2	
	4	11.4 ± 0.1	
	5	11.5 ± 0.2	
	6	13.3 ± 0.1	
	7	13.5 ± 0.1	
	8	11.1 ± 0.1	
	9	10.5 ± 0.1	

5.5 Phycobilisome mobility is faster in cells lacking PsaL

The rate of diffusion of phycobilisomes in *Synechococcus* 7942 cells was measured *in vivo* using the FRAP technique (Sarcina *et al* 2001). Cells were first elongated using DMSO as described in Chapter 2. This causes cells that are typically 3 μm in length to elongate to 10 μm or more by inhibiting cell division (Mullineaux & Sarcina 2002). A highly focused laser beam is used to bleach a line across the centre of a cell under a scanning confocal microscope, causing the chromophores in this region to become bleached. The wavelength of the laser can be altered to target different fluorescent pigments, which could be a constituent of the target or an added tag. The recovery of fluorescence in this region is monitored and used to determine the rate at which unbleached chromophores are able to diffuse into this area (Mullineaux *et al* 1997).

In these experiments, the phycobilisomes were targeted (using excitation at 633 nm and measuring emission at 650 nm) in samples of both wild type and PsaL-minus cells. Figure 5.5 shows a series of images for a typical representative of each cell type. Prior to bleaching, each cell has a relatively uniform level of fluorescence along its length, showing an even distribution of phycobilisomes. After the bleach, a region of reduced fluorescence intensity indicates that the phycobilisomes have been bleached out. Subsequent images from the time series show the fluorescence intensity increasing again, as phycobilisomes diffuse back into this area. Analysis of each series of images is carried out as described in Chapter 2. Figures 5.6 and 5.7 show an example of one wild type cell from this set of FRAP experiments undergoing some of the key steps in the analysis. Figure 5.8 shows examples of the plots used to calculate the diffusion coefficients for each of the cell types. It is interesting that the plot for the PsaL-minus mutant intercepts the y-axis at a higher point, demonstrating that the bleached area was wider for this cell than for the wild type cell when the recording images of the recovery started at time 0 s. Since the experiment was carried out consistently with same timings for each cell, this difference in the width of the bleach at time 0 s suggests that the phycobilisomes were diffusing more rapidly in the mutant, causing an increased spread of the bleached area by time 0 s (the time between photobleaching and recording the first image of the series taken during the

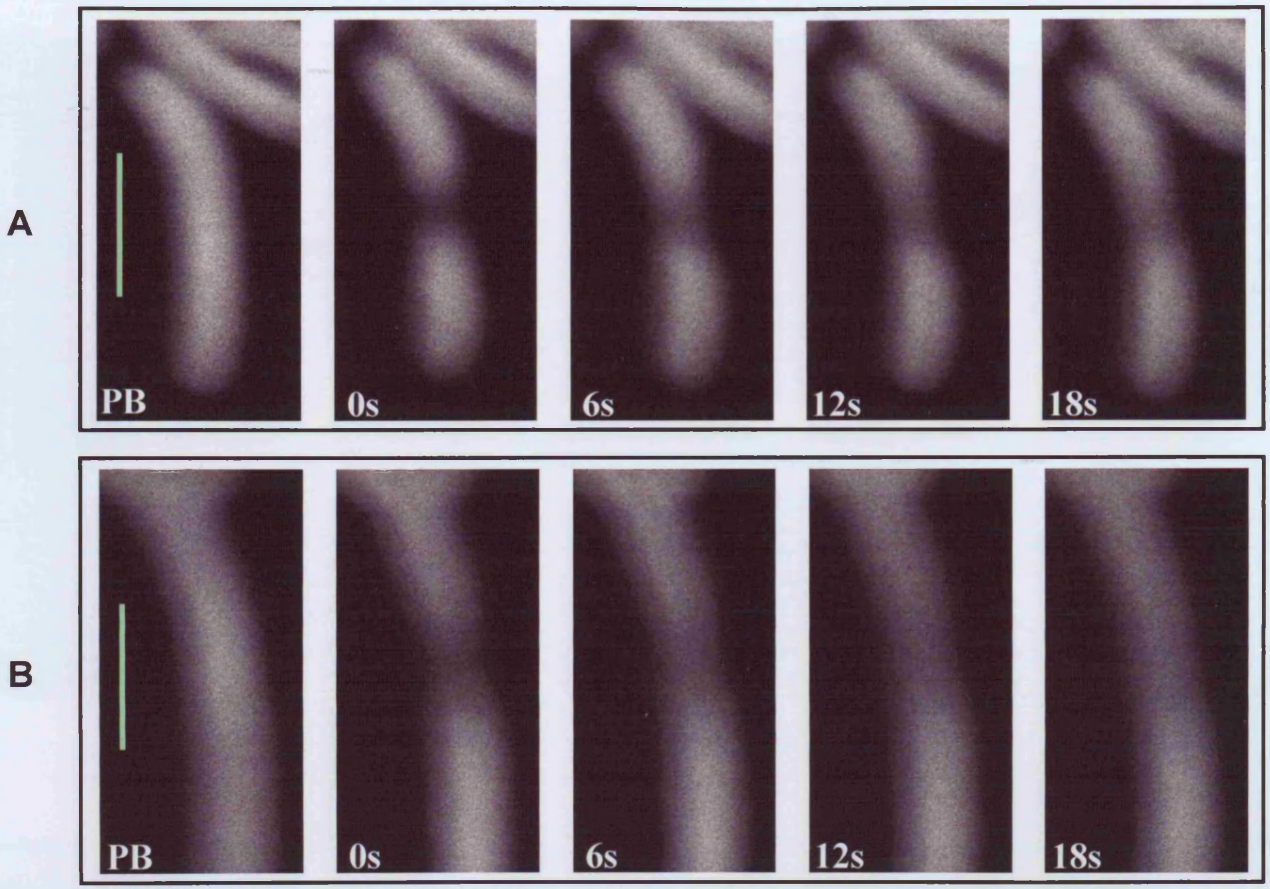

Figure 5.5 FRAP experiments on *Synechococcus* 7942 wild type (series A) and PsaL-minus (series B) cells. For each series, a cell is shown prior to photobleaching (PB), immediately after being photobleached (0 s) and then at 6, 12 and 18 s after bleaching. The images represent a selection from a time series during which images were recorded every 3 s. The bar represents 5 μm. This wild type cell had a phycobilisome diffusion coefficient D of $5.9 \pm 0.1 \times 10^{-10}$ cm^2s^{-1} and the mutant cell had a D of $15.0 \pm 2.0 \times 10^{-10}$ cm^2s^{-1}, values that are typical for their respective cell populations.

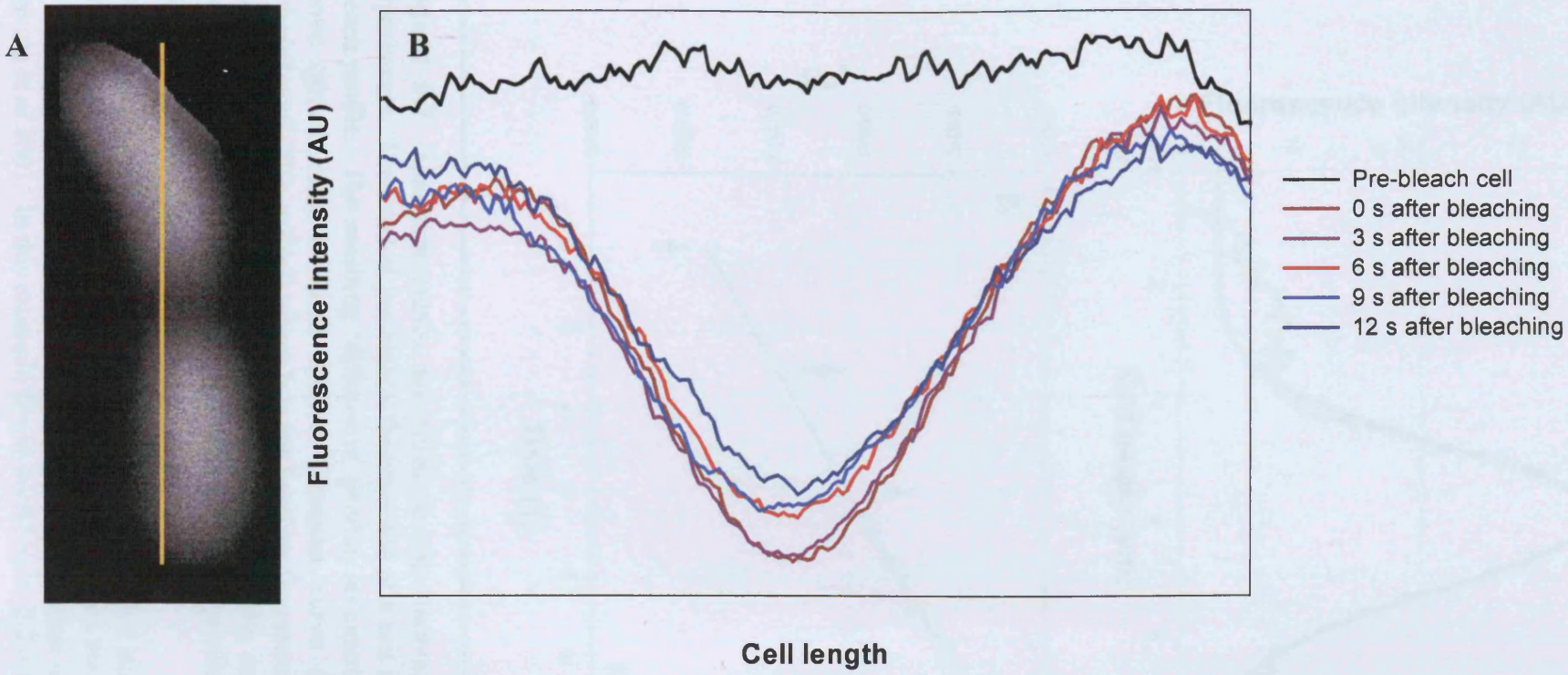

Figure 5.6 Each FRAP image from a time series was converted into a profile of the fluorescence intensity along the cell length. Computer software was used (as described in Chapter 2) to integrate across the cell width along a line drawn to mark out the cell's length as shown in A above. The software is then used to convert the data into a profile showing the fluorescence intensity along the length of the cell as shown in B. The pre-bleach cell has relatively uniform fluorescence along its length. After bleaching, the plot alters shape, showing a dramatic decrease in fluorescence intensity at the bleaching point. As phycobilisomes diffuse back into the area over time, the fluorescence intensity gradually increases again. The difference between the fluorescence profiles at different time points can be used to calculate the rate of diffusion (Sarcina *et al* 2001).

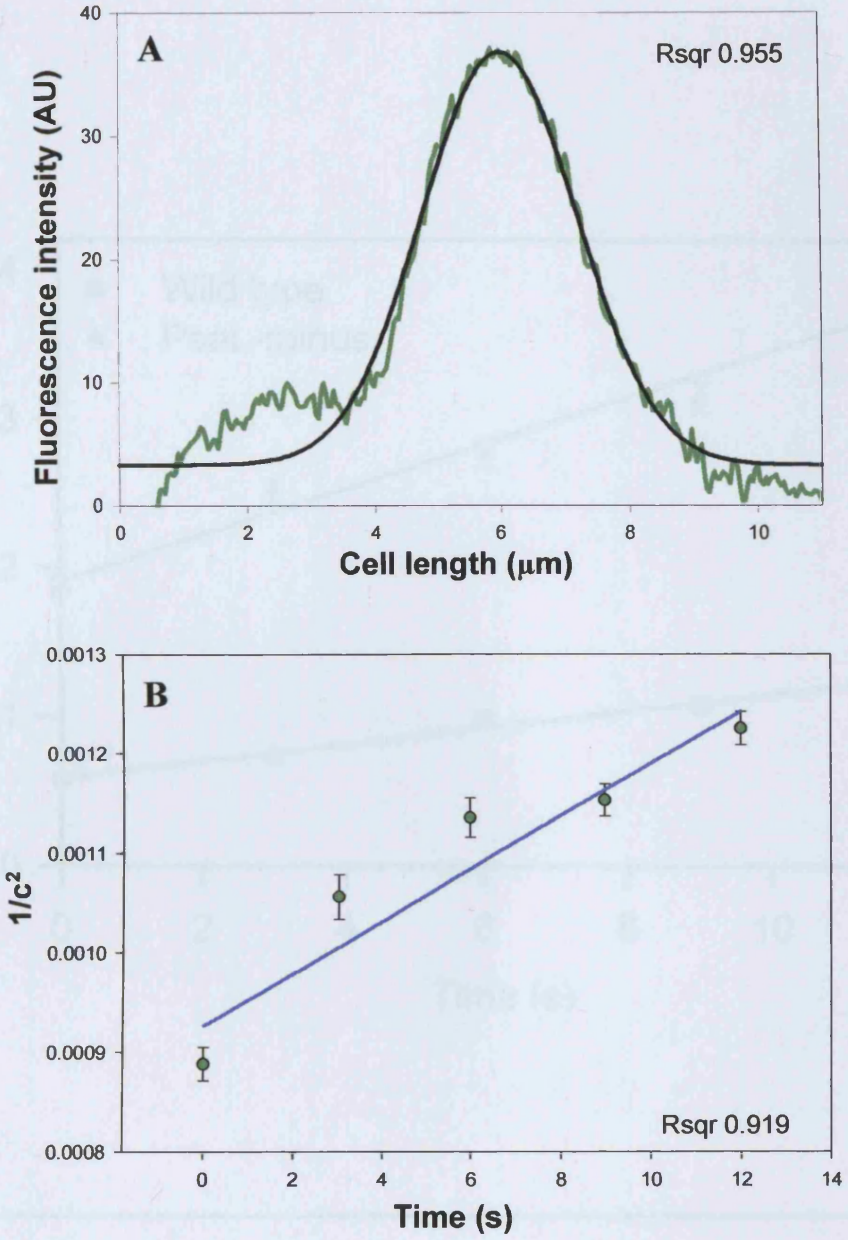

Figure 5.7 Gaussian curves are fitted to the fluorescence profiles from FRAP experiments. The level of pre-bleach fluorescence of a cell is subtracted from each post-bleach profile. The resulting 'difference' profile, an example of which is shown in A above (green line), is fitted with a Gaussian curve (black line) with equation $y=b+(c*\exp((-2*(x-m)^2/a))$ where b is the baseline fluorescence value of the profile, c is the maximum bleach value, a is the bleach half-width squared and m is the centre position of the bleach. The values for each difference profile in a time series are used to calculate the diffusion coefficient.

The value of $1/c^2$ for each time point in a series is plotted against time as shown in B. A straight line is fitted using the equation $y=a+(b*x)$, with the gradient b being equivalent to $8D/C_0^2R_0^2$. This value is used to calculate the diffusion coefficient D, as described in Sarcina *et al* 2001. In this example D was found to be $2.2 \pm 0.4 \times 10^{-10}$ cm^2 s^{-1}.

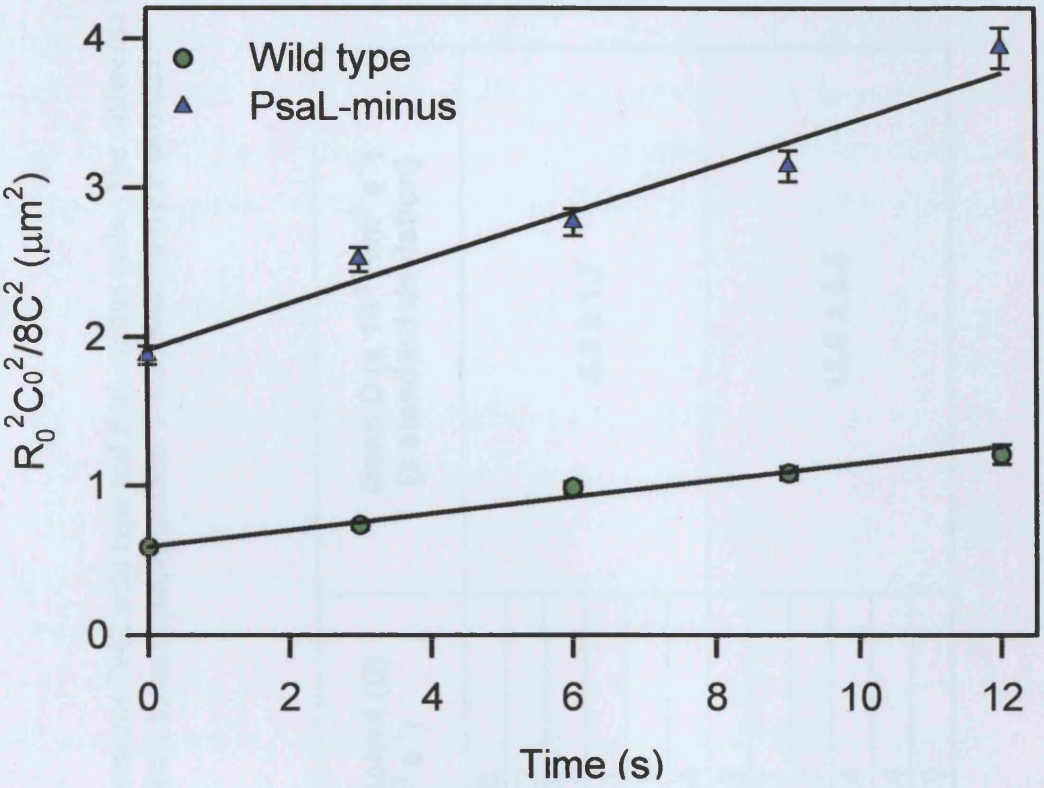

Figure 5.8 Calculation of phycobilisome diffusion coefficients from plots of $R_0^2C_0^2/8C^2$ against time. R_0 is the bleach half width at time 0 s, C_0 is the bleach depth at time 0 s and C is the bleach depth at time *t*. The gradient of a straight line fitted to these points gives the diffusion coefficient D, as described by Mullineaux *et al* (1997). The plots above represent typical wt and PsaL-minus cells with D values of $5.9 \pm 0.1 \times 10^{-10}$ cm^2 s^{-1} and $1.5 \pm 0.2 \times 10^{-9}$ cm^2 s^{-1} respectively.

Table 5.2 Phycobilisome lateral diffusion coefficients for *Synechococcus* 7942 wild type and PsaL-minus cells. The difference between the mean diffusion coefficient for each cell type was found to be significant by an unpaired student T-test, which gave P as 0.023.

Cell type		Diffusion coefficient (D) ($\times 10^{-10}$ cm^2 s^{-1})	Mean D ($\times 10^{-10}$ cm^2 s^{-1}) [± standard deviation]
Wild type	1	3.7 ± 0.6	4.3 ± 1.7
	2	6.2 ± 0.2	
	3	5.3 ± 0.2	
	4	5.9 ± 0.1	
	5	2.6 ± 1.1	
	6	2.2 ± 0.4	
PsaL-minus	1	6.3 ± 0.2	12.0 ± 6.5
	2	11.0 ± 0.7	
	3	23.0 ± 0.7	
	4	9.2 ± 0.4	
	5	5.6 ± 1.4	
	6	15.0 ± 2.0	

recovery). This is confirmed by visual comparison of the images of the time series and calculation of the diffusion coefficients for numerous cells of each type.

Table 5.2 lists the diffusion coefficient values for each cell analysed in this FRAP study. The mean diffusion coefficients for the wild type and PsaL-minus cells were 4.3 ± 1.7 and $12.0 \pm 6.5 \times 10^{-10}$ cm^2 s^{-1} respectively; the rate in the mutant was found to be significantly faster by the unpaired T-test (P value 0.023). Overall the diffusion of phycobilisomes occurred 2.7 times faster in PsaL-minus cells than in wild type.

5.6 Discussion

5.6.1 Tracking phycobilisome diffusion using FRAP

The phycobilisomes are the primary accessory light-harvesting structures in cyanobacterial cells under normal growth conditions. They have the ability to couple with and efficiently transfer energy to both PSI and PSII reaction centres (Mullineaux 1992, Mullineaux 1994). The FRAP technique was used to demonstrate the mobility of phycobilisomes in the cyanobacterium *Dactylococcopsis salina* (Mullineaux *et al* 1997). It was found that phycobilisomes are highly mobile structures, which diffuse rapidly across the thylakoid membrane surface, in contrast with PSII, which appeared to be completely immobile. Measurement of PSI diffusion has not been possible as yet, as it does not fluoresce sufficiently to measure at room temperature.

It is likely that the interaction between phycobilisomes and photosystem reaction centres is transitory, with phycobilisomes attaching to a reaction centre temporarily but then decoupling to diffuse over the membrane and associate with a different reaction centre. Subsequent FRAP studies using different cyanobacterial species have confirmed the mobile nature of phycobilisomes and the unstable nature of the interaction with reaction centres (Sarcina *et al* 2001). Mullineaux *et al* (1997) suggested that phycobilisome mobility could be involved in regulating light-harvesting via state transitions and that the rate of their diffusion could be limited by the transient binding to stationary reaction centres or by steric hindrance in the cytoplasm.

5.6.2 Factors affecting phycobilisome diffusion rates

Studies in *Synechococcus* 7942 have shown that the rate of phycobilisome diffusion is affected by certain factors including the size of the phycobilisome and the membrane lipid composition (Sarcina *et al* 2001). A mutant lacking the rod elements of the phycobilisome structure but retaining functional core assemblies was found to have a diffusion coefficient significantly faster than wild type. The diffusion rate is therefore partially dependent on phycobilisome size, with smaller structures being able to diffuse more quickly. In a mutant with increased levels of unsaturated fatty acids in the thylakoid membranes, increased membrane fluidity was accompanied by a significant decrease in phycobilisome mobility. Sarcina *et al* (2001) proposed that this unexpected result indicates a role for membrane lipids in controlling the phycobilisome-reaction centre interaction. Temperature was found to have only a minor effect on phycobilisome diffusion rate, which suggests that the structures do not have an integral membrane domain (Sarcina *et al* 2001). Their attachment to the membrane surface is more likely to be via interactions with lipid head-groups.

5.6.3 PSI monomerisation leads to faster phycobilisome diffusion

In this FRAP study the mean phycobilisome diffusion coefficient for wild type *Synechococcus* 7942 cells was $4.3 \pm 1.7 \times 10^{-10}$ cm^2 s^{-1}. This is similar to values previously recorded for this organism [$3.1 \pm 1.0 \times 10^{-10}$ cm^2 s^{-1}] (Sarcina *et al* 2001). The mean diffusion coefficient for the PsaL-minus mutant cells was $12.0 \pm 6.5 \times 10^{-10}$ cm^2 s^{-1}. Phycobilisomes diffuse almost 3 times more rapidly when PSI is entirely monomeric. Oligomerisation of reaction centres in the membrane is therefore another factor influencing the diffusion rate of phycobilisomes. As there is no difference in the pigment composition or PSII:PSI ratio in the mutant, the altered rate is unlikely to be due to any general alterations to the membrane arrangement. The monomerisation of PSI has a direct effect on phycobilisome mobility.

The thylakoid membranes, like any biological membranes, are dynamic structures, with protein components being synthesised, degraded, repaired and replaced. The thylakoid membranes contain the protein complexes required for the photosynthetic

and respiratory electron transport chains and are densely packed with protein complexes (Mullineaux 1999). It is therefore possible that the packing of PSI as a large trimeric structure could slow the diffusion of phycobilisomes by steric hindrance. It is expected that, usually, PSII dimers would arrange themselves in parallel rows within the membrane (an arrangement that has been observed in electron micrographs), with PSI trimers occupying the areas between rows (Mullineaux 1999). The organisation of PSII dimers in relatively neat, ordered rows may also explain the immobility of these complexes. The smaller monomeric PSI complexes are likely to be packaged differently from trimers and may cause less hindrance to the movement of phycobilisomes across the surface. The X-ray crystal structure of cyanobacterial PSI shows that the cytoplasmic side of the structure protrudes from the membrane considerably, with the stromal subunits PsaC, PsaD and PsaE forming the protrusion at the site where ferredoxin is predicted to bind with the photosystem (Jordan *et al* 2001).

It has been suggested that the formation of a functional 'supercomplex' consisting of a phycobilisome and a photosystem reaction centre depends on the oligomerisation of the photosystem, with PSII being required as a dimer and PSI as a trimer (Bald *et al* 1996). However, the PsaL-minus mutant showed no detectable reduction in its ability to use phycobilisome-absorbed energy (as determined by low temperature fluorescence spectroscopy shown in Figure 5.1). The phycobilisomes can interact with PSI either as a trimer or as a monomer and efficiently funnel energy into the reaction centre in either case.

There has also been suggestion that alterations to the oligomerisation status of reaction centres could be involved in the mechanism of state transitions, with state 1 requiring dimeric PSII and monomeric PSI and state 2 requiring monomeric PSII and trimeric PSI (Meunier *et al* 1997). In this model, the phycobilisomes would attach preferentially to the oligomerised reaction centres in each state. In this study, the PsaL-minus mutant was fully capable of carrying out state transitions (as shown in Figure 5.2). As the PsaL subunit is essential for the trimerisation of PSI, the PSI complexes in these mutant cells could not alter between monomeric and trimeric

structures as suggested in the proposed model. State transitions are feasible when PSI is present in either form.

It remains possible that there is some difference in the strength of the phycobilisome-PSI reaction centre interaction when the PSI is monomeric. A potentially looser association with monomers could allow faster phycobilisome diffusion in PsaL-minus cells by reducing the strength of the coupling to such reaction centres.

5.6.4 State transitions occur more rapidly when PSI is monomeric

State transitions are a rapid and convenient mechanism by which cyanobacteria can respond to changing light intensity or quality by altering the relative amounts of phycobilisome-harvested light to PSI or PSII complexes. In this way, the efficiency of the photosynthetic apparatus is maintained when the environmental conditions are altered.

In these experiments we found that state transitions occur almost twice as fast in the PsaL-minus mutant of *Synechococcus* 7942 than in wild type. This is in agreement with an earlier study using a PsaL-minus mutant of *Synechococcus* 7002, which found that state transitions occurred about three times faster in the mutant (Schluchter *et al* 1996).

Schluchter *et al* (1996) proposed a 'mobile PSI' model for state transitions, suggesting that the PSI complexes are the mobile element, with the smaller monomers simply being able to travel more quickly, leading to more rapid state transitions in the PsaL-minus mutant. However, FRAP studies have convincingly shown that the phycobilisomes are highly mobile and can move between PSII and PSI complexes to allow state transitions to be effected (Mullineaux 1997, Sarcina *et al* 2001). The immobility of PSII has also been demonstrated by FRAP. The mobility of PSI cannot be determined at this time as its fluorescence at room temperature is insufficient to be detectable.

It is possible that there is a link between the increased rate of state transitions and the more rapid diffusion of phycobilisomes in the PsaL-minus mutant. If the rate of diffusion of phycobilisomes could be considered a rate-limiting step in the state transition, then a direct correlation between more rapid diffusion and more rapid state transitions would be a possibility. It seems doubtful that this could be the case as PSI and PSII complexes are likely to be in close proximity within the cell (Mullineaux 1999) and the rate of phycobilisome diffusion is so rapid compared to the timeframe of a state transition (seconds) that it is unlikely to be a limiting factor. It is estimated that a phycobilisome could travel between reaction centres on a millisecond timescale (Mullineaux *et al* 1997). The phycobilisome diffusion rate as a rate-limiting factor becomes more plausible, however, if the membrane organisation required a longer-range movement of the phycobilisome during a state transition. Sherman *et al* (1994) described a heterogeneous distribution of PSI and ATP synthase, with higher concentrations of these complexes being found in the thylakoid membranes closest to the plasma membrane. PSII complexes were more evenly distributed throughout the membrane system. If there are distinct regions of the membrane containing higher concentrations of PSI, then increased phycobilisome mobility may lead directly to more rapid state transitions.

The association of PSI and phycobilisomes is known to be transient and unstable. It is possible that the interaction of the phycobilisome with monomeric PSI is weaker than with the trimeric form found in wild type cells. As well as creating the potential for more rapid phycobilisome diffusion (by reducing the strength of anchoring of the phycobilisome to the reaction centre), this weaker structural interaction might also permit more rapid state 2 to state 1 transitions. It is predicted that a covalent modification during the signal transduction pathway of the state transition would result in an altered affinity of phycobilisomes for PSI or PSII. There would consequently be a redistribution of the phycobilisomes. If the weaker association with monomers allowed easier decoupling from PSI, then the redistribution to associate with PSII in state 1 could occur more quickly.

CHAPTER SIX

LIGHT-HARVESTING WITH THE CP43′ PROTEIN RING INDUCED UNDER IRON STRESS

CHAPTER SIX

LIGHT-HARVESTING WITH THE CP43' PROTEIN RING INDUCED UNDER IRON STRESS

6.1 Introduction

The concentration of iron in aquatic habitats is often low enough to inhibit the growth rates of cyanobacteria. Cyanobacteria in iron-limited conditions express the genes *isiA* and *isiB* (*i*ron *s*tress *i*nduced genes). The *isiB* gene encodes flavodoxin, which can replace ferredoxin as an electron acceptor for PSI. The protein product IsiA, a chlorophyll *a*-binding protein, is also known as CP43' because it shares significant homology with the CP43 protein of PSII.

The function of the CP43' protein in iron stress conditions has been the subject of some debate (see Chapter 1). In recent years an iron stress-induced supercomplex consisting of PSI trimers and CP43' was described (Bibby *et al* 2001a, Boekema *et al* 2001a). Electron microscopy revealed 18 subunits of CP43' arranged in a ring around the PSI trimer. It is probable that each CP43' subunit can bind 12 chlorophyll *a* molecules, by comparison with CP43 of PSII (Zouni *et al* 2001). The 18-mer ring structure could therefore bind around 200 chlorophyll *a* molecules, giving the capacity to increase the light-harvesting capacity of PSI by 60 to 70% (Bibby *et al* 2001a, Boekema *et al* 2001a). It is likely to be of great importance in iron stress conditions, when the levels of iron-rich PSI and light-harvesting phycobilisomes decrease.

The supercomplex of 18 CP43' subunits and one PSI trimer is a highly efficient mechanism for survival in conditions of iron stress. There do not appear to be many points of contact between the ring and the reaction centre, suggesting that the 18-mer ring itself is needed to ensure the stability of the supercomplex. To investigate whether the trimeric conformation of PSI was necessary for the stability and functionality of this supercomplex, iron stress studies of the *Synechocystis* 6803 PsaL-

minus mutants were conducted. To simplify the isolation of PSI complexes from the membranes of these cells, the *Synechocystis* PSII- *psaL*- double mutant (the construction of which is described in Chapter 3) was used, although the initial experiments on whole cells were also carried out using the single PsaL-minus mutant. Much of the work presented in this chapter was recently published in Aspinwall *et al* (2004a).

6.2 PsaL-minus mutants grow normally under iron stress conditions

The *Synechocystis* 6803 PSII- mutant and the PSII- *psaL*- double mutant were grown under white light in normal iron-replete growth medium with added 5 mM glucose and the same medium lacking added iron compounds. Growth was monitored by recording the optical density at 750 nm at regular intervals. Sufficient cells were added to each experimental culture to give a starting OD_{750} of 0.1. Pelleting and washing of cells before addition to the experimental cultures eliminated carry-over of iron from the starter culture medium.

Typical growth curves are shown in Figure 6.1. Each culture grew at similar rates in both the presence and absence of iron. The doubling times for each culture in the exponential growth phase were determined and were found to be approximately 31 hours for the *Synechocystis* 6803 PSII- cells in either media, and 20 hours for the *Synechocystis* 6803 PSII- *psaL*- cells in either media. Although it might appear that the double mutant grew at a faster rate in this experiment, this was a result of a higher light intensity in the incubator housing these cultures. In terms of growth rate, neither culture was disadvantaged by the absence of an iron source in the medium, suggesting that both possessed the necessary mechanisms to compensate for the lack. In order to determine whether the mechanism being employed was the synthesis of the CP43' antenna ring, we tested iron-starved cultures for the presence of CP43' protein.

6.3 CP43' protein is produced by PsaL-minus cells under iron stress

The accumulation of CP43' protein in cells, as a result of *isiA* gene expression under iron stress, is indicated by a blue shift in the long wavelength absorption maximum of

room temperature absorption spectra (Burnap *et al* 1993, Falk *et al* 1995, Park *et al* 1999). Figure 6.2 compares absorption spectra for *Synechocystis* 6803 PSII- *psaL*- cells grown in the presence and absence of iron for 3 days. The 8 nm shift of the long wavelength absorption maximum indicates that CP43' protein was being synthesised and accumulated in the thylakoid membranes of these cells.

The CP43' protein can also be detected by looking for a characteristic peak at 685nm in 77 K fluorescence emission spectra when exciting chlorophyll *a* at 435nm (Burnap *et al* 1993, Falk *et al* 1995, Park *et al* 1999). Spectra were recorded for a culture of *Synechocystis* 6803 *psaL*- cells in iron-free medium at intervals over several weeks of growth and are shown in Figure 6.3. In the initial spectra at the beginning of the experiment, peaks representing PSI and PSII are present. After several days of growth under iron stress conditions, a sharp peak at 685 nm appears and increases in size relative to the PSI peak (spectra are normalised at 720 nm) as the experiment progresses. This indicates that the *isiA* gene is being induced in these cells and that CP43' proteins are being produced. For about the first week of the experiment, the CP43' is being coupled to PSI reaction centres. After 9 days, the emergence of the large peak at 685 nm implies that CP43' protein is now present in excess in the cells and can therefore be detected in its free form.

A shift in the PSI peak (at around 720 nm) of 3-4 nm occurs over the course of the iron depletion experiment. The appearance of this shift occurs concurrently with the increased size of the CP43' peak after the first few days of the experiment. A shift in the PSI peak of a fluorescence emission spectrum indicates a structural alteration to the PSI. In this instance this structural change is most likely related to the aggregation of PSI reaction centres and CP43' proteins to form supercomplexes. The formation of the supercomplex may cause a small conformational change to PSI.

6.4 PSI monomer-CP43' supercomplexes can be isolated from iron starved cells

Sucrose density gradient centrifugation was used to separate the photosystem complexes in solubilised thylakoid membranes extracted from *Synechocystis* 6803

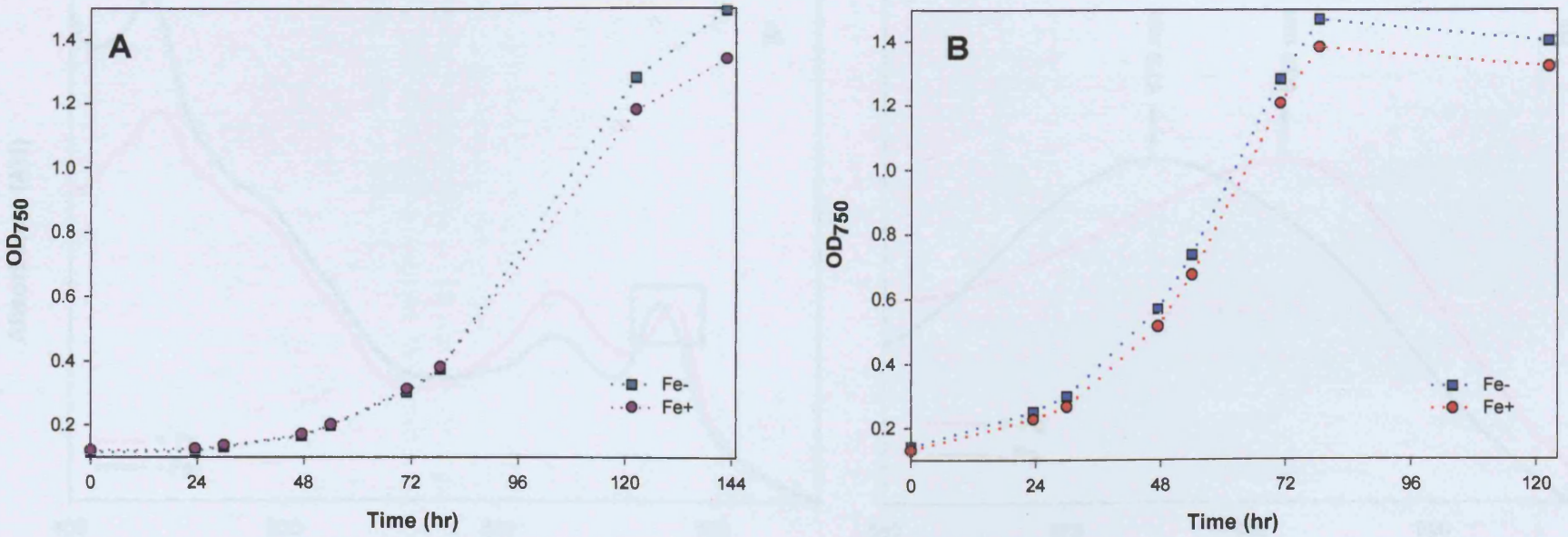

Figure 6.1 Growth curves for *Synechocystis* 6803 PSII- (A) and PSII- *psaL*- (B) cells in the presence and absence of iron. At the start of the experiment, sufficient cells were added to flasks of growth medium to give an OD_{750} of 0.1. The increase in OD_{750} was monitored in triplicate for each cell type and averaged to produce the plots shown (error bars not shown as they interfered with data presented but errors were small). Curves were fitted to the exponentially rising part of each plot, as described in Chapter 2, and used to calculate the doubling times. For PSII- cells, the doubling time was about 31 hours in both the presence and absence of iron. For PSII- *psaL*- cells, the doubling time was 20 hours in both growth media.

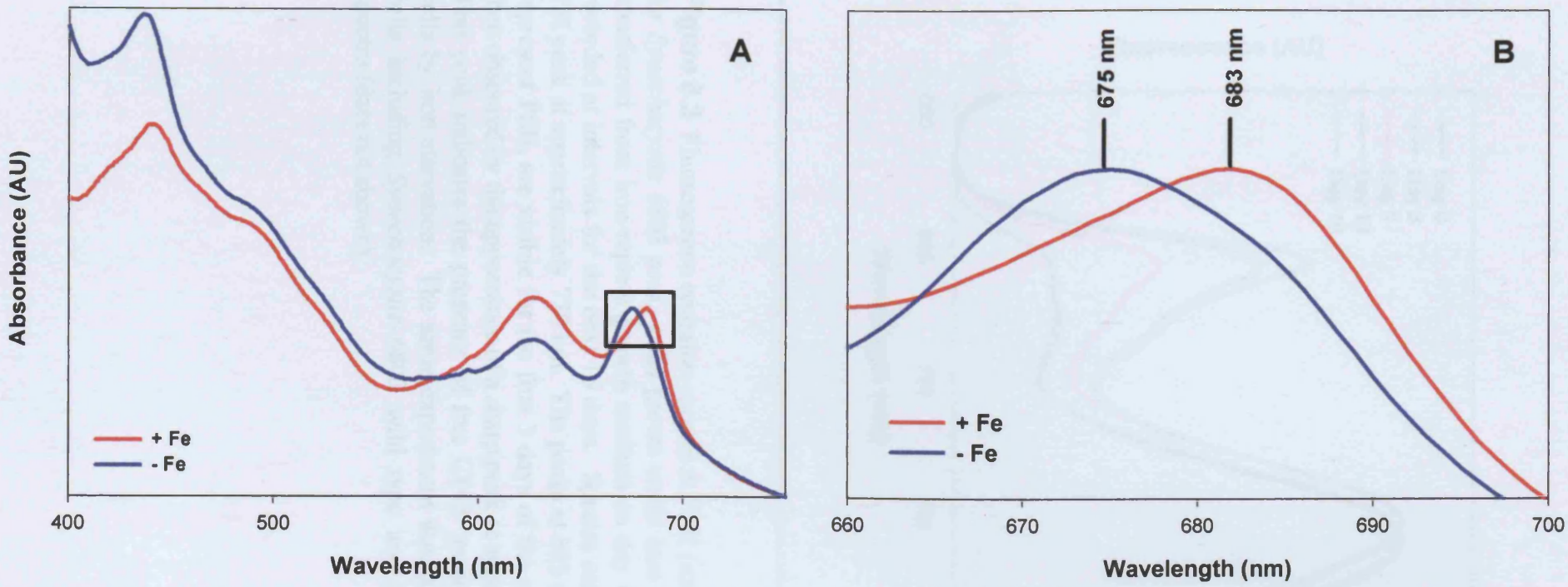

Figure 6.2 Room temperature absorption spectra of *Synechocystis* 6803 *PSII- psaL-* cells grown in standard iron-replete growth medium (red lines) and after transfer to growth medium lacking iron for 3 days (blue lines). A shift in the spectra, shown boxed in A and enlarged in B, from 683 nm to 675 nm, implies the induction of CP43' protein in the iron-stressed cell population.

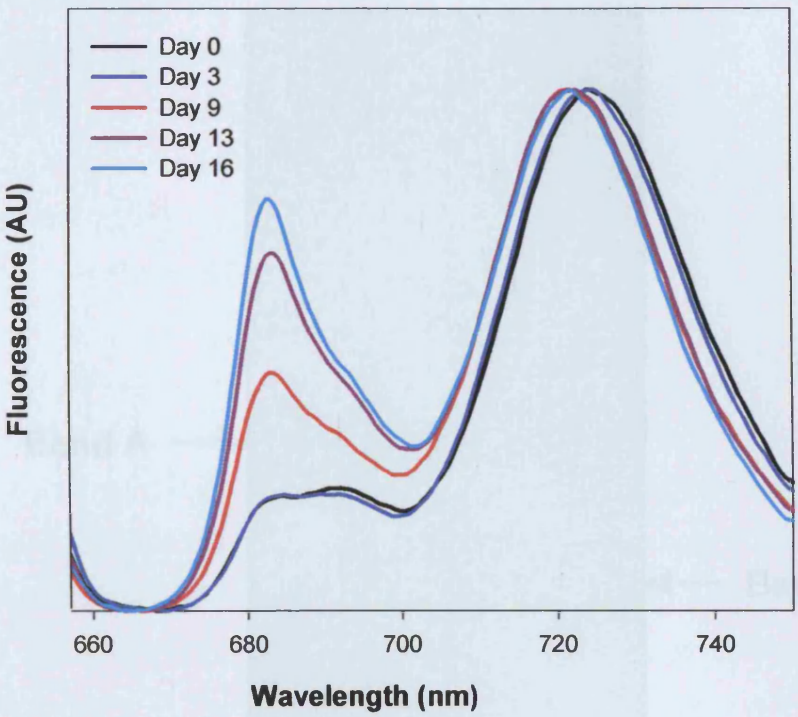

Figure 6.3 Fluorescence emission spectra at 77 K (excitation at 435 nm) for *Synechocystis* 6803 *psaL-* cells grown under iron stress. Cells were transferred from iron-replete growth medium on day 0 and spectra were recorded at intervals for the next 16 days. Spectra are normalised to the PSI peak at approximately 720 nm. The peaks at 685 and 695 nm, which represent PSII, are visible for the first 3 days of the experiment, but are then obscured by the appearance of a sharp peak at approximately 685 nm. This peak indicates the presence of free CP43' protein, induced in the cells by iron starvation. The same experiment was carried out for other cells including *Synechocystis* 6803 wild type and produced identical spectra (data not shown).

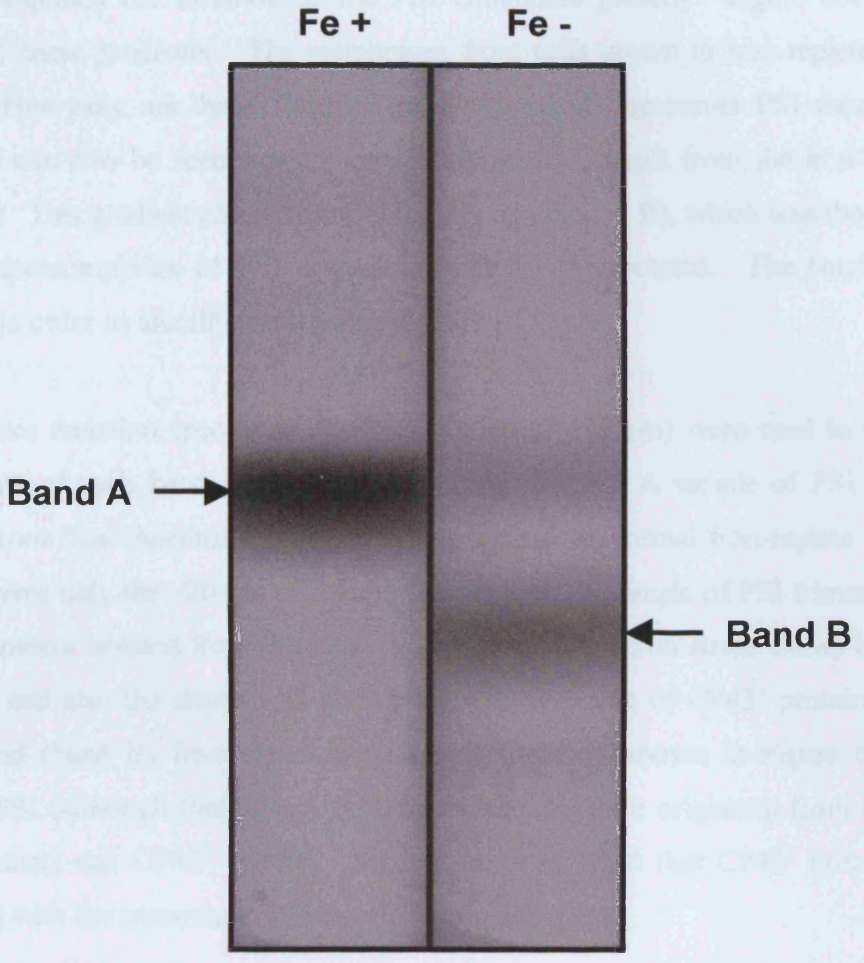

Figure 6.4 Sucrose density gradients to separate solubilised PSI complexes isolated from PSII- *psaL*- cells grown in the presence and absence of iron (Fe+ and Fe- respectively). Band A represents PSI monomers. Band B represents PSI monomer-CP43' supercomplexes.

PSII- *psaL*- cells grown in the presence and absence of iron. The lack of PSII in these samples simplified the isolation of the PSI complexes present. Figure 6.4 shows profiles of these gradients. The membranes from cells grown in iron-replete (Fe+) medium show only one band (labelled band A), which represents PSI monomers. This band can also be seen, albeit more faintly, in the sample from the iron-starved (Fe-) cells. This gradient also revealed a heavier band (band B), which was thought to contain supercomplexes of PSI monomers with CP43' proteins. The bands were extracted in order to identify these complexes.

Fluorescence emission spectra at 77 K (excitation at 435 nm) were used to identify constituents of each band and are shown in Figure 6.5. A sample of PSI trimers isolated from *Synechocystis* 6803 PSII- cells grown in normal iron-replete growth medium gives only the 720 nm peak representing PSI. A sample of PSI trimer-CP43' supercomplexes isolated from the same strain grown under iron stress shows both the PSI peak and also the sharp peak at 685 nm, characteristic of CP43' proteins. The heavy band (band B) from the sucrose density gradient shown in Figure 6.4 also contains PSI (although this time it must be monomeric as it originates from a PsaL-minus mutant) and CP43' protein. These spectra revealed that CP43' protein was associated with the monomeric PSI in cells under iron stress.

Further analysis of the isolated bands using SDS-PAGE is shown in Figure 6.6. The sample of PSI monomers from the Fe+ sample (lane A) revealed many of the constituent protein subunits of this reaction centre, including the core subunits PsaA and PsaB and several of the low molecular mass accessory subunits. The same profile of PSI subunits was found in the putative supercomplex sample (lane B), as well as an additional band corresponding to CP43'. This showed that the supercomplex did indeed consist of PSI monomers and CP43' proteins in an as yet undetermined stoichiometry.

6.5 Characterisation of PSI monomer-CP43' supercomplexes

The absorbance and 77 K fluorescence emission characteristics of isolated PSI monomers, free CP43' proteins and the PSI monomer-CP43' supercomplexes were

compared and are shown in Figure 6.7. The long wavelength absorbance maxima for CP43', PSI monomers and the supercomplex were 670 nm, 680 nm and 673 nm respectively. The supercomplex absorbance maximum was positioned between the wavelengths for its two components. This wavelength was similar to that found for the PSI trimer-CP43' supercomplex isolated previously (Bibby *et al* 2001b). The fluorescence emission spectra for the supercomplex gave peaks corresponding to its PSI monomer and CP43' components.

When the PSI trimer-CP43' supercomplex was isolated, detergent treatment was used to disassociate the photosystem and antenna ring, to show that they were functionally linked when isolated from the membranes (Bibby *et al* 2001b). A sample of the isolated PSI monomer-CP43' supercomplex was treated with 0.1% Triton X-100 and 77 K fluorescence emission spectra of the sample before and after the detergent treatment were compared as shown in Figure 6.8. The large increase in the 685 nm peak is indicative of the disassociation of CP43' proteins from the complex and their presence in a free form. The isolated supercomplex consists, therefore, of PSI monomers with a functional CP43' antenna.

In order to examine the exact nature of the CP43' association with PSI monomers, electron microscopy of negatively stained isolated particles was conducted (in collaboration with James Duncan at Imperial College London). The resulting images are shown in Figure 6.9. X-ray crystallography data for CP43 (Zouni *et al* 2001) and PSI (Jordan *et al* 2001) were used to overlay the images of the supercomplex particles with the structures of these components. The result revealed that each PSI monomer associates with a crescent of 6 CP43' proteins, which arrange themselves along the outside edge of the monomer where the accessory subunits PsaJ and PsaF are located. The monomer supercomplex appears to be equivalent to one third of the trimer supercomplex, which has a complete ring of 18 CP43' proteins around it.

The majority of particles studied had the 6-mer crescent of CP43' shown in Figure 6.9. However, a small number of particles with an additional CP43' subunit were observed. The existence of these particles suggests that CP43' molecules can interact with each other to form a stable linkage. So in the vast majority of cases, a 6-mer

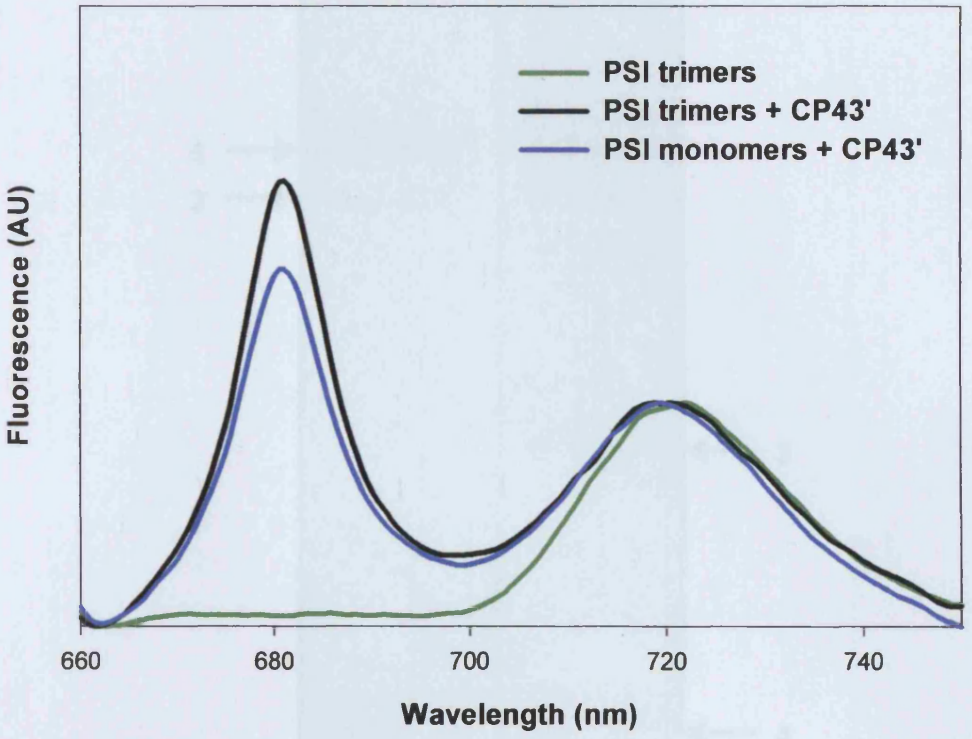

Figure 6.5 Fluorescence emission spectra at 77 K (excitation at 435 nm) of solubilised PSI complexes derived from *Synechocystis* 6803 PSII- and PSII- *psaL*- cell membranes by sucrose density gradient centrifugation. Thylakoid membranes were isolated from the cells, solubilised and the photosystems separated on gradients. The spectra show PSI trimers isolated from PSII- cells grown in iron replete medium (green line), PSI trimers and associated CP43' protein from PSII- cells grown in the absence of iron (black line) and PSI monomers and associated CP43' from PSII- *psaL*- cells grown in the absence of iron (blue line).

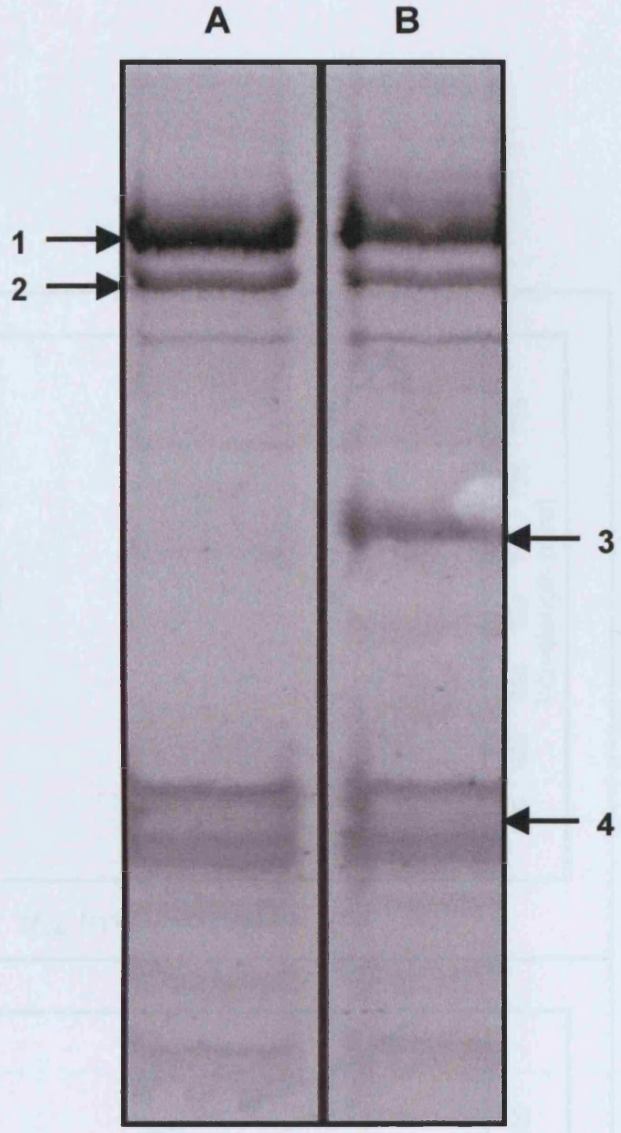

Figure 6.6 SDS-PAGE to separate the constituent protein subunits from the PSI complexes isolated on the sucrose density gradients shown in Figure 6.4. Lane A shows subunits of PSI monomers (from gradient band A of Fig 6.4); lane B shows subunits of PSI monomer-CP43'supercomplexes (from gradient band B of Fig 6.4). Subunits were identified as follows: PsaA (band 1), PsaB (band 2), CP43' (band 3) and stromal subunits PsaC, PsaD and PsaE (bands in region 4). *This gel image was produced in collaboration with James Duncan, Tom Bibby and James Barber of Imperial College London.*

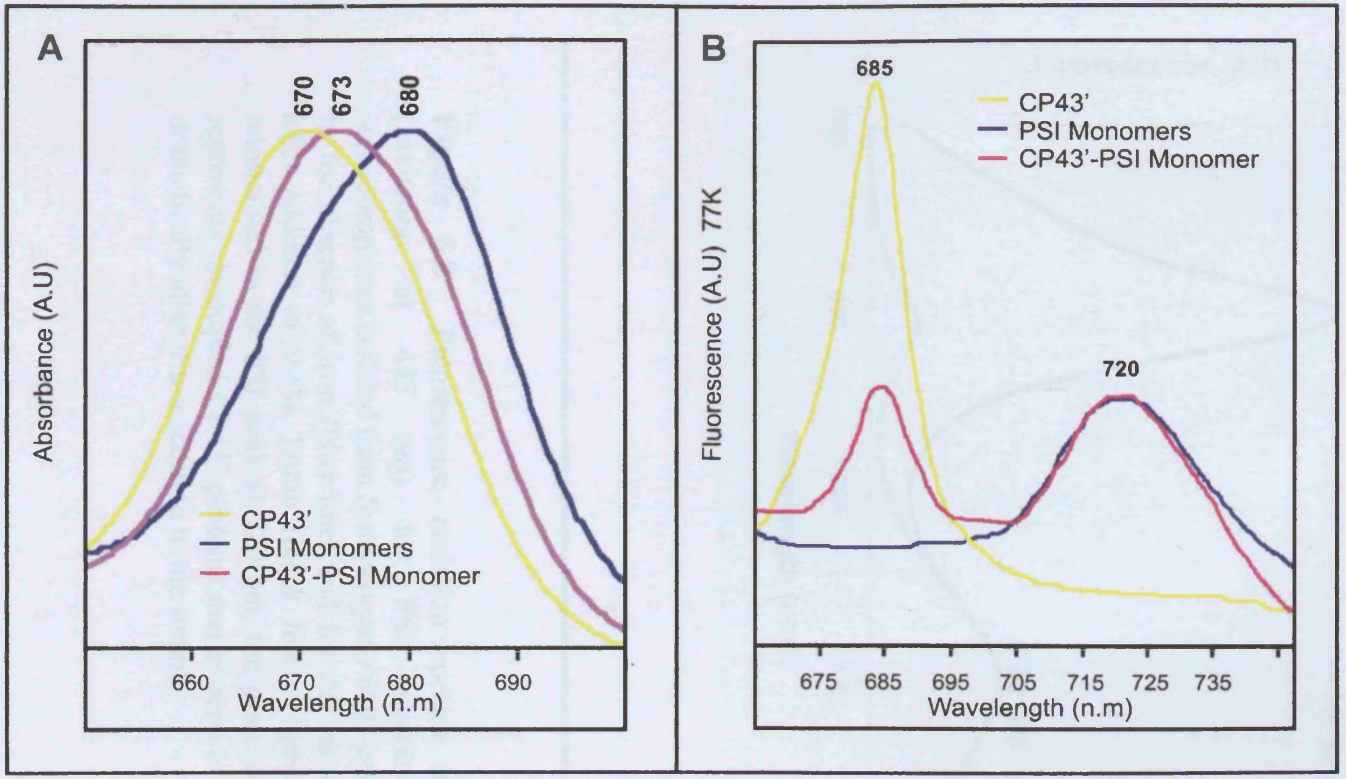

Figure 6.7 Room temperature absorption spectra (A) and 77 K fluorescence emission spectra with excitation at 435 nm (B) of isolated CP43' proteins, PSI monomers and PSI monomer-CP43' supercomplexes isolated from *Synechocystis* PSII- *psaL*- cells grown in the absence of iron. The wavelengths of absorbance or fluorescence maxima are marked.

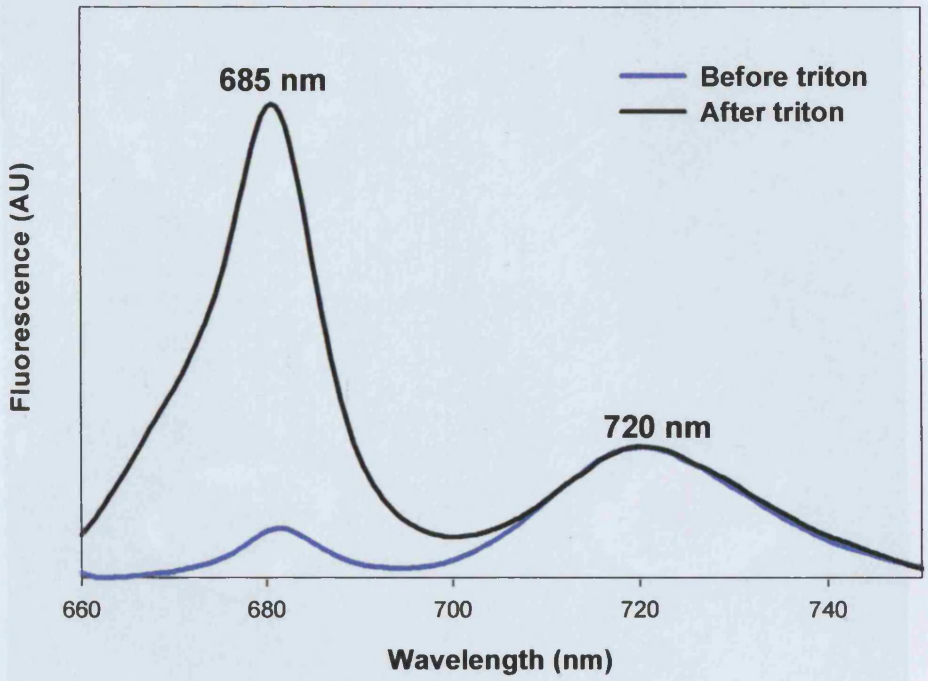

Figure 6.8 Fluorescence emission spectra at 77 K (excitation at 435 nm) for PSI monomer-CP43' supercomplexes isolated from *Synechocystis* 6803 cells grown in the absence of iron (blue line) and for the same sample after addition of 0.1% Triton (black line). Spectra were normalised to the PSI peak at 720 nm, the peak at 685 nm represents uncoupled CP43' proteins and is seen to increase dramatically after triton addition to the sample.

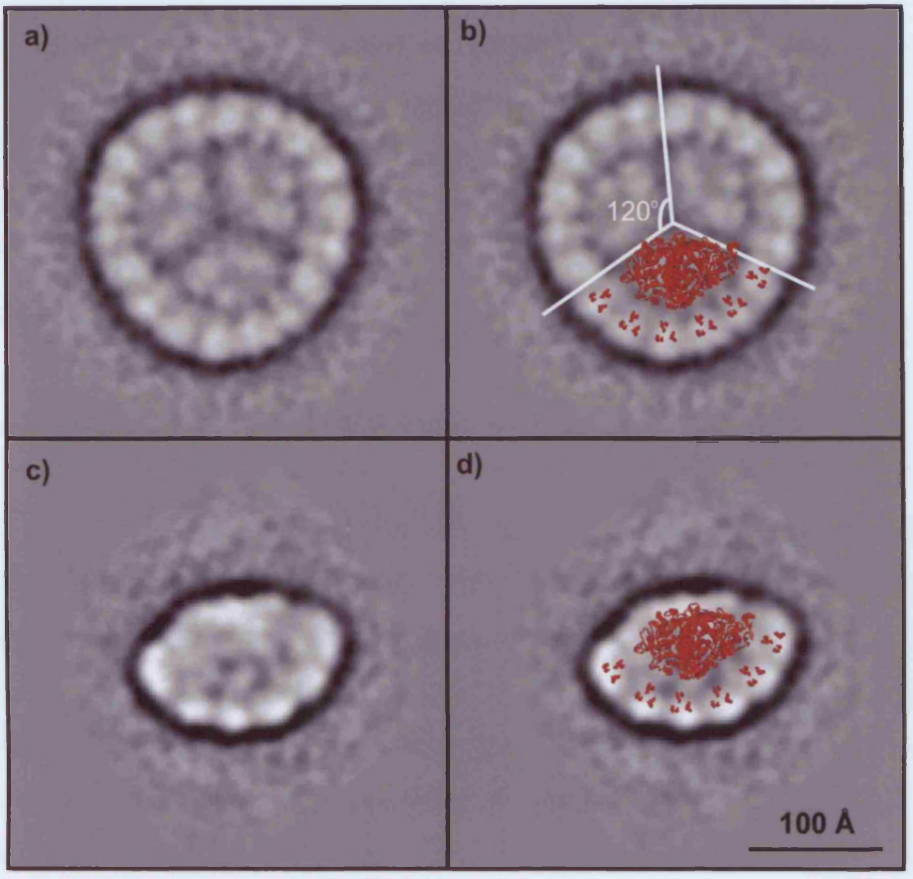

Figure 6.9 Single particle analyses of (a) the PSI trimer-CP43' 18-mer supercomplex induced by iron stress; (b) an overlay of the x-ray structure of PSI (Jordan *et al* 2001) and of CP43 proteins (Zouni *et al* 2001) onto one monomeric segment of the trimer-CP43' supercomplex; a PSI monomer-CP43' supercomplex isolated from the gradients shown in Figure 6.4; (d) an overlay of the PSI x-ray structure and CP43 structure onto the monomer-CP43' supercomplex. *These top projection single particle analysis images were produced in collaboration with James Duncan, Tom Bibby and James Barber of Imperial College London.*

chain of CP43' subunits anchors to a PSI monomer, while in the case of these larger particles, an extra CP43' has attached to the chain. This may provide interesting information about the way the antenna ring attaches to a reaction centre, as it implies that the CP43' subunits can form a stable chain with only few contact points to connect it to the reaction centre.

6.6 Discussion

6.6.1 Light-harvesting proteins in photosynthetic organism

In higher plants PSI is monomeric. The light-harvesting chlorophyll proteins Lhca 1-4 bind along one side of the monomer. This side of the plant monomer would be equivalent to the outside edge of a cyanobacterial PSI trimer (Ben-Shem *et al* 2003). The association of the Lhca with PSI in plants therefore resembles the association of CP43' with monomeric PSI in cyanobacteria. Anoxygenic purple photosynthetic bacteria possess antenna systems consisting of multiple light-harvesting (LH1 and LH2) proteins, which also form rings. The ring structure appears to be a common feature of light-harvesting proteins for photosynthetic reaction centres in photosynthetic bacteria.

6.6.2 Trimerisation of PSI is not required for the CP43' antenna ring to functionally associate with the reaction centre

The induction of the *isiA* gene and subsequent synthesis of CP43' protein leads to accumulation of this protein in the thylakoid membranes of cyanobacterial cells under conditions of iron starvation. The CP43' proteins form an antenna ring comprised of 18 subunits around PSI trimers in wild type cells, allowing a large increase in light-harvesting capability for these reaction centres at a time when both PSI and phycobilisome levels decrease.

The experiments described in this chapter revealed that the CP43' protein is also produced in iron stressed PsaL-minus mutants and can still associate with this reaction centre as a crescent-shaped structure. The antenna system of CP43' proteins do not

require trimerisation of PSI or the presence of the PsaL subunit to functionally associate with this reaction centre. The PsaL-minus mutant was not disadvantaged in terms of growth rate under conditions of iron starvation, presumably because the compensation provided by the complexing of CP43' proteins to the reaction centres caused a sufficient increase in light-harvesting capacity. Although these results showed that the functional significance of PSI trimerisation in cyanobacteria is not to aid survival in iron stress conditions, they did further our understanding of the CP43' antenna system.

Electron microscopy and single particle analysis of the isolated PSI monomer-CP43' supercomplexes were combined with x-ray crystallography data (Figure 6.9) to demonstrate that six CP43' subunits associate with each monomeric PSI reaction centre. These supercomplexes resemble a simple one-third segment of the wild type PSI trimer-CP43' supercomplex, which has a ring of 18 CP43' subunits surrounding the reaction centres (Bibby *et al* 2001a, Boekema *et al* 2001a). The antenna does not need to form this complete ring in order to associate with PSI.

Previous characterisation of the PSI trimer-CP43' supercomplex showed spectroscopically that energy transfer from the 18-mer antenna ring to the trimeric PSI reaction centre is very efficient (Andrizhiyevskaya *et al* 2002, Bibby *et al* 2001a, 2001b). Similar spectroscopic analyses of the PSI monomer-CP43' supercomplexes isolated in for this study demonstrated a good level of energy transfer between the 6-mer antenna and the monomeric reaction centre. A dramatic increase in CP43' fluorescence at 685 nm after dissociation of the supercomplex using a mild detergent treatment shows that the CP43' antenna is efficiently coupled to PSI in the isolated supercomplex (Figure 6.8).

6.6.3 The interaction of the CP43' subunits with PSI shows a degree of flexibility

The results of this chapter have shown that the iron stress-induced CP43' antenna is stabilised by interaction between adjacent CP43' subunits and also by connection of these subunits with the PSI reaction centre. Recent work with a *Synechocystis* 6803

PsaFJ-minus mutant revealed a 17-mer ring of CP43' around PSI trimers (Kouřil *et al* 2003). This suggests a level of flexibility in the way the CP43' interacts with PSI. The structure could be stabilised more by interactions between the CP43' units themselves, although the results of this chapter have demonstrated that an entire ring is not necessary for a stable and functional association with PSI. This work also eliminates PsaF and PsaJ as essential subunits for the interaction of the ring with the reaction centre; further work with mutants lacking other subunits could identify whether there is a single essential point of contact on the reaction centre.

The fact that the 6-mer crescent of CP43' associated specifically with the outside edge of PSI implies that there is some specific point of interaction with PSI. It is possible that one CP43' unit in the chain interacts with a specific subunit of PSI and that the remaining CP43' subunits are primarily linked by interaction with each other. The particles described in this chapter would therefore consist of a chain of 6 CP43' subunits connected to the monomer, perhaps only at one anchoring point. In the wild type 18-mer ring around a PSI trimer, there could be three of these crescents joined together to form the complete ring around the trimer. In the case of the 17-mer ring described by Kouřil *et al* (2003), the absence of the PsaF and PsaJ subunits from the PSI trimer may result in a slightly smaller supercomplex, with the ring of 17 CP43' subunits connecting to the PSI reaction centre by just one anchoring point.

CHAPTER SEVEN

ANALYSIS OF PHOTOSYSTEM I FUNCTION USING EPR

CHAPTER SEVEN

ANALYSIS OF PHOTOSYSTEM I FUNCTION USING EPR

7.1 Introduction

7.1.1 Electrons are carried through PSI via a series of cofactors

PSI catalyses the light-driven transfer of electrons from plastocyanin or cytochrome c_6 in the thylakoid lumen to ferredoxin (or flavodoxin) on the stromal side. The low redox potential of the PSI electron transfer chain allows reduction of $NADP^+$ on the stromal side. Electron transfer through PSI occurs via a series of cofactors bound by the core subunits PsaA and PsaB as well as PsaC. When light is absorbed, the primary electron donor, the chlorophyll dimer P700, is photooxidised and excited, generating the strong reductant $P700^*$, which reduces the chlorophyll acceptor A_0. Electrons are then transferred via the chlorophyll electron carrier, A_0, to a series of electron acceptors; the phylloquinone A_1 and iron-sulphur centres F_X, F_A and F_B (Brettel 1997, Nugent 1996).

As described in Chapter 1, the PSI reaction centre core consists of two proteins: PsaA and PsaB. This heterodimer plus the PsaC protein bind the electron cofactors described above. The exact spatial arrangement of the cofactors has an impact on the electron transfer chain through PSI. The functionality of the electron transfer chain can be monitored using EPR spectroscopy.

7.1.2 EPR provides information about the electron transfer chain

EPR is a method for studying unpaired electron spins such as those found in organic free radicals and in paramagnetic species such as transition metal ions (e.g. Fe^{3+}) and is therefore useful for analysing photosynthetic reaction centres (Hall & Rao 1999). EPR allows detection of photosystem components and provides information about the environment of the electron spins and light-induced changes to their redox states (Evans 1977).

It has previously been shown that the reaction centre can be modified as a result of changes to proteins external to the reaction centre core (Evans *et al* 1999). This chapter describes EPR analysis of the PsaL-minus and PsaE-minus mutants of *Synechocystis* 6803 in an attempt to discover whether these mutations had any effect on electron transfer through PSI. A comparison of the EPR signals generated by monomeric and trimeric isolates of cyanobacterial PSI is included.

7.2 CW-EPR measurements

7.2.1 CW-EPR conditions

EPR spectra were recorded using a Jeol RE1X spectrometer (Kyoto, Japan) fitted with a helium cryostat (Oxford Instruments, Abingdon, Oxfordshire, UK). Illumination was with a 150 W light source. Measurements were recorded in dark and light.

7.2.2 Oxidation of P700

Samples of thylakoid membranes or isolated photosystems were prepared as described in Chapter 2 and reduced using sodium ascorbate. CW-EPR spectra were recorded in the g = 2.00 region at 12 K before and after illumination. Figure 7.1 shows the resulting spectra for *Synechocystis* 6803 thylakoids; illumination of the sample results in a large radical signal due to the oxidation of P700. Additional signals indicate the transfer of electrons to the iron-sulphur centres F_A and F_B and these are indicated on the figure. The presence of the large P700 signal demonstrates that electron transfer from P700 is functional in this sample. A similar signal was generated in experiments using samples from the PsaL-minus and PsaE-minus mutants (data not shown), indicating that electron transfer is unimpaired in PSI lacking these accessory subunits.

7.2.3 Electron transfer to iron-sulphur centres

Light minus dark spectra were plotted for each ascorbate reduced sample as shown in Figure 7.2. The large P700 peak has been deleted so that the signals from the iron-

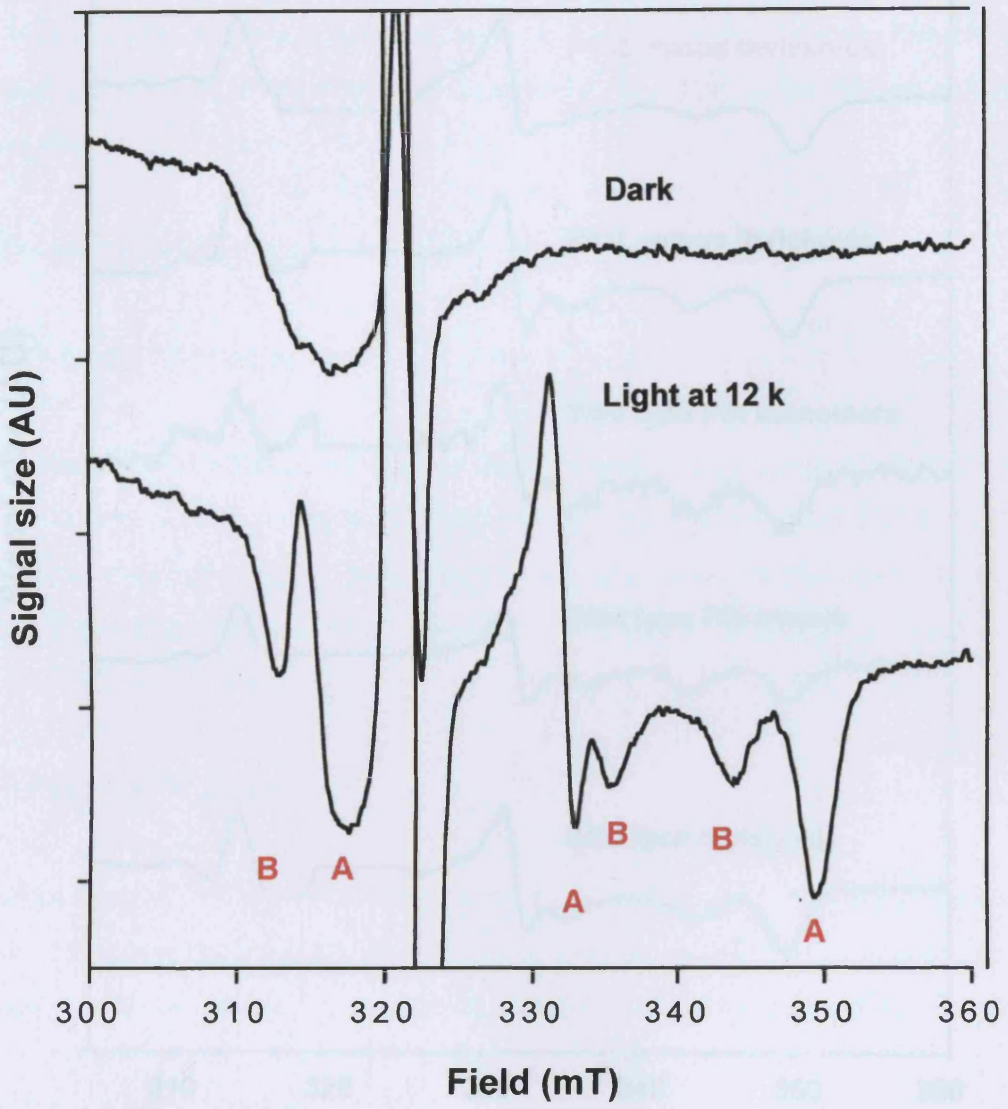

Figure 7.1 CW-EPR spectra of the light-induced $P700^+$ signal of *Synechocystis* 6803 wild type photosystem I. Wild type thylakoids were reduced with sodium ascorbate and EPR spectra recorded at 12 K. The spectra shown are of the g = 2.00 region. When the sample is illuminated, a large P700 peak is seen. The signals corresponding to the iron-sulphur centres F_A/F_B are indicated. EPR conditions were: microwave frequency 9.09 GHz, microwave power 10 mW, modulation amplitude 0.1 mT.

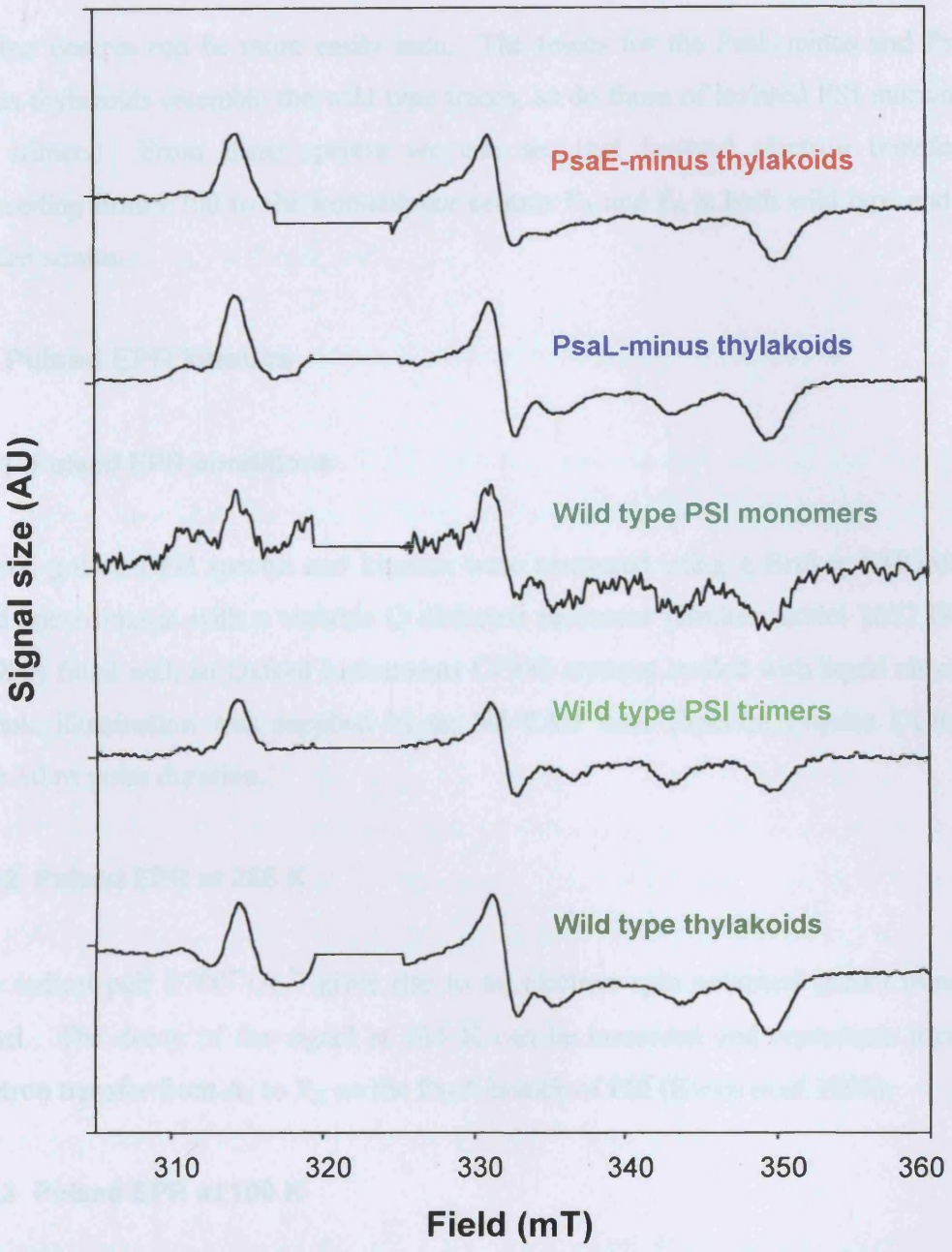

Figure 7.2 CW-EPR spectra of the iron-sulphur centres F_A/F_B in *Synechocystis* 6803 wild type, PsaL-minus and PsaE-minus thylakoids or in isolated monomeric or trimeric PSI particles. Samples were reduced with sodium ascorbate and EPR spectra were recorded at 12 K. The light minus dark spectra for the g = 2.00 region are shown, with the oxidation of P700 deleted to ease comparison. In all cases, the iron-sulphur centres signals are present and resemble the wild type signals (see Figure 7.1). EPR conditions were: microwave frequency 9.09 GHz, microwave power 10 mW, modulation amplitude 0.1 mT.

sulphur centres can be more easily seen. The traces for the PsaL-minus and PsaE-minus thylakoids resemble the wild type traces, as do those of isolated PSI monomers and trimers. From these spectra we can see that forward electron transfer is proceeding from P700 to the iron-sulphur centres F_A and F_B in both wild type and the mutant strains.

7.3 Pulsed EPR kinetics

7.3.1 Pulsed EPR conditions

Kinetic pulsed EPR spectra and kinetics were measured using a Bruker ESP380 X-band spectrometer with a variable Q dielectric resonator (Bruker model 1052 DLQ-H8907) fitted with an Oxford Instruments CF935 cryostat cooled with liquid nitrogen. Actinic illumination was supplied by an Nd-YAG laser (Spectra Physics DCR-11) with 10 ns pulse duration.

7.3.2 Pulsed EPR at 265 K

The radical pair $P700^{\bullet+}/A_1^{\bullet-}$ gives rise to an electron spin polarised (ESP) transient signal. The decay of the signal at 265 K can be measured and represents forward electron transfer from A_1 to F_X on the PsaA branch of PSI (Evans *et al* 1999).

7.3.3 Pulsed EPR at 100 K

At 100 K, forward electron transfer is blocked on the PsaA side of PSI (Schlodder *et al* 1998). The rate measured by pulsed EPR experiments at this temperature results from a mixture of the back reaction between $P700^+$ and A_1^- and the decay of correlation between the two radicals. This rate can be affected by changes to the local environment of A_1 and by the distance between the two electron spins. In ascorbate reduced samples, essentially irreversible electron transfer from P700 to the iron-sulphur centres occurs on the PsaB side of PSI, such that virtually all of the signal seen reflects the formation and decay of the $P700^{\bullet+}/A_1^{\bullet-}$ on the PsaA side. In certain conditions signals from the $P700^{\bullet+}/A_1^{\bullet-}$ pair on the PsaB side can also be detected

(Muhiuddin *et al* 2001). In the present experiments only reactions occurring on the PsaA side of the reaction centre were investigated. The decay of the PsaB side radical pair is approximately 10 times faster than the PsaA side. When both sides of the PSI reaction centre are functional mixed signals are always present, hence no attempt was made to measure the PsaB side rate.

7.3.4 Pulsed EPR analysis of thylakoids and isolated photosystems

Samples of thylakoids or isolated PSI particles were reduced with sodium ascorbate and used to determine the rate of decay of the ESP signal at 265 and/or 100 K as shown in Figures 7.3 and 7.4. Exponential curves were fitted to the data and the values for several experiments were averaged and are presented in Table 7.1.

Although there is some variation in the rates at 265 K, no sample gave a dramatically different rate from the wild type rate. This suggests that functional forward electron transfer from A_1 to F_X on the PsaA branch is occurring normally in the mutants with altered PSI subunit composition. The rates for the PsaL-minus samples and also for the wild type grown under dim blue light conditions (as described in Chapter 4) show slightly reduced forward electron transfer rates. However, as the rate for isolated wild type monomeric PSI particles (equivalent to the type of PSI found in the PsaL-minus mutant) does not differ in rate from that wild type thylakoids, it is unlikely that the slower rate reflects a direct effect on the electron transfer chain.

Likewise, there is no meaningful difference in the signal decay rates for wild type and mutant samples analysed at 100 K. This implies that there has not been a major effect on the properties of the electron transfer chain as a result of the mutations to the accessory subunits of PSI. There are some slight differences in the rates for the isolated photosystems, perhaps as a result of the detergent preparations affecting the quinone (A_1) binding site.

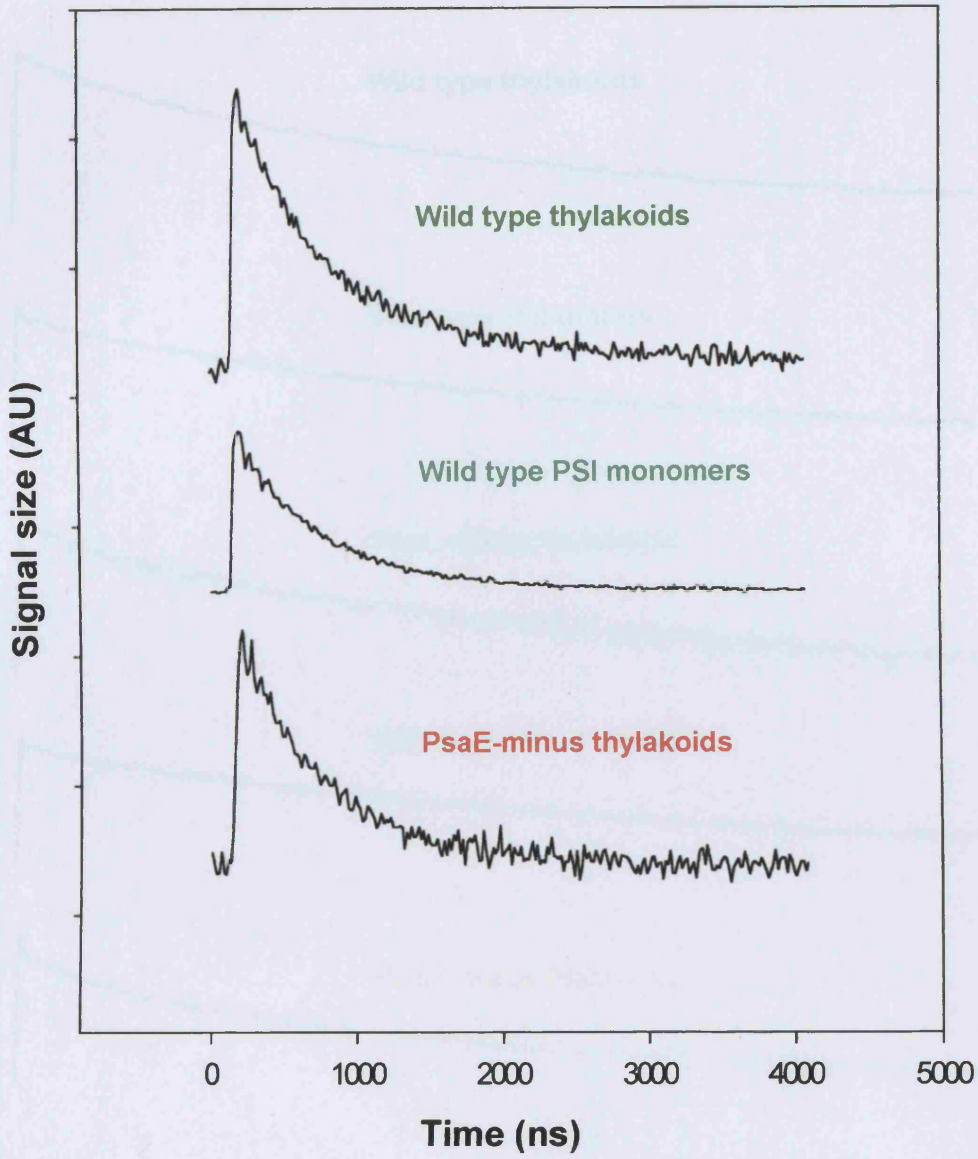

Figure 7.3 Decay of polarisation signal in ascorbate reduced *Synechocystis* 6803 PSI at 265 K arising from the flash induced P700+/A1A- radical pair. Exponential fits to the data were calculated and are shown in Table 7.1. EPR conditions were: flash repetition rate 1 Hz, signal intensity was measured in the g = 2.00 region, field 3465 mT, frequency 9.71. The pulse sequence used to detect the radical was Laser -- T -- 8 ns - t - 16 ns -- echo, t=128 ns, T varies from 0 to 4000 ns from the laser Q switch.

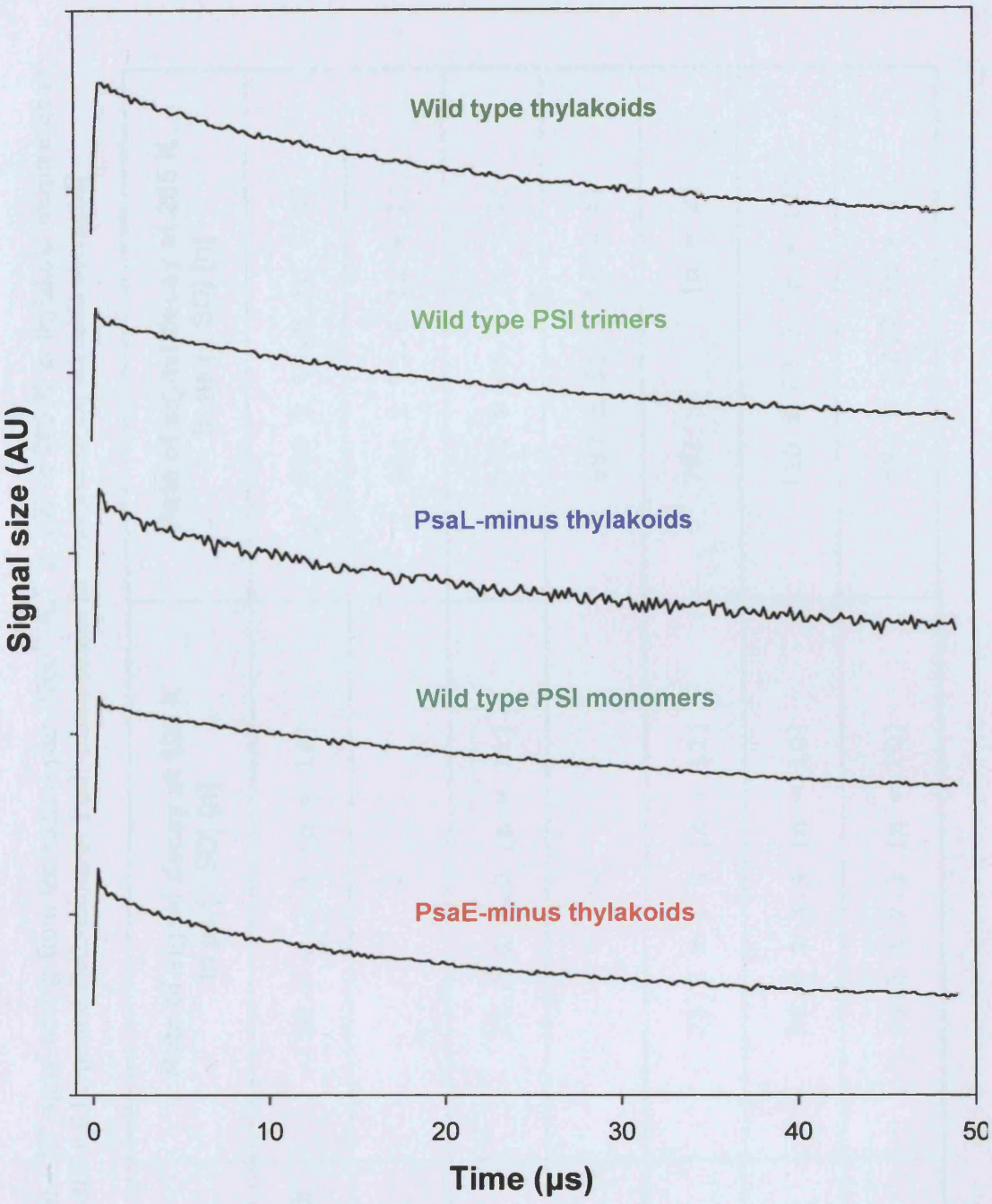

Figure 7.4 Decay of polarisation signal in ascorbate reduced *Synechocystis* 6803 PSI at 100 K. Exponential fits to the data were calculated and are shown in Table 7.1. EPR conditions were: flash repetition rate 10 Hz, signal intensity was measured in the g = 2.00 region.

Table 7.1 Rates of disappearance of the ESP signal arising from the radical pair $P700^{\bullet+}/A_1^{\bullet-}$ at 100 or 265 K in thylakoid membranes or isolated PSI particles from *Synechocystis* 6803 wild type and PsaL-minus or PsaE-minus strains [n = number of experiments averaged]

Sample	Rate of signal decay at 100 K in µs (± SD) [n]	Rate of signal decay at 265 K in ns (± SD) [n]
Wild type (thylakoids), white light growth	20.5 ± 3.3 [n = 14]	645 ± 40.6 [n = 4]
Wild type (thylakoids), blue light growth	-	894 ± 73.6 [n = 7]
Wild type (isolated PSI trimers)	28.2 ± 2.0 [n = 11]	500 ± 45.1 [n = 9]
Wild type (isolated PSI monomers)	-	587 ± 51.3 [n = 4]
PsaL-minus mutant (thylakoids)	25.6 ± 1.5 [n = 12]	781 [n = 2]
PsaL-minus mutant (isolated monomers)	36.0 ± 3.4 [n = 10]	710 ± 82.8 [n = 12]
PsaE-minus mutant (thylakoids)	19.5 ± 2.2 [n = 20]	594 ± 22.7 [n = 4]

7.4 Discussion

7.4.1 CW-EPR indicates functional PSI in the PsaL-minus and PsaE-minus mutants

The CW-EPR spectra revealed no detectable difference between the traces for wild type and PsaL-minus or PsaE-minus mutant samples. This demonstrates that the oxidation of P700 and subsequent electron transfer to the iron-sulphur centres is unimpaired in either mutant and that PSI electron transfer is fully functional. Likewise, there was no discernable difference in spectra for isolated PSI monomers and trimers, implying that any physiological difference between these two PSI conformations is more likely to be connected with light-harvesting or some other function than with electron transfer through the photosystem.

7.4.2 Pulsed EPR demonstrates rates of electron transfer comparable with wild type

Rates of decay of the $P700^{\bullet+}/A_1^{\bullet-}$ radical pair measured from pulsed EPR experiments give an indication of the efficiency of electron transfer through the PsaA side of the core PSI subunits.

The rates obtained for the PsaE-minus mutant were comparable with those of wild type samples. Although the rate for the PsaL-minus mutant appears to be slightly slower than that of wild type (Table 7.1), it is still close to the range typical for wild type and does not therefore signify that there has been an effect on electron transfer through PSI in these cells. The rates for isolated PSI monomers also appeared a little slower than the PSI trimer rate but, once again, it is not sufficiently reduced to imply any particular impact on PSI function.

CHAPTER EIGHT

DISCUSSION

CHAPTER EIGHT

DISCUSSION

8.1 Characterisation of mutants lacking PSI subunits

Cyanobacterial mutants lacking particular accessory subunits of PSI are relatively straightforward to construct as a result of the availability of genome sequences, their ability to undergo natural transformation and the fact that they incorporate the transformed DNA by homologous recombination with the chromosome. Such mutants can be used to explore the function of the missing subunit. Many of the accessory subunits are dispensable for photosynthesis and growth, raising questions as to their function. The primary role of some subunits appears to be to stabilise or orient other subunits, for example PsaI interacts with PsaL; a lack of PsaI results in a decrease in the proportion of trimerised PSI that can be isolated from the thylakoids (Schluchter *et al* 1996). The construction of a set of mutants lacking the PsaL and PsaE subunits is described in Chapter 3.

Characterisation of the PsaL-minus mutants is presented in Chapter 4. It has been established for some time that the PsaL subunit is the main component of the trimerisation domain of cyanobacterial PSI, forming the point of contact between the three monomers (Chitnis & Chitnis 1993, Jordan *et al* 2001). We found that the growth rate of PsaL-minus cells was indistinguishable from that of wild type cells, which concurs with earlier studies (Chitnis *et al* 1993). The question as to whether trimerisation of PSI has any physiological significance for cyanobacterial cells is an intriguing one, particularly as eukaryotic PSI is monomeric. As PsaL-minus mutants are unimpaired in terms of their ability to grow and photosynthesise effectively, it was postulated that the main purpose of trimerisation of PSI is to modulate light-harvesting (Chitnis & Chitnis 1993). Low temperature fluorescence emission spectroscopy was used to show that monomeric PSI interacts with the light-harvesting phycobilisomes and that energy can be transferred to the reaction centres. Monomers and trimers are equally capable of receiving energy from phycobilisomes.

DNA microarray analysis to determine which genes are induced during salt stress was performed and it was found that increased expression of *psaL* occurred under such conditions (N Yeremenko & HCP Matthijs, personal communication). However, studies presented in Chapter 4 demonstrated that the PsaL-minus mutant was no more adversely affected by growth in high salt than wild type cells. Furthermore, salt stress did not result in an increased proportion of trimerised PSI complexes in wild type cells. A later DNA microarray study was published and did not report up-regulation of *psaL* under salt stress (Kanesaki *et al* 2002).

Sucrose density gradients and 77 K fluorescence emission spectra depicted in Chapter 4 demonstrate that wild type cells produce large amounts of strongly trimeric PSI under conditions of dim blue light (as suggested by P Fromme, personal communication). Under this light regime, PsaL-minus cells grow significantly more slowly than wild type and produce an increased level of carotenoids, suggesting that the cells are experiencing stress (this could be further investigated by applying a double stress and/or competition assays). These results reveal that there are conditions, not uncommon in the natural habitat of cyanobacteria, in which cells that cannot produce trimeric PSI are at a disadvantage. This adds weight to the supposition that trimers are physiologically useful in some environmental conditions. The reason for the blue light effect is, as yet, undetermined but we speculate that the monomeric PSI may be more difficult to pack into the thylakoid membrane in conditions were large amounts of PSI are being synthesised or that a thylakoid membrane with a large amount of monomeric PSI functions less efficiently than normal. Oxygen evolution by cells grown under dim blue light was measured and showed that photosynthesis and respiration were occurring normally.

The role of the PsaE subunit, which forms part of the stromal side of PSI, has been debated for several decades, as reviewed in Chapter 1. Several possible functions have been proposed and it is generally accepted that PsaE forms part of the docking site for ferredoxin (Rousseau *et al* 1993, Xu *et al* 1994c) and plays some role in cyclic electron transport (Yu *et al* 1993; Zhao *et al* 1993).

The PsaE-minus mutant was found to grow at a slightly reduced rate compared to wild type cells (Chapter 4). Early reports on the PsaE subunit stated that PSI activity was reduced in the mutant (Chitnis *et al* 1989a). It was decided to use EPR analysis of PSI function to determine whether loss of either the PsaE or PsaL subunits had an effect on electron transfer through the PSI reaction centre core; the results were presented in Chapter 7 and are summarised in Section 8.4

8.2 Interaction of phycobilisomes and PSI monomers and trimers

The light-harvesting structures within cyanobacterial cells are the phycobilisomes - highly mobile structures that diffuse rapidly across the thylakoid membrane surface (Mullineaux *et al* 1997). Phycobilisomes can couple with and efficiently transfer energy to both PSI and PSII reaction centres (Mullineaux 1992, Mullineaux 1994). It is likely that the contact between a phycobilisome and a photosystem reaction centre is short-lived, with each phycobilisome diffusing over the membrane and associating transiently with different reaction centres. FRAP studies have confirmed the mobile nature of phycobilisomes and the unstable nature of the interaction with reaction centres (Sarcina *et al* 2001). Mullineaux *et al* (1997) suggested that phycobilisome mobility could be involved in regulating light-harvesting via state transitions and that the rate of their diffusion could be limited by the transient binding to stationary reaction centres or by steric hindrance in the cytoplasm.

In Chapter 5 of this thesis, FRAP analysis of the PsaL-minus mutant of *Synechococcus* 7942 (a species that has thylakoid membranes conveniently arranged as concentric rings that facilitate FRAP measurements) is presented. This analysis revealed that phycobilisomes diffuse almost three times more rapidly when PSI is entirely monomeric (Aspinwall *et al* 2004b). As there is no difference in the pigment composition or PSII:PSI ratio in the mutant, the altered rate is unlikely to be due to any general alterations to the membrane arrangement: the monomerisation of PSI has a direct effect on phycobilisome mobility. The thylakoid membranes contain the protein complexes required for the photosynthetic and respiratory electron transport chains and are densely packed with protein complexes (Mullineaux 1999). It is possible that the packing of PSI as a large trimeric structure could slow the diffusion

of phycobilisomes across the thylakoid membrane by steric hindrance. The smaller monomeric PSI complexes are likely to be packaged differently from trimers and may cause less obstruction to the movement of phycobilisomes across the surface. It is also possible that there is some difference in the strength of the phycobilisome-PSI reaction centre interaction when the PSI is monomeric. A potentially looser association with monomers could allow faster phycobilisome diffusion in PsaL-minus cells by reducing the strength of the coupling to such reaction centres.

It has been suggested that the formation of a functional 'supercomplex' consisting of a phycobilisome and a photosystem reaction centre depends on the oligomerisation of the photosystem, with PSII being required as a dimer and PSI as a trimer (Bald *et al* 1996). However, the PsaL-minus mutant showed no detectable reduction in its ability to use phycobilisome-absorbed energy (determined by low temperature fluorescence spectroscopy). The phycobilisomes can interact with PSI either as a trimer or as a monomer and efficiently funnel energy into the reaction centre in either case.

State transitions are a rapid and convenient mechanism by which cyanobacteria can respond to changing light intensity or quality by altering the relative amounts of phycobilisome-harvested light to PSI or PSII complexes. In experiments described in Chapter 5 we found that state transitions occur almost twice as fast in the PsaL-minus mutant of *Synechococcus* 7942 than in wild type. This is in agreement with an earlier study using a PsaL-minus mutant of *Synechococcus* 7002, which found that state transitions occurred about three times faster in the mutant (Schluchter *et al* 1996).

It is possible that there is a link between the increased rate of state transitions and the more rapid diffusion of phycobilisomes in the PsaL-minus mutant. The phycobilisome diffusion rate as a rate-limiting factor for state transitions is plausible if the membrane organisation requires a long movement of the phycobilisome during a state transition. Sherman *et al* (1994) described a heterogeneous distribution of PSI, with higher concentrations being found in the thylakoid membranes closest to the plasma membrane, whereas PSII complexes were more evenly distributed throughout the membrane system. If there are distinct regions of the membrane containing higher

concentrations of PSI, then increased phycobilisome mobility may lead directly to more rapid state transitions.

The association of PSI and phycobilisomes is known to be transient and unstable. It is possible that the interaction of the phycobilisome with monomeric PSI is weaker than with the trimeric form found in wild type cells. As well as creating the potential for more rapid phycobilisome diffusion (by reducing the strength of anchoring of the phycobilisome to the reaction centre), this weaker structural interaction might also permit more rapid state 2 to state 1 transitions.

8.3 PSI trimerisation is not required for association of the CP43' antenna ring

The induction of the *isiA* gene and subsequent synthesis of CP43' protein leads to accumulation of this protein in the thylakoid membranes of cyanobacterial cells under conditions of iron starvation. The CP43' proteins form an antenna ring comprised of 18 subunits around PSI trimers in wild type cells, allowing a large increase in light-harvesting capability for these reaction centres at a time when both PSI and phycobilisome levels decrease.

The experiments described in Chapter 6 revealed that the CP43' protein is also produced in iron stressed PsaL-minus mutants and can still associate with the PSI reaction centre as a crescent-shaped structure. The antenna system of CP43' proteins do not, therefore, require trimerisation of PSI, or the presence of the PsaL subunit, to functionally associate with the reaction centre (Aspinwall *et al* 2004a). The PsaL-minus mutant was not disadvantaged in terms of growth rate under conditions of iron starvation, presumably because the compensation provided by the chlorophyll bound to the CP43' proteins caused a sufficient increase in light-harvesting capacity. Electron microscopy and single particle analysis of the isolated PSI monomer-CP43' supercomplexes were combined with x-ray crystallography data to demonstrate that six CP43' subunits associate with each monomeric PSI reaction centre. A dramatic increase in CP43' fluorescence at 685 nm after dissociation of the supercomplex using a detergent treatment shows that the CP43' antenna is efficiently coupled to PSI in the

isolated supercomplex. Recent work with a *Synechocystis* 6803 PsaFJ-minus mutant revealed a 17-mer ring of CP43' around PSI trimers (Kouřil *et al* 2003). This suggests a level of flexibility in the way the CP43' interacts with PSI.

8.4 Electron transfer is not perturbed in PsaL-minus and PsaE-minus mutants

EPR analysis of photosystem I particles and thylakoid membrane samples from the PsaL and PsaE mutants is presented in Chapter 7. CW-EPR revealed no detectable difference between the wild type, PsaL-minus or PsaE-minus samples. This demonstrates that the oxidation of P700 and subsequent electron transfer to the iron-sulphur centres is unimpaired in either mutant and that PSI electron transfer is fully functional. Likewise, there was no discernable difference between the spectra for isolated PSI monomers and trimers, implying that any physiological difference between these two PSI conformations is more likely to be connected with light-harvesting or some other function than with electron transfer through the photosystem.

Rates of decay of the $P700^{\bullet+}/A_1^{\bullet-}$ radical pair measured from pulsed EPR experiments give an indication of the efficiency of electron transfer through the PsaA side of the core PSI subunits. The rates obtained for the PsaE-minus mutant were comparable with those of wild type samples. Although the rate for the PsaL-minus mutant appears to be slightly slower than that of wild type, it is still close to the range typical for wild type and does not therefore signify that there has been an effect on electron transfer through PSI in these cells. The rates for isolated PSI monomers also appeared a little slower than the PSI trimer rate but, once again, it is not sufficiently reduced to imply any particular impact on PSI function.

8.5 Future work

It is known that the PsaE subunit forms part of the docking side for ferredoxin on the stromal side of PSI. As it has also been suggested that the subunit is required for cyclic electron transport, it would be interesting to grow the PsaE-minus cells under

conditions that favour cyclic electron transport, in which they should be disadvantaged.

The physiological significance of PSI trimerisation remains unsolved. However, growth conditions in which cells with only monomeric PSI are disadvantaged have been discovered – dim blue light. A northern blot could be used to determine whether the *psaL* gene is actually up-regulated in order to enhance the level of trimerisation in wild type cells, as the results presented in Chapter 4 suggest. A similar blot could also be used to establish whether this gene is up-regulated under salt stress, although the results in Chapter 4 gave no indication that the absence of PsaL posed any problem for cells growing in high salt media.

Thylakoid membranes isolated from cells grown under dim blue light membrane could be used for electron microscopic imaging. This would perhaps reveal whether PSI trimers are favoured in these conditions because (a) they can be packaged more efficiently in the membrane when PSI is being produced in large amounts (b) trimers themselves are better distributed, while monomers form arrangements that in some way impair electron transport and photon utilisation.

The *chlL*-minus genetic background provides a means of eliminating pigments and photosystems from cells, followed by a re-greening period in which new photosystems are synthesised. In theory, this could provide a useful method for studying the effect of a mutation on the assembly of the photosynthetic apparatus. Although the *psaL* and *psaE* genes were knocked out in cells with this genetic background to create double mutants, the de-greening/re-greening experiments were unsuccessful due to difficulties in maintaining viable conditions under LAHC and were abandoned. However, this study could be resurrected and used to establish whether the absence of an accessory subunit has an impact on photosystem assembly.

It has been shown that the trimerisation of PSI is not necessary for the functional association of the light-harvesting phycobilisome structures or the iron stress-induced CP43' antenna ring. It would be interesting to learn more about the factors that are

necessary for the CP43' to attach to the reaction centre. A systematic mutagenesis strategy could be employed to discover which PSI components are required.

To learn more about the interaction of phycobilisomes and PSI, it would be useful to find a mutant that was affected in terms of its ability to transfer phycobilisome-harvested energy to the reaction centre. If this mutation was combined with the *psaL* deletion and studied to find out whether the energy transfer was improved or further impaired, it may give us information about the interaction of phycobilisomes and reaction centres rather than their movement between them.

Several possibilities that may reveal a reason for PSI trimerisation remain untested. For example, the effects of photoinhibitory light intensity could be investigated. Indeed, a crude test in which *Synechocystis* 6803 wild type and PsaL-minus cells were placed beneath a high intensity light found that the wild type cells survived while the mutant cells appeared to die (data not shown). Due to time constraints this was not pursued further for this thesis, but it provides a starting point for further studies on these mutants.

Additionally, work with monomers and trimers of PSI in *Spirulina platensis* suggested that trimers could be necessary for the use of long wavelength-emitting chlorophyll (called 'red' chlorophyll) in the PSI reaction centre, which could increase the range of wavelengths of light that can be utilised (Kruip *et al* 1999). It would be useful to investigate this in other species to determine whether the red chlorophylls do require trimerisation of the reaction centre.

8.6 Summary

The experiments presented in this thesis have demonstrated the following:

- The absence of the PsaE subunit of PSI results in a slightly reduced growth rate. Electron transfer through PSI in this mutant is not adversely affected.
- The PsaL-minus mutant grew normally under standard light conditions but was at a disadvantage under dim blue light.
- Salt stress did not have an adverse effect on PsaL-minus cells.
- Phycobilisomes interact efficiently with either PSI trimers or monomers.
- Phycobilisomes diffuse more rapidly across membranes containing entirely monomeric PSI.
- State transitions occur more rapidly in cells with entirely monomeric PSI.
- Trimerisation of PSI is not required for interaction between the reaction centre and the iron stress-induced CP43' ring.

Cyanobacteria provide excellent model systems for studying photosynthesis. The analysis of deletion mutants that lack one or more of the photosystem subunits can provide insights into the function of the missing subunit and the factors affecting the interaction of the altered photosystem with other structures such as the light-harvesting apparatus.

REFERENCES

REFERENCES

Allen JF (1992) Protein phosphorylation in regulation of photosynthesis. *Biochimica Biophysica Acta* 1098: 275-335

Ali K (2004) Photosystem I in *Chlamydomonas reinhardtii*. PhD thesis. University College London,

Andersen B, Scheller HV and Moller BL (1992) The PSI-E subunit of photosystem I binds ferredoxin:NADP+ oxidoreductase. *FEBS Letters* 311: 169-173

Andrizhiyevskaya EG, Schwabe TME, Germano M, D'Haene S, Kruip J, van Grondelle R and Dekker JP (2002) Spectroscopic properties of PSI-IsiA supercomplexes from the cyanobacterium *Synechococcus* PCC 7942. *Biochimica et Biophysica Acta* 1556: 265-272

Aspinwall CL, Duncan J, Bibby T, Mullineaux CW and Barber J (2004a) The trimeric organisation of photosystem I is not necessary for the iron-stress induced CP43' protein to functionally associate with this reaction centre. *FEBS Letters* 574: 126-130

Aspinwall CL, Sarcina M and Mullineaux CW (2004b) Phycobilisome mobility in the cyanobacterium *Synechococcus* sp. PCC7942 is influenced by the trimerisation of photosystem I. *Photosynthesis Research* 79: 179-187

Bald D, Kruip J and Rögner M (1996) Supramolecular architecture of cyanobacterial thylakoid membranes: how is the phycobilisome connected with the photosystems? *Photosynthesis Research* 49: 103-118

Barber J and Andersson B (1994) Revealing the blueprint of photosynthesis. *Nature* 370: 31-34

Barth P, Lagoutte B and Setif P (1998) Ferredoxin reduction by photosystem I from *Synechocystis* sp. PCC 6803: toward an understanding of the respective roles of subunits PsaD and PsaE in ferredoxin binding. *Biochemistry* 37: 16233-16241

Behrenfeld MJ, Bale AJ, Zbigniew SK, Aiken J and Falkowski PG (1996) Confirmation of the iron limitation of phytoplankton photosynthesis in the equatorial Pacific Ocean. *Nature* 383: 508-511

Bendall DS and Manasse RS (1995) Cyclic photophosphorylation and electron transport. *Biochimica et Biophysica Acta: Bioenergetics* 1229: 23-38

Ben-Shem A, Frolow F and Nelson N (2003) Crystal structure of plant photosystem I. *Nature* 426: 630-635

Bibby TS, Nield J and Barber J (2001a) Iron deficiency induces the formation of an antenna ring around trimeric photosystem in cyanobacteria. *Nature* 412: 743-745

Bibby TS, Nield J and Barber J (2001b) Three-dimensional model and characterisation of the iron stress-induced CP43'-photosystem I supercomplex isolated from the cyanobacterium *Synechocystis* PCC 6803. *Journal of Biological Chemistry* 276: 43246-43252

Bibby TS, Nield J, Partensky F and Barber J (2001c) Antenna ring around photosystem I. *Nature* 413: 590

Biggins GS and Mathis P (1988) Functional role of vitamin K1 in photosystem I of the cyanobacterium *Synechocystis* 6803. *Biochemistry* 27: 1494-1500

Boekema EJ, Hifney A, Yakushevska AE, Piotrowski M, Keegstra W, Berry S, Michel K-P, Pistorius EK and Kruip J (2001a) A giant chlorophyll-protein complex induced by iron deficiency in cyanobacteria. *Nature* 412: 745-748

Boekema E, Jensen PE, Schlodder E, van Breeme JFL, an Roon H, Scheller HV and Dekker JP (2001b) Green plant photosystem I binds light-harvesting complex on one side of the complex. *Biochemistry* 40: 1029-1036

Brettel K (1997) Electron transfer and arrangement of the redox cofactors in photosystem I. *Biochimica et Biophysica Acta* 1318: 322-373

Burnap RL, Troyan T and Sherman LA (1993) The highly abundant chlorophyll-protein complex of iron-deficient *Synechococcus* sp. PCC7942 (CP43') is encoded by the *isiA* gene. *Plant Physiology* 103: 893-902

Castenholz RW (1998) Culturing methods for cyanobacteria. *Methods in Enzymology* 167: 68-92. Ed. Packer L and Glazer AN. Academic Press, San Diego.

Chitnis PR (1996) Photosystem I. *Plant Physiology* 111: 661-669

Chitnis VP and Chitnis PR (1993) PsaL subunit is required for the formation of photosystem I trimers in the cyanobacterium *Synechocystis* sp. PCC 6803. *FEBS Letters* 336: 330-334

Chitnis VP, Xu Q, Yu L, Golbeck JH, Nakamoto H, Xie DL ad Chitnis PR (1993) Targeted inactivation of the gene *psaL* encoding a subunit of photosystem I of the cyanobacterium *Synechocystis* sp. PCC 6803. *Journal of Biological Chemistry* 268: 11678-11684

Chitnis PR, Reilly PA, Miedel MC and Nelson N (1989a) Structure and targeted mutagenesis of the gene encoding 8-kDa subunit of photosystem I from the cyanobacterium *Synechocystis* sp. PCC 6803. *Journal of Biological Chemistry* 264: 18374-18380

Chitnis PR, Reilly PA and Nelson N (1989b) Insertional inactivation of the gene encoding subunit II of photosystem I from the cyanobacterium *Synechocystis* sp. PCC 6803. *Journal of Biological Chemistry* 264: 18381-18385

Chitnis PR, Xu Q, Chitnis VP and Nechushtai R (1995) Function and organisation of photosystem I polypeptides. *Photosynthesis Research* 44: 23-40

Duncan J, Bibby T, Tanaka A and Barber J (2003) Exploring the ability of chlorophyll *b* to bind to the CP43' protein induced under iron deprivation in a mutant of *Synechocystis* PCC 6803 containing the *cao* gene. *FEBS Letters* 541: 171-175

Emlyn-Jones D, Ashby MK and Mullineaux CW (1999) A gene required for the regulation of photosynthetic light harvesting in the cyanobacterium *Synechocystis* 6803. *Molecular Microbiology* 33: 1050-1058

Evans MCW (1977) Electron paramagnetic resonance studies in photosynthesis. In *Primary Processes of Photosynthesis*. Topics in Photosynthesis volume 2. Editor J. Barber. Elsevier Scientific Publishing Company.

Evans MCW, Purton S, Patel V, Wright D, Heathcote P and Rigby SEJ (1999) Modification of electron transfer from the quinone electron carrier, A_1, of photosystem I in the site directed mutant D576→L within the Fe-S_X binding site of PsaA and in the second site suppressors of the mutation in *Chlamydomonas reinhardtii*. *Photosynthesis Research* 61: 33-42

Fairclough WV, Forsyth A, Evans MCW, Rigby EJ, Purton S and Heathcote P (2003) Bidirectional electron transfer in photosystem I: electron transfer on the PsaA side is not essential for phototrophic growth in *Chlamydomonas*. *Biochimica Biophysica Acta* 1606: 43-55

Falk S, Samson G, Bruce D, Hunter NPA and Laudenbach DA (1995) Functional analysis of the iron-stress induced CP43' polypeptide of PSII in the cyanobacterium *Synechococcus* sp. PCC7942. *Photosynthesis Research* 45: 51-60

Farah J, Rappaport F, Choquet Y, Joliot P and Rochaix JD (1995) Isolation of a psaF-deficient mutant of *Chlamydomonas reinhardtii*: efficient interaction of plastocyanin

with the photosystem I reaction centre is mediated by the PsaF subunit. *The EMBO Journal* 14: 4976-4984

Ferreira F and Straus NA (1994) Iron deprivation in cyanobacteria. *Journal of Applied Phycology* 6: 199-210

Fischer N, Boudreau E, Hippler M, Drepper F, Haehnel W and Rochaix J-D (1999) A large fraction of PsaF is non-functional in photosystem I complexes lacking the PsaJ subunit. *Biochemistry* 38: 5546-5552

Fischer N, Hippler M, Setif P, Jacquot JP and Rochaix JD (1998) The PsaC subunit of photosystem I provides an essential lysine residue for fast electron transfer to ferredoxin. *EMBO Journal* 17: 849-858

Fork DC and Herbert SK (1993) Electron transport and photophosphorylation by photosystem I in vivo in plants and cyanobacteria. *Photosynthesis Research* 36: 149-168

Frank H and Cogdell RJ (1995) Carotenoids in photosynthesis. *Photochemistry and Photobiology* 63: 257-264

Fromme P, Melkozernov A, Jordan P and Krauss N (2003) Structure and function of photosystem I: interaction with its soluble electron carriers and external antenna systems. *FEBS Letters* 555: 40-44

Geiß U, Vinnemeier J, Schoor A and Hagemann M (2001) The iron-regulated *isiA* gene of *Fischerella muscicola* strain PCC 73103 is linked to a likewise regulated gene encoding a Pcb-like chlorophyll-binding protein. *FEMS Microbiology Letters* 197: 123-129

Ghassemian M and Straus NA (1996) Fur regulates the expression of iron-stress genes in the cyanobacterium *Synechococcus* sp. strain PCC 7942. *Microbiology-UK* 142: 1469-1476

Guergova-Kuras M, Bordreaux A, Joliot A, Joliot P and Redding K (2001) Evidence for two active branches for electron transfer in photosystem I. *Proceedings of the National Academy USA* 98: 4437-4442

Guikema J and Sherman LA (1983) Organization and function of chl in membranes of cyanobacteria under iron starvation. *Plant Physiology* 73: 250-256

Haldrup A, Jensen PE, Lunde C and Scheller HV (2001) Balance of power: a view of the mechanism of photosynthetic state transitions. *Trends in Plant Science* 6: 301-305

Haldrup A, Naver H and Scheller HV (1999) The interaction between plastocyanin and photosystem I is inefficient in transgenic *Arabidopsis* plants lacking the PSI-N subunit of photosystem I. *The Plant Journal* 17: 689-698

Haldrup A, Simpson DJ and Scheller HV (2000) Down-regulation of the PSI-F subunit of photosystem I (PSI) in *Arabidopsis thaliana*. *Journal of Biological Chemistry* 275: 31211-31218

Hall DO and Rao KK (1999) Photosynthesis. 6th edition. Cambridge University Press.

Hillier W and Babcock GT (2001) Photosynthetic reaction centres. *Plant Physiology* 125: 33-37

Hippler M, Drepper F, Rochaix JD and Muhlenhoff (1999) Insertion of the N-terminal part of PsaF from *Chlamydomonas* reinhardtii into photosystem I from *Synechococcus elongatus* enables efficient binding of algal plastocyanin and cytochrome c_6. *Journal of Biological Chemistry* 274: 4180-4188

Hutber GN, Hutson KG and Rogers LG (1977) Effect of iron deficiency on levels of two ferredoxins and flavodoxin in a cyanobacterium. *FEMS Microbiology Letters* 1: 193-196

Ivanov AG, Park Y-I, Miskiewicz E, Raven JA, Huner NPA and Öquist G (2000) Iron stress restricts photosynthetic intersystem electron transport in *Synechococcus* sp. PCC 7942. *FEBS Letters* 485: 173-177

Iwata S and Barber J (2004) Structure of photosystem II and molecular architecture of the oxygen-evolving centre. *Current Opinion in Structural Biology* 14: 447-453

Jeanjean R, Zuther E, Yeremenko N, Havaux M, Matthijs HCP and Hagemann M (2003) A photosystem 1 psaFJ-null mutant of the cyanobacterium Synechocystis PCC 6803 expresses the isiAB operon under iron replete conditions. *FEBS Letters* 549: 52-56

Jensen PE, Gilpin M, Knoetzel J and Scheller HV (2000) The PSI-K subunit of photosystem I is involved in the interaction between light-harvesting complex I and the photosystem I reaction centre core. *Journal of Biological Chemistry* 275: 24701-24708

Joliot P and Joliot A (1999) In vivo analysis of the electron transfer within photosystem I: are the two phylloquinones involved? *Biochemistry* 38: 11130-11136

Jordan P, Fromme P, Witt HT, Klukas O, Saenger W and Krauβ (2001) Three-dimensional structure of cyanobacterial photosystem I at 2.5 Å resolution. *Nature* 411: 909-917

Kaneko T, Sato S, Kotani H *et al* (1996) Sequence analysis of the genome of the unicellular cyanobacterium *Synechocystis* sp. strain PCC 6803. II. Sequence determination of the entire genome and assignment of potential protein-coding regions. *DNA Research* 3: 109-136

Kanesaki Y, Suzuki I, Allakhverdiev SI, Mikami K and Murata N (2002) Salt stress and hyperosmotic stress regulate the expression of different sets of genes in

Synechocystis sp. PCC 6803. *Biochemical and Biophysical Research Communications* 290: 339-348

Kouřil R, Yeremenko N, D'Haene S, Yakushevska AE, Keegstra W, Matthijs HCP, Dekker JP and Boekema E (2003) Photosystem I trimers from *Synechocystis* PCC 6803 lacking the PsaF and PsaJ subunits bind an IsiA ring of 17 units. *Biochimica et Biophysica Acta* 1607: 1-4

Kruip J, Bald D, Boekema EJ and Rögner M (1994) Evidence for the existence of trimeric and monomeric photosystem I complexes in the thylakoid membranes from cyanobacteria. *Photosynthesis Research* 40: 279-286

Kruip J, Karapetyan NV, Terekhova IV and Rögner M (1999) *In vitro* oligomerization of a membrane protein complex. Liposome-based reconstitution of trimeric photosystem I from isolated monomers. *Journal of Biological Chemistry* 274: 18181-18188

Li D, Xie J, Zhao Y and Zhao J (2003) Probing connection of PBS with the photosystems in intact cells of *Spirulina platensis* by temperature-induced fluorescence fluctuation. *Biochimica et Biophysica Acta* 1557: 35-40

Lunde C, Jensen PE, Haldrup A, Knoetzet J and Scheller HV (2000) The PSI-H subunit of photosystem I is essential for state transitions in plant photosynthesis. *Nature* 408: 613-615

Lunde C, Jensen PE, Rosgaard L, Haldrup A, Gilpin MJ and Scheller HV (2003) Plants impaired in state transitions can to a large degree compensate for their defect. *Plant Cell Physiology* 44: 44-54

Meimberg K, Lagoutte B, Bottin H and Mühlenhoff U (1998) The PsaE subunit is required for complex formation between photosystem I and flavodoxin from the cyanobacterium *Synechocystis* sp. PCC 6803. *Biochemistry* 37: 9759-9767

Meimberg K and Mühlenhoff U (1999) Laser-flash absorption spectroscopy study of the competition between ferredoxin and flavodoxin photoreduction by photosystem I in *Synechococcus* sp. PCC 7002: evidence for a strong preference for ferredoxin. *Photosynthesis Research* 61: 253-267

Meunier PC, Colón-López MS and Sherman LA (1997) Temporal changes in state transitions and photosystem organization in the unicellular, diazotrophic cyanobacterium *Cyanothece* sp. ATCC 51142. *Plant Physiology* 115: 991-1000

Michel K-P and Pistorius EK (2004) Adaptation of the photosynthetic electron transport chain in cyanobacteria to iron deficiency: the function of IdiA and IsiA. *Physiologia Plantarum* 120: 36-50

Muhiuddin IP, Heathcote P, Carter S, Purton S, Rigby SEJ and Evans MCW (2001) Evidence from time resolved studies of the $P700^{+}/A_1^{-}$ radical pair for photosynthetic electron transfer on both the PsaA and PsaB branches of the photosystem I reaction centre. *FEBS Letters* 503: 56-60

Muhlenhoff U, Zhao J and Bryant DA (1996) Interaction between photosystem I and flavodoxin from the cyanobacterium *Synechococcus* sp. PCC 7002 as revealed by chemical cross-linking. *European Journal of Biochemistry* 235: 324-331

Mullineaux CW (1992) Excitation energy transfer from phycobilisomes to photosystem I in a cyanobacterium. *Biochimica et Biophysica Acta* 1100: 285-292

Mullineaux CW (1994) Excitation energy transfer from phycobilisomes to photosystem I in a cyanobacterial mutant lacking photosystem II. *Biochimica et Biophysica Acta* 1184: 71-77

Mullineaux CW (1999) The thylakoid membranes of cyanobacteria: structure, dynamics and function. *Australian Journal of Plant Physiology* 26: 671-677

Mullineaux CW and Allen JF (1990) State 1-State 2 transitions in the cyanobacterium *Synechococcus* 6301 are controlled by the redox state of electron carriers between photosystems I and II. *Photosynthesis Research* 23: 297-311

Mullineaux CW and Sarcina M (2002) Probing the dynamics of photosynthetic membranes with fluorescence recovery after photobleaching. *Trends in Plant Science* 7: 237-240

Mullineaux CW, Tobin MJ and Jones GR (1997) Mobility of photosynthetic complexes in thylakoid membranes. *Nature* 390: 421-424

Munekage Y, Hojo M, Meurer J, Endo T, Tasaka M and Shikani T (2003) *PGR5* is involved in cyclic electron flow around photosystem I and is essential for photoprotection in *Arabidopsis. Cell* **110**

Munekage Y, Hashimoto M, Miyake C, Tomizawa K, Endo T, Tasaka M and Shikanai T (2004) Cyclic electron flow around photosystem I is essential for photosynthesis. *Nature* **429**: 579-582

Naithani S, Hou JM and Chitnis PR (2000) Targeted inactivation of the *psaK1, psaK2* and *psaM* genes encoding subunits of photosystem I in the cyanobacterium *Synechocystis* sp. PCC 6803. *Photosynthesis Research* 63: 225-236

Nield J, Morris EP, Bibby TS and Barber J (2003) Structural analysis of the photosystem I supercomplex of cyanobacteria induced by iron deficiency. *Biochemistry* 42: 3180-3188

Naver H, Haldrup A and Scheller HV (1999) Cosuppression of photosystem I subunit PSI-H in *Arabidopsis thaliana. The Journal of Biological Chemistry* 274: 10784-10789

Nugent JHA (1996) Oxygenic photosynthesis. Electron transfer in photosystem I and photosystem II. *European Journal of Biochemistry* 237: 519-531

Pakrasi HB, Riethman HC and Sherman LA (1985) Organization of pigment proteins in the photosystem II complex of the cyanobacterium *Anacystis nidulans* R2. *Proceedings of the National Academy of Science USA* 82: 6903-6907

Park Y, Sandström S, Gustafsson P and Öquist G (1999) Expression of the *isiA* gene is essential for the survival of the cyanobacterium *Synechococcus* sp. PCC 7942 by protecting photosystem II from excess light under iron limitation. *Molecular Microbiology* 32: 123-129

Porra RJ, Thompson WA and Kriedeman PE (1989) Determination of accurate extinction coefficients and simultaneous equations for assaying chlorophyll *a* and chlorophyll *b* extracted with four different solvents; verification of the concentration of chlorophyll standards by atomic absorption spectroscopy. *Biochimica et Biophysica Acta* 975: 384-394

Purton S, Stevens DR, Muhiuddin IP, Evans MCW, Carter S, Rigby SEJ and Heathcote P (2001) Site-directed mutagenesis of PsaA residue W693 affects phylloquinone binding and function in the photosystem I reaction centre of *Chlamydomonas reinhardtii*. *Biochemistry* 40: 2167-2175

Riethman HC and Sherman LA (1988) Purification and characterization of an iron-stress-induced chlorophyll-protein from the cyanobacterium *Anacystis nidulans* R2. *Biochimica et Biophysica Acta* 935: 141-151

Rigby SEJ, Muhiuddin IP, Evans MCW, Purton S and Heathcote P (2002) Photoaccumulation of the PsaB phyllosemiquinone in photosystem I of Chlamydomonas reinhardtii. *Biochimica et Biophysica Acta Bioenergetics* 1556: 13-20

Rousseau F, Setif P and Lagoutte B (1993) Evidence for the involvement of PSI-E subunit in the reduction of ferredoxin by photosystem I. *The EMBO Journal* 12: 1755-1765

Ruffle SV, Mustafa AO, Kitmitto A, Holzenburg A and Ford RC (2000) The location of the mobile electron carrier ferredoxin in vascular plant photosystem I. *Journal of Biological Chemistry* 275: 36250-36255

Sambrook J and Russell DW (2001) Molecular Cloning – A Laboratory Manuel. 3rd edition. Cold Spring Harbour Laboratory Press, New York.

Sandström S, Ivanov AG, Park Y-I, Öquist G and Gustafsson P (2002) Iron stress responses in the cyanobacterium *Synechococcus* sp. PCC 7942. *Physiologica Plantarium* 116: 255-263

Sarcina M, Tobin MJ and Mullineaux (2001) Diffusion of phycobilisomes on the thylakoid membranes of the cyanobacterium *Synechococcus* 7942. *Journal of Biological Chemistry* 276: 46830-46834

Satoh S, Ikeuchi M, Mimuro M and Tanaka A (2001) Chlorophyll *b* expressed in cyanobacteria functions as a light-harvesting antenna in photosystem I through flexibility of the proteins. *Journal of Biological Chemistry* 276: 4293-4297

Scheller HV, Jensen PE, Haldrup A, Lunde C and Knoetzel (2000) Role of subunits in eukaryotic photosystem I. *Biochimica Biophysica Acta* 1507: 41-60

Schlodder E, Falkenberg K, Gergeleit M and Brettel K (1998) Temperature dependence of forward and reverse electron transfer from $A_1^{\bullet-}$, the reduced secondary electron acceptor in Photosystem I. *Biochemistry* 37: 9466-9476

Schluchter WM, Shen G, Zhao J and Bryant DA (1996) Characterisation of *psaI* and *psaL* mutants of *Synechococcus* sp Strain PCC 7002: a new model for state transitions in cyanobacteria. *Photochemistry and Photobiology* 64: 53-66

Schwabe TME and Kruip J (2000) Biogenesis and assembly of photosystem I. *Indian Journal of Biochemistry and Biophysics* 37: 351-359

Setif P and Brettel K (1993) Forward electron transfer from phylloquinone A1 to iron-sulphur centres in spinach photosystem I. *Biochemistry* 32: 7846-7854

Sherman DM, Troyan TA and Sherman LA (1994) Localization of membrane proteins in the cyanobacterium *Synechococcus* sp. PCC7942: radial asymmetry in the photosynthetic complexes. *Plant Physiology* 106: 251-262

Sherman M, Soejima T, Shui W and van Heel M (1998) Multivariate analysis of single unit cells in electron crystallography. *Ultramicroscopy* 74: 179-199

Sonoike K, Hatanaka H and Katoh S (1993) Small subunits of photosystem I reaction centre complexes from *Synechococcus elongatus*. II. The *psaE* gene product has a role to promote interaction between the terminal electron acceptor and ferredoxin. *Biochimica et Biophysica Acta* 1141: 52-57

Straus NA (1994) Iron deprivation: physiology and gene regulation. In *The Molecular Biology of Cyanobacteria*. Ed. Bryant DA. Kluwer Academic Publishers, Dordrecht. P731-750.

van Heel M, Gowen B, Matedeen R, Orlova EV, Finn R, Pape T, Cohen D, Stark H, Schmidt R, Schatz M and Partwardhan A (2000) Single-particle electron cryo-microscopy: towards atomic resolution. *Quarterly Reviews of Biophysics*. 33: 307-369

van Heel M, Harauz G and Orlova EV (1996) A New Generation of the IMAGIC Image Processing System. *Journal of Structural Biology* 116: 17-24

Varotto C, Pesaresi P, Meurer J, Oelmuller R, Steiner-Lange S, Salamini F and Leister D (2000) Disruption of the *Arabidopsis* photosystem I gene psaE1 affects photosynthesis and impairs growth. *The Plant Journal* 22: 115-124

Vermaas WFJ, Charite J and Eggers B (1990) System for site-directed mutagenesis in the *psbD1/C* operon of *Synechocystis* sp. PCC6803. In: *Current Research in*

Photosynthesis. (Editor Baltscheffsky M). Volume 1, pp 231-238. Kluwer Academic Publishers, Dordrecht.

Vinnemeier J, Kunert A and Hagemann M (1998) Transcriptional analysis of the *isiAB* operon in salt-stressed cells of the cyanobacterium *Synechocystis* sp. PCC 6803. *FEMS Microbiology Letters* 169: 323-330

Webb EA, Moffett JW and Waterbury JB (2001) Iron stress in open-ocean cyanobacteria (*Synechococcus, Trichodesmium,* and *Crocosphaera* spp.): identification of the IdiA protein. *Applied and Environmental Microbiology* 67: 5444-5452

Webber AN and Bingham SE (1998) Structure and Function of Photosystem I. In The Molecular Biology of Chloroplasts and Mitochondria in Chlamydomonas. pp 323-348. Edited by Rochaix J , Goldschmidt M and Merchant S. Kluwer Academic Publishers.

Webber AN, Su H, Bingham SE, Kass H, Krabben L, Kuhn M, Jordan R, Schlodder E and Lubitz W (1996) Site-directed mutations affecting the spectroscopic characteristics and midpoint potential of the primary donor in photosystem I. *Biochemistry* 35: 12857-12863

Weber N and Strotmann H (1993) On the function of subunit PsaE in chloroplast photosystem I. *Biochimica et Biophysica Acta* 1143: 204-210

Wu Q and Vermaas WFJ (1995) Light-dependent chlorophyll a biosynthesis upon chlL deletion in wild-type and photosystem I-less strains of the cyanobacterium *Synechocystis* sp. PCC 6803. *Plant Molecular Biology* 29: 933-945

Xu Q, Armbrust TS, Guikema JA and Chitnis PR (1994a) Organisation of photosystem I polypeptides. *Plant Physiology* 106: 1057-1063

Xu Q, Guikema JA and Chitnis PR (1994b) Identification of surface-exposed domains on the reducing side of photosystem I. *Plant Physiology* 106: 617-624

Xu Q, Hoppe D, Chitnis VP, Odom WR, Guikema JA and Chitnis PR (1995) Mutational analysis of photosystem I polypeptides in the cyanobacterium *Synechocystis* sp. PCC 6803 – Targeted inactivation of psaI reveals the function of PsaI in the structural organisation of PsaL. *Journal of Biological Chemistry* 270: 16243-16250

Xu Q, Jung YS, Chitnis VP, Guikema JA, Golbeck JH and Chitnis PR (1994c) Mutational analysis of photosystem I polypeptides in *Synechocystis* sp. PCC 6803. *Journal of Biological Chemistry* 269: 21512-21518

Xu Q, Odom WR, Guikema JA, Chitnis VP and Chitnis PR (1994d) Targeted deletion of psaJ from the cyanobacterium *Synechocystis* sp. PCC 6803 indicates structural interactions between the PsaJ and PsaF subunits in photosystem I. *Plant Molecular Biology* 26: 291-302

Xu W, Chitnis P, Valieva A, van der Est A, Pushkar YN, Krzystyniak M, Teutloff C, Zech SG, Bittl R, Stehlik D, Zybailov B, Shen G and Goldbeck JH (2003a) Electron transfer in cyanobacterial photosystem I. I. Physiological and spectroscopic characterization of site-directed mutants in a putative electron transfer pathway from A_0 through A_1 to F_X. *Journal of Biological Chemistry* 278: 27864-27875

Xu W, Chitnis P, Valieva A, van der Est A, Brettel K, Guergova-Kuras M, Pushkar YN, Krzystyniak M, Teutloff C, Zech SG, Bittl R, Stehlik D, Zybailov B, Shen G and Goldbeck JH (2003b) Electron transfer in cyanobacterial photosystem I. II. Determination of forward electron transfer rates of site-directed mutants in a putative electron transfer pathway from A_0 through A_1 to F_X. *Journal of Biological Chemistry* 278: 27876-27887

Yang F, Shen G, Schluchter WM, Zybailov BL, Ganago AO, Vassiliev IR, Bryant DA and Golbeck JH (1998) Deletion of the PsaF polypeptide modifies the

environment of the redox-active phylloquinone (A_1). Evidence for unidirectionality of electron transfer in photosystem I. *Journal of Physical Chemistry* B 102: 8288-8299

Yeremenko N, Kouril R, Ihalainen JA, D'Haene SD, van Oosterwijk N, Andrizhiyevskaya EG, Keegstra W, Dekker HL, Hagemann M, Boekema EJ, Matthijs HCP and Dekker JP (2004) Supramolecular organization and dual function of the IsiA chlorophyll-binding protein in cyanobacteria. *Biochemistry* 43: 10308-10313

Yoon HS, Hackett JD, Ciniglia C, Pinto G and Bhattacharya D (2004) A molecular timeline for the origin of photosynthetic eukaryotes. *Molecular Biology and Evolution* **21**: 809-818

Yu L, Zhao J, Muhlenhoff U, Bryant DA and Golbeck JH (1993) PsaE is required for in vivo cyclic electron flow around photosystem I in the cyanobacterium *Synechococcus* sp. PCC 7002. *Plant Physiology* 103: 171-180

Zhao J, Snyder WB, Muhlenhoff U, Rhiel E, Warren PV, Golbeck JH and Bryant DA (1993) Cloning and characterisation of the *psaE* gene of the cyanobacterium *Synechococcus* sp. PCC 7002: characterisation of a *psaE* mutant and overproduction of the protein in *Escherichia coli*. *Molecular Microbiology* 9: 183-194

Zouni A, Witt HT, Kern J, Fromme P, Kraub N, Saenger W and Orth P (2001) Crystal structure of photosystem II from *Synechococcus elongatus* at 3.8 Å resolution. *Nature* 409: 739-743